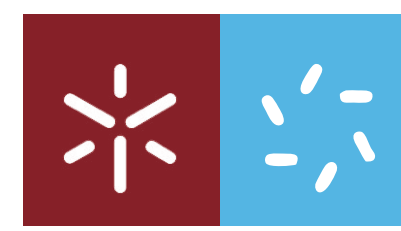




**Molecular Mechanisms Involved in 3-Bromopyruvate
Effect in Colorectal Cancer Cell Lines**

Joana Margarida Pereira Vieira

UMinho | 2017

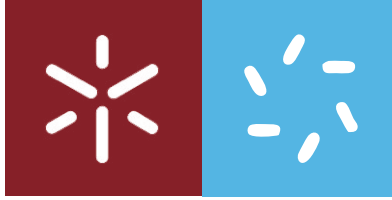


Universidade do Minho
Escola de Ciências

Joana Margarida Pereira Vieira

**Molecular Mechanisms Involved
in 3-Bromopyruvate Effect in
Colorectal Cancer Cell Lines**

Março de 2017



Universidade do Minho

Escola de Ciências

Joana Margarida Pereira Vieira

Molecular Mechanisms Involved in 3-Bromopyruvate Effect in Colorectal Cancer Cell Lines

Tese de Mestrado

Mestrado em Genética Molecular

Trabalho efetuado sob a orientação de:

Professora Doutora Odília Marques de Queirós

Professora Doutora Margarida Casal

DECLARAÇÃO

Nome: Joana Margarida Pereira Vieira

Endereço electrónico: joana.m.vieira@live.com.pt

Telefone: 910684802

Número do Bilhete de Identidade: 13925429

Título tese: Molecular Mechanisms Involved in 3-Bromopyruvate Effect in Colorectal Cancer Cell Lines

Orientador(es):

Professora Doutora Odília Marques de Queirós

Professora Doutora Margarida Casal

Ano de conclusão: 2017

Designação do Mestrado: Mestrado em Genética Molecular

É AUTORIZADA A REPRODUÇÃO INTEGRAL DESTA TESE/TRABALHO APENAS PARA EFEITOS DE INVESTIGAÇÃO, MEDIANTE DECLARAÇÃO ESCRITA DO INTERESSADO, QUE A TAL SE COMPROMETE.

Universidade do Minho, ____/03/2017

Assinatura: _____

Acknowledgments/ Agradecimientos

Acknowledgments/ Agradecimentos

À Professora Doutora Odília Queirós, orientadora desta tese, gostaria de agradecer pela oportunidade que me deu em trabalhar neste projeto. Pela confiança que depositou no meu trabalho, conhecimento e incentivo ao longo deste percurso. Pela disponibilidade e simpatia que sempre partilhou. Muito obrigada.

À Professora Doutora Margarida Casal, no título de co-orientador, agradeço pela orientação, pelos ensinamentos e confiança, pela disponibilidade e simpatia ao longo de todo o trabalho.

A todas as colegas de laboratório, Andrea Cunha, Joana Barbosa, Juliana Faria, Ana Barbosa, Joana Miranda e Diana Valente, que sem elas certamente esta seria uma tarefa mais difícil! Em especial à Patrícia Silva pela paciência nos western. À Ana Barbosa e Joana Miranda, que já terminaram os seus percursos académicos, mas a amizade prevalece para além do laboratório.

Um especial e sincero agradecimento à Diana Valente! Muito obrigada pela partilha de conhecimento e pelas produtivas discussões de foro científico, mas não só! Obrigada pelo companheirismo, apoio nos momentos bons e menos bons e, principalmente pela boa disposição. Muito obrigada, meu bem!

Agradeço ao Joaquim Soares, principalmente pela paciência e compreensão nos atrasos e no pouco tempo que por vezes tinha. Obrigada pelo companheirismo, pelos conselhos, pela amizade e carinho, por me ouvir e por estar sempre ao meu lado em todos os momentos.

Por último, agradeço à minha família, aos meus pais e irmão, pelo apoio incondicional, pela motivação e encorajamento. Um especial obrigada aos meus pais por me terem dado mais esta oportunidade, pela educação e princípios incutidos. Pela compreensão e sacrifícios que fizeram, por estarem sempre presentes, pelos conselhos e sobretudo por confiarem em mim. Muito obrigada!

Abstract/Resumo

Abstract

Tumor cells present predominantly a glycolytic profile with increased glucose consumption and lactate production, even under aerobic conditions (Warburg effect). The high glycolytic rates in several tumors lead to the production of large amounts of lactate and upregulation of monocarboxylate transporters (MCTs), whose function is to export lactate into the extracellular milieu. This metabolic reprogramming enables cells to sustain the high proliferative rates and promotes an acidic microenvironment. 3-bromopyruvate (3BP) is an alkylating agent, which targets cancer cell metabolism and it has been demonstrated to be a powerful and specific antitumor agent either in *in vitro* or *in vivo* models. 3BP is an analogous compound of lactate, whose uptake into the cell occurs through MCTs, leading to depletion of intracellular ATP and thus acting as a cytotoxic agent. As tumor cells overexpress MCTs, they can serve as trap, allowing the uptake of 3BP. However, MCTs expression can change according to microenvironment conditions, including extracellular pH, hypoxia, starvation and, in the case of colorectal cancer (CRC), by the presence of short-chain fatty acids (SCFA) produced by intestinal microbiota. The aim of this work was to understand the regulation of MCTs in these different conditions in CRC cell lines and how it correlates with 3BP toxic effect.

Our study showed that the three cell lines presented different sensitivities for 3BP: HCT-15 < Caco-2 < HT-29. In all these cell lines, 3BP decreased lactate production and cell viability and migration capacity. Concerning the expression of MCT1 and MCT4, proteins involved in 3BP uptake, it was observed that the HCT-15 cell line, the most sensitive to 3BP, presented an increased expression of MCT1 and MCT4, while the most resistant cell lines HT-29 and Caco-2 showed a lower expression of both proteins. The effect of different environment conditions on MCT1 and MCT4 expression was evaluated in the HCT-15 cell line. HCT-15 cells were more resistant to 3BP when exposed to hypoxia or glucose starvation, although an increase in MCT expression levels has been observed in these conditions. Treatment with both butyrate and acetate, sensitized HCT-15 cells to 3BP and an increased expression of MCT4 was observed. Thus, the overall results suggest that MCTs can be involved in 3BP mechanism of action, possibly mediating 3BP uptake into the cell, but the resistance observed under the different should involve other factors beyond MCTs.

Keywords: "Warburg effect", 3-bromopyruvate, Monocarboxylate transporters, Colorectal Cancer.

Resumo

As células tumorais apresentam um perfil glicolítico com elevados níveis de consumo de glicose e produção de lactato, mesmo sob condições aeróbias (efeito Warburg). Este fenótipo glicolítico presente em vários tumores resulta na produção excessiva de lactato e na sobre-expressão dos transportadores de monocarboxilatos (MCTs), envolvidos no transporte de lactato para o meio extracelular. Esta reprogramação metabólica suporta a elevada taxa de proliferação e promove um microambiente ácido. O 3-bromopiruvato (3BP) é um agente alquilante, que tem como alvo o metabolismo células tumorais e demonstrou ser um agente antitumoral poderoso, quer em modelos *in vitro* quer em *in vivo*. O 3BP é um análogo do lactato, cuja transporte ocorre via MCTs, levando à depleção de ATP intracelular, sendo um agente citotóxico. Os MCTs podem servir como armadilha para as células tumorais, onde estão sobre-expressos, permitindo a entrada do 3BP. Porém, a expressão dos MCTs pode alterar-se com as condições do microambiente tumoral, tais como o pH extracelular, a hipoxia, a escassez de glicose e, no caso de cancro colorectal (CRC), a presença de ácidos monocarboxílicos produzidos pela flora intestinal. O objetivo deste trabalho foi compreender a regulação dos MCTs nestas condições em linhas celulares de CRC e correlacionar com o efeito tóxico do 3BP.

Neste estudo mostrámos que as três linhas celulares têm sensibilidades diferentes ao 3BP: HCT-15 < Caco-2 < HT-29. Em todas as linhas celulares, o tratamento com o 3BP diminuiu a produção de lactato e a capacidade de migração. Quanto à expressão do MCT1 e MCT4, proteínas envolvidas no transporte do 3BP, observou-se que a linha HCT-15, a mais sensível ao 3BP, teve maior expressão de MCT1 e MCT4, enquanto que as linhas mais resistentes HT-29 e Caco-2 tiveram uma expressão mais baixa de ambas as proteínas. Avaliou-se a expressão dos MCTs nas diferentes condições do microambiente tumoral. As células HCT-15 foram mais resistentes ao 3BP em hipoxia e em privação de glicose, embora tenha sido observado um aumento nos níveis de expressão dos MCTs nestas condições. O pré-tratamento com o butirato e o acetato, sensibilizou as células HCT-15 ao 3BP e aumentou a expressão do MCT4. Assim, os resultados sugerem que os MCTs estão envolvidos no mecanismo de ação do 3BP, mediando o transporte do composto, mas a resistência observada nas diferentes condições deverão envolver outros factores para além dos MCTs.

Palavras-chave: “Efeito de Warburg”, 3-Bromopiruvato, Transportadores de monocarboxílicos, Cancro do Colorectal

Table of Contents

Table of Contents

Acknowledgments/ Agradecimientos	v
Abstract	ix
Resumo	xi
Abbreviation List	xxi
Figures	xxvii
Tables	xxix
Chapter 1	
Introduction	1
1.1. Cell metabolism.....	3
1.2. Tumor cell metabolism: Warburg effect.....	3
1.2.1. Tumor Microenvironment.....	6
1.2.1.1. Hypoxia	6
1.2.1.2. Acidosis	8
1.2.1.3. Nutrient Availability and Metabolic Symbiosis.....	10
1.3. Monocarboxylic Transporters.....	11
1.3.1. Structure of Monocarboxylate Transporters family	14
1.3.2. Regulation of Monocarboxylate Transporters family	16
1.3.2.1. MCT1 isoform	17
1.3.2.2. MCT4 isoform	18
1.3.2.3. MCT1 and MCT4 Accessory Protein: CD147.....	19
1.3.2.4. Inhibitors	20
1.3.2.5. MCT1 and 4: role in cancer and potential target for therapy.....	21
1.4. Tumor metabolism as a target for anticancer therapy.....	22
1.4.1. 3-Bromopyruvate	25
1.5. Colorectal Cancer	26
1.5.1. Relevance of short-chain fatty acid in colorectal cancer	28
1.6. Rationale and aim	29
Chapter 2	
Material and Methods	31
2.1. Cell Lines and Cell Culture	33

2.2. Preparation of Monocarboxylic Acids.....	33
2.2.1. 3-Bromopyruvate.....	33
2.2.2. Butyrate, acetate and lactate.....	34
2.3. Determination of Cell Viability by the Sulforhodamine B assay.....	34
2.4. Determination of the appropriate cell density.....	35
2.5. Determination of 3BP IC ₅₀	35
2.5.1. Extracellular pH.....	36
2.5.2. Hypoxia.....	36
2.5.3. Glucose Starvation.....	37
2.5.4. Pre-treatment with monocarboxylic acids.....	37
2.6. Metabolic profile determination.....	38
2.6.1. Extracellular Glucose Quantification.....	39
2.6.2. Extracellular Lactate Quantification.....	40
2.7. Wound-healing assay.....	40
2.8. MCT1 and MCT4 expression assessment.....	41
2.8.1. RNA isolation and analysis.....	41
2.8.2. Real-Time Quantitative Polymerase Chain Reaction.....	42
2.8.3. Protein extraction and quantification.....	44
2.8.4. Western Blotting.....	44
2.8.5. Immunofluorescence.....	45
2.9. Statistical Analysis.....	46
Chapter 3	
Results	47
3.1. 3-Bromopyruvate effect different colorectal cancer cell lines: evaluation of viability, metabolism and cell migration.	49
3.1.1. Assessment of MCT1 and MCT4 expression in CRC cell lines.	54
3.2. Effect of tumor microenvironment in MCTs expression and cell sensitivity to 3BP.....	56
3.2.1. Hypoxia.....	56
3.2.2. Extracellular pH.....	61
3.2.3. Glucose Starvation.....	66
3.3. Influence of the short-chain fatty acids in 3-bromopyruvate cytotoxicity and monocarboxylate transporters expression in HCT-15 cell line.	70

3.3.1 Cells pre-treated with short-chain fatty acids.....	70
3.1.2. Assessment of MCT1 and MCT4 expression	73
Chapter 4	
Discussion.....	77
Chapter 5	
Final Remarks and Future Perspectives	87
References	95

Abbreviation List

Abbreviation List

2-DG: 2-Deoxyglucose

3BP: 3-Bromopyruvate

18F-FDG: 18F-Fluorodeoxyglucose

α -KG: alpha-Ketoglutarate

ABC: ATP Binding Cassette

AE: Anion Exchanger

AJCC/UICC: American Joint Cancer Committee/Union for International Cancer Control

ATCC: American Type Culture Collection

ATP: Adenosine Triphosphate

CA: Carbonic Anhydrase

CAF: Cancer-associated Fibroblast

CBP: CREB-binding Protein

CHC: α -cyano-4-hydroxycinnamate

ccRCC: clear cell Renal Cell Carcinoma

cDNA: complementary Deoxyribonucleic Acid

CHO: Chinese Hamster Ovary

CoCl₂: Cobalt Chloride

CRC: Colorectal Cancer

DIDS: 4,4'-diisothiocyano-2,2'-disulphonate

DMEM: Dulbecco's Modified Eagle's Medium

DMSO: Dimethylsulphoxide

DNA: Deoxyribonucleic Acid

EDTA: Ethylenediaminetetraacetic acid

EPO: Erythropoietin

EST: Expressed Sequences Tags

FBS: Fetal Bovine Serum

FIH-1: Factor Inhibiting HIF-1

GAPDH: Glyceraldehyde-3-phosphate Dehydrogenase

GLS: Glutaminases

GLUT: Glucose Transporter

HDAC: Histone Deacetylase

HEPES: 4-(2-hydroxyethyl)-1-piperazineethanesulfonic acid

HG: High-glycosylated

HIF-1: Hypoxia-inducible Factor 1

HK: Hexokinase

HRE: Hypoxia-responsive Element

IC₅₀: 50% Inhibition Concentration

LDH: Lactate Dehydrogenase

LDN: Lonidamine

LG: Low-glycosylated

MCT: Monocarboxylate Transporter

MDR: Multidrug resistance

miRNA: microRNA

MMP: Matrix Metalloproteinases

MPC: Mitochondrial Pyruvate Carrier

NADH: Nicotinamide Adenine Dinucleotide Dehydrogenase

NADPH: Nicotinamide Adenine Dinucleotide Phosphate

NF- κ B: Nuclear Factor-Kappa B

NHE: Sodium-Hydrogen Exchanger

OD: Optical Density

ODD: Oxygen-dependent Degradation

PBS: Phosphate Buffer Saline

pCMBS: p-chloromeranibenzene sulphonate

PDH: Pyruvate Dehydrogenase

PDK: Pyruvate Dehydrogenase Kinase

PET: Positron Emission Tomography

PHD: Proline Hydroxylase

pHe: Extracellular pH

pHi: Intracellular pH

PI3K/Akt: Phosphatidylinositol 3-OH Kinase/serine/threonine-specific protein kinase

PPP: Pentose Phosphate Pathway

RPE: Retinal Pigment Epithelium

qRT-PCR: quantitative Real-Time Polymerase Chain Reaction

RNA: Ribonucleic acid

ROS: Reactive Oxygen Species

RT: Room Temperature

SCFA: Short-Chain Fatty Acid

SD: Standard Deviation

SDS-page: Sodium Dodecyl Sulfate polyacrylamide gel electrophoresis

siRNA: small interfering Ribonucleic Acid

SLC: Solute Carrier

SMCT: Sodium-coupled Monocarboxylate Transporter

SRB: Sulforhodamine B

TBST: Tris-Buffered Saline /Tween-20

TCA cycle: Tricarboxylic Acid cycle

TAD-C: COOH-terminal Transactivation Domain

TAD-N: NH₂-terminal Transactivation Domain

TEMED: N,N,N',N'- Tetramethylethylenediamine

TMS: Transmembrane helices segment

V-ATPase: Vacuolar ATPase

VDAC: Voltage Dependent Anion Channel

VEGF: Vascular endothelial growth factor

VHL: Van Hippel Lindau complex

Figures and Tables

Figures

Figure 1. Representative illustration of the ten Hallmarks of cancer.	4
Figure 2. Representative scheme of glucose metabolism by oxidative phosphorylation and anaerobic or aerobic glycolysis.....	5
Figure 3. Schematic representation of the oxygen-sensitive subunit, HIF-1 α	8
Figure 4. Representative illustration of pH regulators in a tumor cell.....	9
Figure 5. Metabolic symbiosis in the tumor microenvironment.	11
Figure 6. Representative scheme of predicted topology of the MCTs family.....	15
Figure 7. Representative scheme of the predicted structure of MCT1.....	15
Figure 8. The schematic diagram illustrated a several factors involved in monocarboxylate transporter 1 and 4 (MCT1 and MCT4) regulation.....	16
Figure 9. MTC1 and MCT4 as potential anticancer targets.	22
Figure 10. Glycolysis as potential target for anticancer therapy.....	24
Figure 11. Mechanism of 3BP action.....	26
Figure 12. Colorectal carcinogenesis from normal epithelium to CRC.....	27
Figure 13. Representative scheme of the 96-well plate for the assays described above showing the pre-treatment with the carboxylic acids followed by 3BP treatment in the appropriate range of concentrations.....	38
Figure 14. Effect of 3BP on HCT-15, Caco-2 and HT-29 cell survival assessed by the SRB assay after 16 h of exposure to the compound.....	50
Figure 15. Effect of 3BP in metabolic profile of HCT-15, HT-29 and Caco-2 cell lines.....	51
Figure 16. Inhibitory effect of 3BP on cell migration capacity of HCT-15 cell line.	52
Figure 17. Inhibitory effect of 3BP on cell migration capacity of Caco-2 cell line.....	53
Figure 18. Inhibitory effect of 3BP on cell migration capacity of HT-29 cell line.....	53
Figure 19. Expression levels of <i>SLC16A1</i> and <i>SLCIA3</i> genes in HCT-15, HT-29 and Caco-2 cell lines determined by qRT-PCR.....	55
Figure 20. MCT 1 expression analysis in HCT-15, HT-29 and Caco-2 cell lines.	55

Figure 21. MCT1 and MCT4 cellular localization in HCT-15, Caco-2 and HT-29 cell lines. Representative images of immunofluorescence are shown at 400x magnification.....	56
Figure 22. Effect of hypoxia in metabolic profile of HCT-15 cells.....	57
Figure 23. Effect of hypoxia on cell migration capacity of HCT-15 cell line.	58
Figure 24. Effect of hypoxia in the expression levels of <i>SLC16A1</i> , <i>SLC1A3</i> and <i>HIF-1</i> genes in HCT-15 cells determined by qRT-PCR.....	59
Figure 25. Effect of hypoxia on MCT1 and MCT4 cellular localization of HCT-15 cell line	60
Figure 26. Effect of hypoxia on cell viability of HCT-15 cells treated with 3BP.	61
Figure 27. Effect of extracellular pH in metabolic profile of HCT-15 cell line.....	62
Figure 28. Effect of extracellular pH on cell migration capacity of HCT-15 cells.....	63
Figure 29. Effect of extracellular pH in the expression levels of <i>SLC16A1</i> , <i>SLC1A3</i> genes in HCT-15 cells determined by qRT-PCR.	64
Figure 30. Effect of extracellular pH on MCT1 and MCT4 cellular localization of HCT-15 cell line.	65
Figure 31. Effect of extracellular pH on cell viability of HCT-15 cells treated with 3BP.....	65
Figure 32. Effect of glucose starvation in metabolic profile of HCT-15 cell line.	66
Figure 33. Effect of glucose starvation on cell migration capacity of HCT-15 cell line.	67
Figure 34. Effect of glucose starvation in the expression levels of <i>SLC16A1</i> and <i>SLC1A3</i> genes in HCT-15 cells (gray bars) determined by qRT-PCR.	68
Figure 35. Effect of glucose starvation on MCT1 and MCT4 cellular localization of HCT-15 cell line.	69
Figure 36. Effect of glucose starvation on cell viability of HCT-15 cell line.	69
Figure 37. Cell viability, evaluated by the SRB assay, of HCT-15 cells incubated during 24 h and 48 h in medium containing butyrate (A) , lactate (B) or acetate (C) in a range of concentrations (up to 70 mM), followed by 16 h incubation in medium with (gray bars) or without 3BP (black bars) using the IC ₅₀ previously determined.	71
Figure 38. Effect of short-chain fatty acids on cell sensitivity of HCT-15 cells to 3BP.....	72
Figure 39. Effect of short-chain fatty acids in the expression levels of <i>SLC16A1</i> , <i>SLC1A3</i> genes in HCT-15 cells determined by qRT-PCR.	74
Figure 40. Effect of butyrate on MCT1 and MCT4 cellular localization of HCT-15 cell line.....	75

Figure 41. Effect of lactate on MCT1 and MCT4 cellular localization of HCT-15 cell line. 76

Figure 42. Effect of acetate on MCT1 and MCT4 cellular localization of HCT-15 cell line.76

Tables

Table 1. Members of Monocarboxylate Transporter Family..... 13

Table 2. Km values (mM) of mammalian MCT isoforms for a range of monocarboxylates. 19

Table 3. Sequences of forward and reverse primers, corresponding to *SLC16A1*, *SLC16A3* and *actin* genes. 42

Table 4. Primary antibodies used in the present study. 45

Table 5. IC₅₀ values for 3BP for the cell lines HCT-15, Caco-2 and HT-29..... 50

Table 6. IC₅₀ values for 3BP for the cell line HCT-15 after pre-incubation with concentration of each short-chain fatty acids. 73

Chapter 1
Introduction

1.1. Cell metabolism

Cell metabolism involves several metabolic pathways, composed by a complex set of biochemical reactions. These metabolic pathways are highly coordinated to sustain vital cell processes, obtaining biosynthetic precursors and chemical energy from nutrient molecules. The cell proliferation is an important process for growth and right function of mammalian adult tissues, involving growth-factor signal transduction pathways activation, translating in adenosine triphosphate (ATP) production and macromolecules synthesis for cell division [1]. The differentiated cells may resort to mitochondrial oxidative phosphorylation or anaerobic glycolysis to obtain energy, depending on the presence or absence of oxygen, respectively [2], while proliferative or tumor cells resort essentially to aerobic glycolysis [3], obtaining the energy and biosynthetic precursors that require for cell proliferation [1,4].

1.2. Tumor cell metabolism: Warburg effect

Cancer is a genetic disease involving gradual changes in the genome that allow the acquisition of a malignant and invasive profile by normal cells. This profile involves multistep processes, known by tumorigenesis, which lead to a deregulation of pathways that govern the normal cells proliferation and homeostasis, giving a phenotype that confers a selective advantage to cells, turning them gradually in malignant cells [5-7]. In 2000, Hanahan and Weinberg suggested six changes in the cellular physiology that define cancer cells, which have posteriorly been complemented with four hallmarks more (**Figure 1**): two enabling characteristics (genome instability and tumor-promoting inflammation) and two emerging hallmarks (avoiding immune destruction and deregulating cellular energetics) [8,9].

The normal differentiated cells depend mainly on the mitochondrial oxidative phosphorylation to obtain the energy needed to cellular processes. In the absence of mitochondrial systems or in anaerobic conditions, differentiated cells follow the fermentative pathway, producing large amounts of lactate. However, in the presence of oxygen, the Pasteur Effect occurs and these cells convert glucose into pyruvate, which in turn is converted into acetyl-CoA that enters in the mitochondrial tricarboxylic acid (TCA) cycle. This metabolic pathway generates NADH that maximize ATP production by oxidative phosphorylation, reducing the production of lactate [2]. Instead, cancer cells use mainly aerobic glycolysis to obtain energy, a phenomenon called "Warburg effect" [3]. As result, cancer cells convert

most glucose into lactate, in either the presence or absence of oxygen (**Figure 2**) [2, 10]. However, glycolysis is an unproductive way to generate ATP, with a yield of two ATPs per molecule of glucose against thirty-six ATPs obtained by the complete oxidation of one glucose molecule [3]. Otto Warburg hypothesized that cancer cells developed defects in mitochondria, disabling them to generate normal levels of energy by respiration [3,11,12]. Nevertheless, recent researches have demonstrated that some cancer cells have active and functional mitochondria, as well as oncogenes and tumor suppressor genes that are important to this metabolic switch, contributing for higher glycolytic rates and a raised glucose consumption through the upregulation of glucose transporters (GLUTs) and overexpression of genes involved in glycolysis, allowing these cells to obtain the necessary supply of energy [13-16].



Figure 1. Representative illustration of the ten Hallmarks of cancer that are involved in the set of functional capabilities acquired by the tumor. Adapted from [9].

Being altered energy metabolism a hallmark of cancer, it can be used to diagnosis, as well as targets to explore new therapies (discussed later in this thesis). This high glucose consumption has been explored in tumor imaging, allowing tumors' detection and monitoring by positron emission

tomography (PET). This clinical technique uses labeled glucose with 18F-fluorodeoxyglucose (18F-FDG), which is transported into the cells by overexpressed GLUTs and phosphorylated by hexokinase (HK). Once inside the cell, 18F-FDG cannot be further metabolized and becomes trapped, and consequently accumulate into the cells. This accumulation of the isotope into tumor cells allow to distinguish them from normal tissue cells by PET, which detects 18F-FDG signal [2,17]. However, not all cancers are easily detected by PET imaging and not all positive PET signal corresponds to a malignant tissue [18].

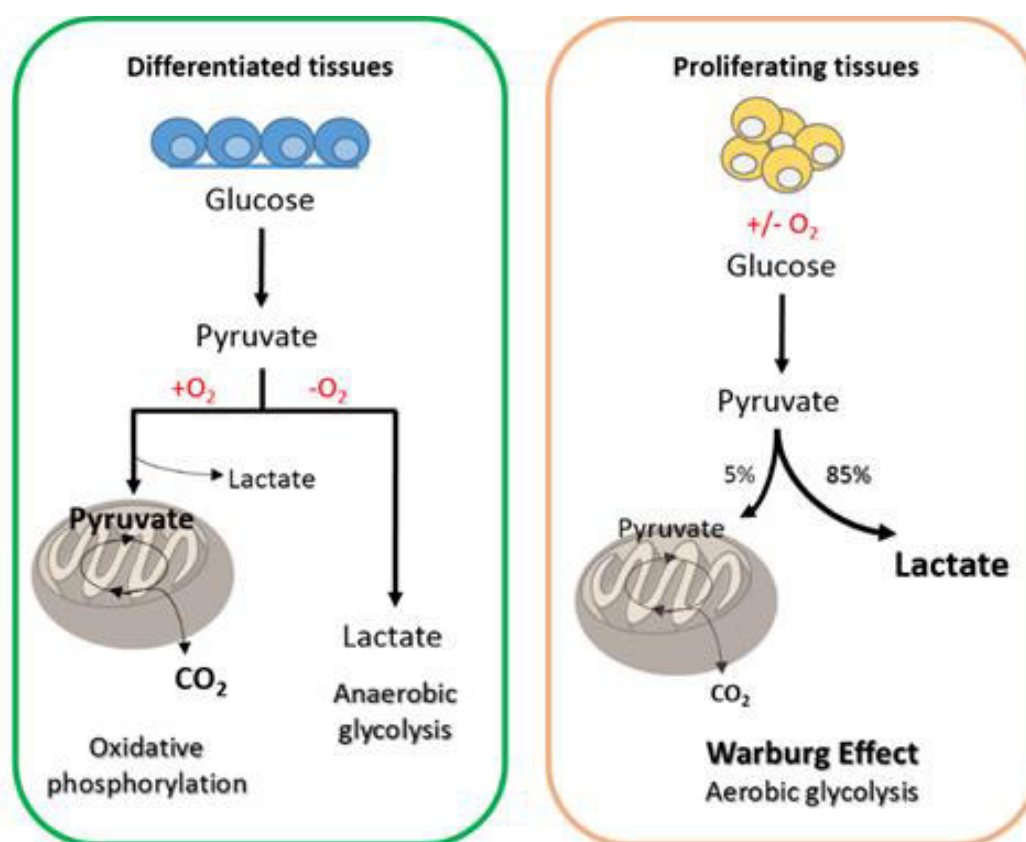


Figure 2. Representative scheme of glucose metabolism by oxidative phosphorylation and anaerobic or aerobic glycolysis. Differentiated tissues convert glucose into pyruvate that enters in the mitochondrial tricarboxylic acid (TCA) cycle to obtain energy, in the presence of oxygen. In contrast, in anaerobic conditions, glucose is converted mainly into lactate. In proliferative or tumor tissues, glucose is essentially metabolized into lactate either absence or presence of oxygen (Warburg effect) [10].

Even though glucose is the preferential substrate of cancer cells, they can reprogram their metabolism and use other substrates as glutamine. Glutamine is converted into glutamate in reactions that either give the amide nitrogen to biosynthetic pathways or release it as ammonia [19]. These reactions are catalyzed by the glutaminases (GLS), being their activity in certain tumors correlated to growth and malignancy [20]. Glutamate is the main source of α -ketoglutarate (α -KG), an intermediate of the TCA cycle and anabolism, providing oxaloacetate [19-23]. Glutamine oxidation also supports nonessential amino acids synthesis and is involved in redox homeostasis by producing nicotinamide adenine dinucleotide phosphate (NADPH) [19]. Thus, metabolism of both glucose and glutamine is relevant to the maintenance of biosynthetic precursors production and energy require for tumor cells survival [2,24].

1.2.1. Tumor Microenvironment

A solid tumor consists of a heterogeneous cellular population, where different cancer and stroma cells co-exist with diverse genetic backgrounds [5]. The fact of cancer cells present metabolic flexibility during tumor progression cause a dynamic between the solid tumor and microenvironment, where the concentration of several nutrients and oxygen are variable in spatially and temporally, leading to an abnormal vasculature and hypoxic stress, being these related to the glycolytic phenotype and consequently, with altered pH of tumor microenvironment [5,9].

1.2.1.1. Hypoxia

A persistent hypoxia exerts a pressure for glycolysis upregulation. The Hypoxia-Inducible Factor (HIF)-1 is an important transcription factor regulated by the levels of oxygen in the cellular environment. HIF-1 activates the expression of several genes through binding to hypoxia-responsive element (HRE) located in their promoter regions. HIF-1 targets genes responsible for cell growth and proliferation, glucose metabolism, angiogenesis, invasion and metastasis [25]. Therefore, a hypoxic environment facilitates tumor development and growth, besides enhancing the resistance to drugs and inhibition of apoptosis [26]. HIF-1 activates vascular endothelial growth factor (VEGF) and erythropoietin (EPO), which are main growth factors involved in tumor angiogenesis. It also promotes upregulation of glucose

transporter (GIUT-1) and of several enzymes involved in the glycolytic metabolism, like lactate dehydrogenase (LDH), pyruvate dehydrogenase kinase-1 (PDK1) or HKII, enhancing glucose uptake and glycolysis [26-28]. At the same time, these alterations promote the efflux of the lactate and protons by the activation of the monocarboxylate acid transporter (MCT) 4 and carbonic anhydrase (CA) IX, respectively, preventing apoptosis and inhibiting the immune system by acidifying the extracellular environment [29,30].

HIF-1 is the major regulator of the cell response to hypoxia and its expression level is closely controlled by its synthesis and degradation. HIF-1 is a heterodimeric transcription factor expressed or degraded in absence or presence of the oxygen, respectively [25]. It consists of two subunits, an oxygen-sensitive HIF-1 α and a constitutively expressed HIF-1 β . Both contain basic helix-loop-helix motifs that bind DNA, occurring subunits dimerization [31]. The α -subunit has an oxygen-dependent degradation (ODD) domain and two transactivation domains: NH₂-terminal transactivation domain (TAD-N) and COOH-terminal transactivation domain (TAD-C), being involved in the stabilization and in modulating the transcriptional activation of HIF-1 α under hypoxic conditions, respectively (**Figure 3**) [25,31,32].

In normoxic conditions, HIF-1 α subunit is hydroxylated by proline-hydroxylase (PHD) enzymes, promoting the binding of the van Hippel-Lindau tumor suppressor (VHL) E3 ligase complex and consequently its degradation by ubiquitination in proteasome. Oxygen also regulates the interaction of the TAD-C domain of HIF-1 α blocking the binding of the co-activators (p300/CREB-binding protein-CBP) by the factor inhibiting HIF-1 (FIH-1) enzyme and, therefore inhibits HIF-1-mediated gene transcription [25,31]. Under hypoxic conditions, the rate of hydroxylation decreases resulting in stability and activity HIF-1 α by inhibiting VHL proteins and FIH-1 [31]. Therefore, co-activators can bind to HIF-1 α allowing transcriptional activation of HIF-1 target genes [25,33].

In addition to the multiple microenvironment stimuli, the HIF-1 α regulation is dependent not only of oxygen concentration. Diverse tumor suppressor genes (p53 and PTEN) and oncogenes (Myc, PI3K, AKT, RAS and RAF) can regulate its activation, being responsible by a constitutive activation of HIF pathway, increasing HIF-1 α protein synthesis and stability in many cancer types and activating the Warburg phenotype [33-36].

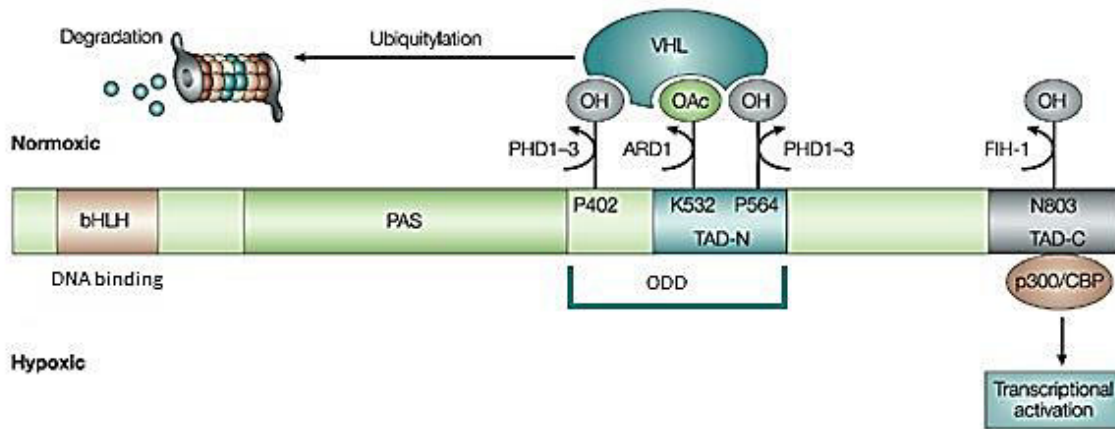


Figure 3. Schematic representation of the oxygen-sensitive subunit, HIF-1 α . In normoxic conditions, the proline (P) residues 402 and 564 present in TAD-N are hydroxylated by the PHD 1-3 enzymes, allowing that the van Hippel–Lindau (VHL) E3 ubiquitin-protein ligase complex binds it and promotes by acetylation of lysine (K) residue 532 by the ARD1 acetyltransferase. The HIF-1 α ubiquitination targets the protein for degradation by the proteasome. In the presence of oxygen, FIH-1 enzyme blocks the binding of co-activators p300/CBP through O₂-dependent hydroxylation of asparagine (N) residue 803 in TAD-C, inhibiting HIF-1-mediated gene transcription. In hypoxic conditions, the hydroxylation rate decreases, decreasing HIF-1 α degradation. However, p300/CBP can bind to N803, allowing transcriptional activation of HIF-1 target genes. bHLH, basic helix–loop–helix; PAS, Per-Arnt-Sim; TAD-C, carboxy-terminal transactivation domain; TAD-N, amino-terminal transactivation domain; ODD, oxygen-dependent degradation; PHD, proline-hydroxylase enzyme; FIH-1, Factor Inhibiting HIF-1 enzyme. Adapted from [32].

1.2.1.2. Acidosis

Intracellular pH (pHi) should be within a narrow range 7.1-7.2, which is regulated through membrane proton pumps and transporters, maintaining pHi homeostasis [29]. As shown in **Figure 4**, this regulation involves the activity of several plasma membrane proteins, including H⁺ pumps and exchangers like V-ATPase and Na⁺/H⁺ exchanger (NHE) family members, respectively and transporters that facilitate H⁺ efflux like carbonic anhydrases (CAs) family and monocarboxylate transporter (MCTs) family. The HCO₃⁻ transporters are also involved in pHi homeostasis, facilitating the movement of HCO₃⁻ ions across plasma membrane. They are upregulated by growth factors, oncogenes, hypoxia and low pHi [30].

The combination of factors like poor vasculature, hypoxia and increased acids production through fermentative glycolysis, can lead to intracellular acidosis in cancer cells, which can be restored to physiological values by these proteins. Consequently, the extracellular pH (pHe) values decrease to 6.5-6.8, being this environmental acidification associated to tumor progression [30]. Acidic pHe affects the expression of some genes, activates proteinases and stimulates disruption of adherence junctions, inducing migration and invasion of tumor cells, and inhibits monocyte motility and cytokine release, escaping the immune system [37,38].

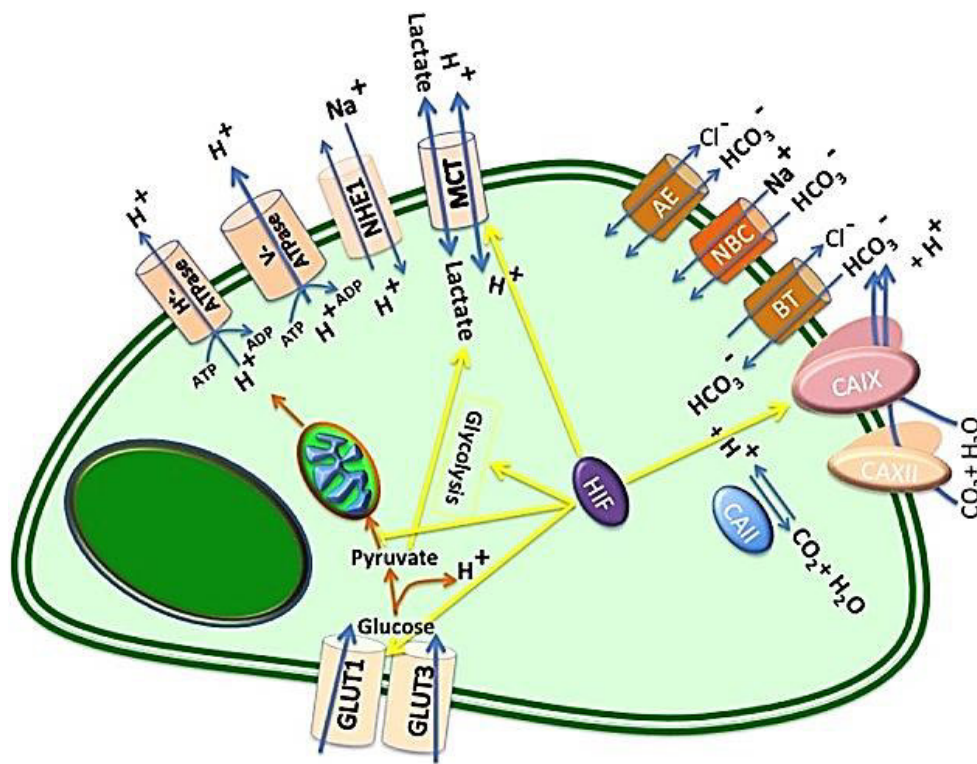


Figure 4. Representative illustration of pH regulators in a tumor cell. Main proteins involved in intracellular and extracellular pH regulation in tumors, such as monocarboxylate transporters (MCTs), the plasma membrane proton pump vacuolar ATPase (V-ATPase); Na⁺/H⁺ exchangers (NHEs); anion exchangers (AEs); carbonic anhydrases (CAII, CAIX and CAXII); Na⁺/HCO₃⁻ co-transporters (NBCs), and HCO₃⁻ transporters (BTs) [30].

1.2.1.3. Nutrient Availability and Metabolic Symbiosis

The abnormal proliferation of tumor mass leads to resources scarcity and long periods under hypoxic stress that, as already mentioned, are responsible for glycolytic phenotype. However, the heterogeneous cellular population that characterize the solid tumor, as well as other surrounding cells, present a great metabolic diversity, existing metabolic symbiosis between them (**Figure 5**) [39]. In the metabolic symbiosis model, they represent essentially two tumor cell populations, hypoxic and oxygenated cells, with distinct metabolism, in which one of them is responsible to produce lactate that will be oxidized by the other population [40]. In this model, cancer-associated fibroblasts (CAF) are also involved in increase of lactate production, in a phenomenon called “Reverse Warburg Effect” [41,42]. This process consists in the capacity of tumor cells to create ROS-mediated “pseudo-hypoxic” conditions, leading to HIF-1 accumulation and oxidative stress of CAF [43]. Consequently, autophagy pathway is activated, as well as aerobic glycolysis, producing recycling nutrients, as lactate and pyruvate [44]. These nutrients are transported for the extracellular environment, being available for tumor cells that present mitochondrial activation. On the other hand, glucose is available for the tumor cells that resort glycolysis [18,45].

This metabolic variety leads to acute and chronic acidification of tumor microenvironment by co-transport of a proton and lactate to the extracellular space mediated by MCTs. While there are more pH regulators, only the MCTs transport lactate and its high production can be correlated with extracellular environmental acidification [30]. As known, the extracellular pH (pHe) is associated with an invasive behavior of tumor through the activation of matrix metalloproteinases (MMPs) at lower pHe [46]. Such activation, together with lactate production, potentiates tumor progression and malignancy by escaping immune system, providing angiogenesis and enhancing resistance to treatments [47-51]. In clinical practice, lactate production, as well as the MCTs overexpression, has been associated to poor prognosis in prostate, non-small-cell lung and gastric cancers [52-54], [55]. These transporters have an important role in tumor, essentially MCT1 and MCT4, which will be discussed later. In this way, cancer cells take advantage of the cooperation with surrounding cells, where the more glycolytic cells produce lactate that can be used by oxidative tumor cells that in this way obtain energy through

mitochondrial oxidative phosphorylation, maintaining favorable microenvironmental conditions to cancer development.

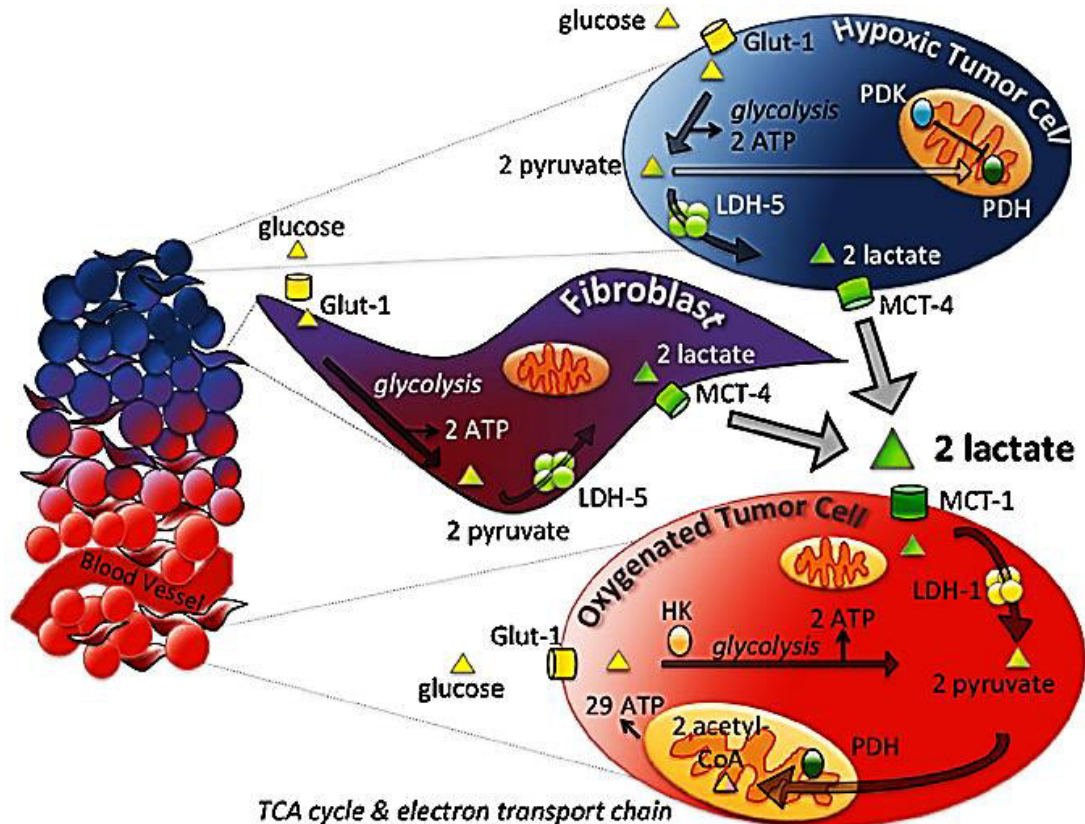


Figure 5. Metabolic symbiosis in the tumor microenvironment. GLUT1, glucose transporters1; LDH, lactate dehydrogenase; PDK, pyruvate dehydrogenase kinase; MCT1-4, monocarboxylate transporters 1-4; HK, Hexokinase; PDH, pyruvate dehydrogenase [39].

1.3. Monocarboxylic Transporters

Most tumor cells, as well as red blood cells and tissues, such as white skeletal muscle, which rely mainly on glycolysis for energy source, produce large quantities of lactate. This increased intracellular concentration of lactate would cause pH decrease in the cytosol and cellular stress [56]. Therefore, cells present a self-defensive strategy, transporting it out of the cell by a proton symport mechanism, avoiding the acidification of intracellular environment. On the other hand, lactate could be a major source of energy in organs like brain and heart, and the major gluconeogenic substrate for kidney and

liver [56]. It can be also used by the most oxidative cancer cells, in a symbiotic metabolism [39]. The transport of lactate and other monocarboxylates, like pyruvate or ketone bodies, is mediated by the proton-linked MCTs, belonging to the solute carrier (SLC)16 family [56-59]. Although there are 14 MCTs, only four members of the family (MCT1–4) are well characterized and involved in this proton-linked monocarboxylate transport [60,61]. The sodium-coupled monocarboxylate transporters (SMCTs) family also transport short-chain organic acids, like lactate, pyruvate or acetate, in an electrogenic sodium dependent process [62].

The **Table 1** reviews the substrate specificity and tissue localization of MCT isoforms [61]. In contrast with MCT1, which is found in the majority of tissues, MCT2 MCT3 and MCT4 have a more restrict distribution. MCT4 appears essentially in strongly glycolytic tissues (heart, brain, skeletal muscle), MCT2 is found mostly in brain, liver and kidney, and MCT3 appears only in retinal pigment epithelium (RPE) [60]. This can be explained by the different roles that MCTs can perform, depending on the tissue/cell types, their metabolic requirements and environmental conditions. For example, ketone bodies, which are produced in the liver under starvation conditions, are exported into the blood through MCT1-2 and be taken up through MCT1-2 present in neurons and red muscle fibers as a respiratory source [57,60]. MCT4 is mainly involved in lactate efflux, and so its expression is relevant in tissues that rely in glycolysis, producing large amount of lactate, which is uptake by more oxidative cells via MCT2 and mainly via MCT1. MCT3 is also responsible for lactate efflux, but only across the RPE and into the blood [57, 63]. Therefore, the different MCT isoforms can have different substrates specificity and affinity and have a special relevance in lactate metabolism and transport, being an important element for cellular metabolic diversity and pH regulation, as well as a signaling agent to promote angiogenesis and immunosuppression [61,64].

Table 1. Members of Monocarboxylate Transporter Family, adapted from [60] and [61].

Protein name	Human Gene name	Reference Sequence	Tissue Distribution	Accessory Protein	Transport Mechanism	Substrate
MCT1	SLC16A1	NM_003051	Ubiquitous	CD147	H ⁺ cotransporter exchanger	Lactate, pyruvate, ketone bodies
MCT2	SLC16A7	NM_004731	Testis, liver, kidney, skeletal, muscle, heart, brain, spleen, pancreas	EMBIGIN	H ⁺ cotransporter	Pyruvate, lactate, ketone bodies
MCT3	SLC16A8	NM_013356	Retinal pigment epithelium (RPE), choroids plexus, aorta, placenta,	CD147	H ⁺ cotransporter	Lactate
MCT4	SLC16A3	NM_004207	White muscle, white blood cells, tumors, RPE, brain kidney, placenta, small intestine, lung, heart	CD147	H ⁺ cotransporter	Lactate, pyruvate, ketone bodies
MCT5	SLC16A4	NM_00469	Placenta, intestine, colon			?
MCT6	SLC16A5	NM_004695	Kidney, muscle, placenta, intestine, brain, heart, pancreas, prostate, lung		Facilitated diffusion	?
MCT7	SLC16A6	NM_00469	Pancreas, brain, muscle			?
MCT8	SLC16A2	NM_00651	Liver, brain, kidney, heart, placenta			T3, T4
MCT9	SLC16A9	BN000144	Endometrium, testis, ovary, breast, brain, kidney, adrenal, retina			?
MCT10	SLC16A10	NM_018593	Intestine, kidney, skeletal muscle, heart, liver, placenta		Facilitated diffusion/	Aromatic amino acids
MCT11	SLC16A11	NM_153357	Skin, lung, ovary, breast, pancreas, RPE, choroid plexus			?
MCT12	SLC16A12	ENSG00000152779	Kidney			?
MCT13	SLC16A13	BN000145	Breast, bone marrow			?
MCT14	SLC16A14	BN000146	Brain, heart, ovary, breast, lung, pancreas, RPE, choroid plexus			?

1.3.1. Structure of Monocarboxylate Transporters family

The MCTs family is composed by 14 members belonging to the *SLC16* gene family (**Table 1**). The MCT family isoforms have conserved structural attributes and sequence motifs, not only in humans but also in several species, such as chicken, rat and mouse [56,60]. All MCT isoforms are predicted to have cytoplasmic N- and C-termini and 12 transmembrane α -helix segments (TMS) domains organized in two domains with the N- or C terminus, each one with 6 TMS and an intracellular loop between TMS 6 and 7 (**Figure 6**) [56,60]. The TMS present the greatest conservation, while the intracellular C- and N termini and the loop between TMS 6 and 7 present more variability [61, 65]. The predicted model for MCT1 is composed by the 6-helix N-terminal domain and the similar 6-helix C-terminal domain linked by a 30 residues loop (**Figure 7**) [66, 67].

Two conformational structure were predicted for MCTs: the inside- and outside-open conformation (**Figure 7**) [67]. In this mechanism, there are amino acid residues that perform an important role in the transport function, the substrate selection and the protein stability. By site-directed mutagenesis, modeling and computational studies, it has been demonstrated that a lysine residue (K38) located in the extracellular region of the MCT1, is involved in the transport process, providing a binding site for the monocarboxylate upon accepting a proton. The monocarboxylate binds through electrostatic interactions changing the protein conformation from a closed to open state (**Figure 7**) [61,67]. Additionally, phenylalanine, aspartate and arginine residues (F360, D302, R306) at the intracellular substrate-binding site are also essential for MCT1 activity and specificity. A site-directed mutagenesis replacing phenylalanine (F360) into cysteine allowed the transport of mevalonate, which is not a MCT1 substrate [65,68]. Therefore, these three critical residues, in both halves of MCTs, have significant role in the proposed translocation cycle. They are also present in MCT2, MCT3, and MCT4. The model predicted that the N-terminus domain is involved in bind of monocarboxylate upon protonation of K38 residues (TMS1). Additionally, the C-terminus domain is involved in substrate specificity and affinity, involving D302 and R306 residues (TMS 8) and F360 residue (TMS 10). This model suggests that, especially TMS7-TMS12, are determinants for substrate affinity [65,67,69].

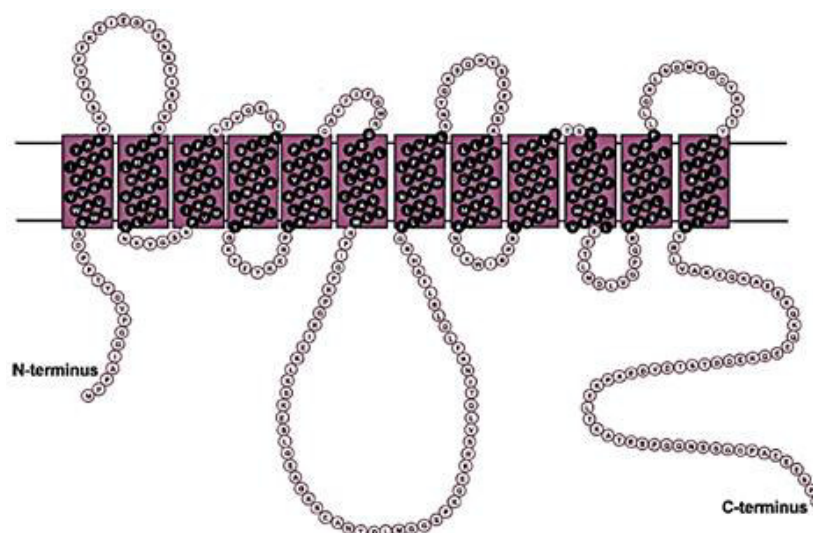


Figure 6. Representative scheme of predicted topology of the MCTs family. The presented sequence is referent to human MCT1 [56].

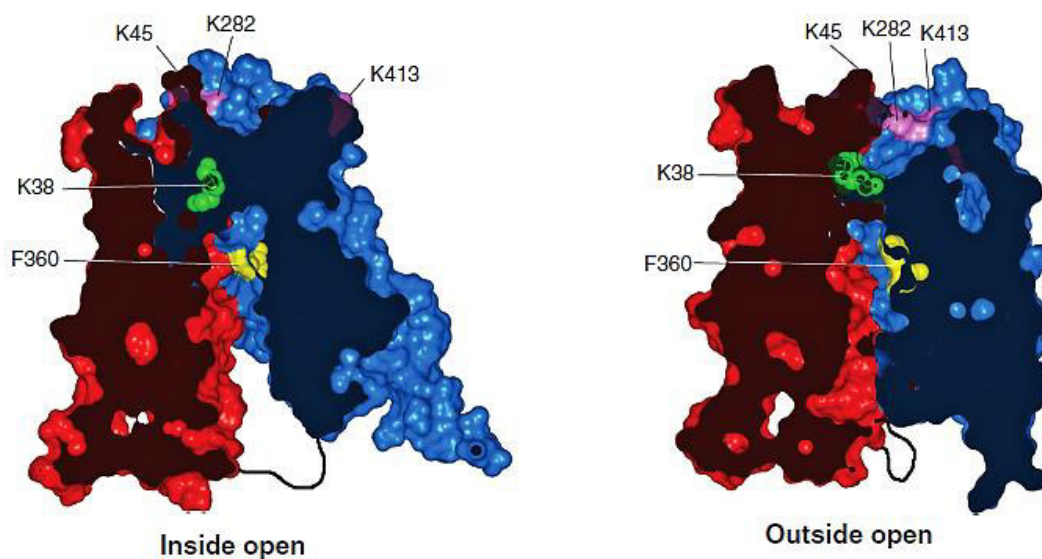


Figure 7. Representative scheme of the predicted structure of MCT1. Molecular model corresponding to two forms, “inside open” and “outside open”. The N-terminal domain is colored red and the C-terminal domain colored blue, while the intracellular loop connecting the two is shown as a connecting line. The green and yellow color are represented critical residues (K38 and F360, respectively) for the translocation cycle and substrate specificity, respectively. Lysine residues (K45, K282, and K413) represented purple are involved in DIDS binding. Adapted from [65].

1.3.2. Regulation of Monocarboxylate Transporters family

Several researches have demonstrated the importance of MCTs in the metabolism and metabolic communication between cells, but cellular and molecular regulation mechanisms of MCTs expression is still an open field. MCTs regulation can occur via transcriptional, post-transcriptional and post-translation mechanisms, affecting proteins amount as well as their activity, which can also be regulated by chaperone proteins [70]. MCTs expression appears to be regulated in a tissue specific way, being dependent of physiological or pathological conditions, including MCT substrate concentration, signals arising from changes in cellular metabolism, dietary conditions, and hypoxia [71]. As describe above, there are different MCT isoforms, being the MCT1-4 the best characterized. Nevertheless, this introduction will give more emphasis to on MCT1 and MCT4 isoforms, being briefly represented in **Figure 8**, several factors involve in MCT1 and MCT4 regulation [72].

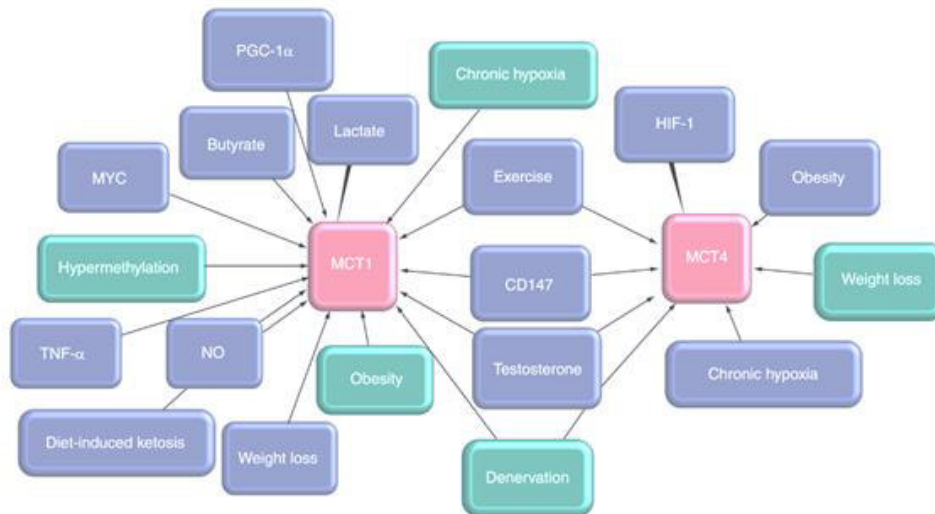


Figure 8. The schematic diagram illustrated a several factors involved in monocarboxylate transporter 1 and 4 (MCT1 and MCT4) regulation. Blue boxes indicate upregulation and green boxes indicate a downregulation of the specific MCTs (pink boxes). There is no distinction between transcriptional and translational regulation. HIF: Hypoxia-Inducible transcription Factor; MCT: Monocarboxylate Transporter; NO: Nitric Oxide; TNF: Tumor Necrosis Factor [72].

1.3.2.1. MCT1 isoform

MCT1 is the isoform most well studied and characterized of the MCT family. It was first identified in Chinese hamster ovary (CHO) cells and posteriorly in human cells [61,70], being the only MCT expressed in human erythrocytes [73,74]. The human MCT1 coding gene, *SLC16A1*, is located in chromosome 1 (1p13.2-p12) and, in 2002, Cuff and Shirazi Beechey described the structural organization of gene, as well as the characterization of *SLC16A1* promoter [75]. The *SLC16A1* gene comprises five coding exons and four introns. It has been found six alternative spliced transcripts in this gene, resulting in four proteins of different sizes and two with no translation product [57,60,61,70,75]. MCT1 functional protein has a molecular weight between 40 to 55 kDa and it is composed by 494 amino acids [71,76].

MCT1 has ubiquitous distribution in human tissues, being capable of transport a wide variety of monocarboxylates, in addition to lactate [60]. The vast distribution of MCT1 may be explained by its substrate affinity, demonstrating a possible involvement of MCT1 in both uptake and efflux of monocarboxylates from cells. Michaelis-Menten kinetics proved that different substrates present different K_m for MCT1 (**Table 2**) [57,77]. However, its main physiological role is the stereoselective lactate transport to inside or outside of the cell depending of the concentration gradient and pH [58,70]. Additionally, there are evidences that high concentrations of lactate have increased MCT1 mRNA and protein levels by stimulating the reactive oxygen species (ROS) synthesis, triggering a signaling cascade that induce the expression of several genes, including MCT1 [78]. Butyrate, which is produced by intestinal bacteria [79], across the colonocyte plasma membrane by MCT1, also enhanced the concentration- and time-dependent increase of both MCT1 mRNA and protein by modulating gene transcription through inhibition of histone deacetylases, increasing mRNA stability and stimulating MCT1 promoter activity through the NF- κ B pathway [72,80-83]. Posterior research demonstrated that butyrate also induced an increase in MCT4 expression in breast cancer cell lines, turning the cells more sensitive to the glycolytic inhibitor 3-bromopyruvate (3BP) [84].

In response to intense exercise in skeletal muscle cells, it occurs an increase in intracellular $[Ca^{2+}]$ and AMP, inducing MCT1 upregulation by the activation of calcineurin and AMP-activated protein

kinase (AMPK) [85]. On the other side, there are evidences of down-regulation of MCT1 and MCT4 in adipose tissue, heart and skeletal muscle in diabetes and obesity situations [86-88].

Hypoxia was also reported to increase in neuronal, astrocytic and endothelial MCT1 expression [65,89]. However, there is no evidence that MCT1 promoter contains HRE, and the upregulation of MCT1 expression in the presence of hypoxia has been shown to be dependent of p53 status and not of HIF-1 α [90, 91]. In this way, it is unclear the exact mechanism of regulation, needing more investigation about it.

1.3.2.2. MCT4 isoform

MCT4 isoform was identified through of a search of the Expressed Sequence Tags (EST) database and was originally called MCT3, according with the sequence homology with chicken MCT3 [56,92]. It was renamed MCT4 after the mammalian MCT3 was identified in mammalian RPE [92]. The human *SLC16A3* gene is located in chromosome 17 (17q25.3), and comprises five exons and three transcripts [93]. MCT4 functional protein is constituted by 465 residues, corresponding to a molecular weight of about 50 kDa [76,92].

MCT4 expression in different cell types is more abundant in cells where glycolysis rates are high, such as white skeletal muscle fibers, astrocytes, white blood cells, chondrocytes and tumor cells [61,94]. This isoform has a particular importance to these tissues, because they need to export lactate. Like MCT1, MCT4 also recognize different substrate, including lactate, pyruvate and ketone bodies [60]. However, the MCT4 kinetic properties indicate that this isoform is adapted to the export of lactate with Km values about 5–10-fold higher than MCT1 [70,94,95]. On the other hand, the Km value is higher for pyruvate than L-lactate, preventing pyruvate loss from the cells, which is crucial in cells that rely in glycolysis [58].

MCT4 expression is increased under hypoxia in agreement with its role of lactate exporter in glycolytic cells. In hypoxic conditions, the MCT4 is upregulated through HIF-1 binding to HRE present in MCT4 promoter [30,85,90]. However, in the neonatal heart, which presents a more glycolytic metabolism than the adult heart and where MCT4 expression is higher than in the adult heart, there are no evidences that the HIF-1 α is responsible for this increased MCT4 expression [65,96].

Recently, it has been demonstrated that epigenetic modifications, as well as microRNAs (miRNA) with mRNA targets are responsible by mRNA degradation and translational repression [85,97,98]. In the case of clear cell renal cell carcinoma (ccRCC), it has been shown that DNA methylation of *SLC16A3* regulate MCT4 expression and it has been demonstrated that this mechanism may be used as a novel predictive marker for disease prognosis [97].

Table 2. Km values (mM) of mammalian MCT isoforms for a range of monocarboxylates, h) human; m) mouse; r) rat; *) tumor cells; n.d.) not determined. Adapted from [77].

Monocarboxylates	MCT1	MCT4
L-Lactate	2.2(r)–4.5(m*)	28.0(h)–34.0(r)
D-Lactate	51.0(r)	519.0(h)
Pyruvate	0.6(r)–1.0(r)	153.0(h)
L-β-hydroxybutyrate	8.1(r)–11.4(m*)	824.0(h)
D-β-hydroxybutyrate	8.1(r)–10.1(m*)	130.0(h)
Butyrate	9.1(h*)	n.d.
Acetoacetate	5.5(r)	n.d.
Propionate	1.5(r)	n.d.
Acetate	3.7(m*)	n.d.

1.3.2.3. MCT1 and MCT4 Accessory Protein: CD147

MCT1 and MCT4 transporters require a right association with transmembrane glycoproteins for proper folding, trafficking and anchoring to specific localization in the cell membrane [99,100]. In this context, CD147, also known as EMMPRIN, OX-47, basigin and HT7, appears as central regulator of MCTs expression [56,101].

CD147 is encoded by the *BSG* gene located on chromosome 19 at p13.3 and is a single-chain transmembrane protein and a member of the immunoglobulin superfamily. The predicted molecular mass of CD147 is dependent of low-glycosylated (LG) or high-glycosylated (HG) glycoforms, representing ~32 kDa and ~45–65 kDa, respectively [102-105]. It appears in many cell types, including tumor cells, being expressed and functional during development processes, nutrient transport

and inflammation, among others functions with a critical role in tumor progression [72,105-107]. As ancillary protein, it is associated to both MCT1 and MCT4 for correct localization in cell membrane, as well as in expression and activity regulation [101,108].

1.3.2.4. Inhibitors

Several non-physiological agents are capable of inhibit MCTs activity and can fall into the following categories [56]: substituted aromatic monocarboxylates as α -cyano-4-hydroxycinnamate (CHC); inhibitors of anion transport as 4,4'-diisothiocyanostilbene-2,2'-disulphonate (DIDS); bioflavonoids such as phlorentin and quercetin; irreversible inhibitors like p-chloromercuribenzenesulphonate (pCMBS) and amino reagents [56,57]. Some these compounds compete with MCTs substrates (CHC and DIDS) and others can have as target not MCT directly, but the ancillary protein CD147, as pCMBS [57,102]. Although these agents inhibit the MCT1, there is no evidence of their specificity. In others words, the same inhibitor can have as target others transporters. The CHC has been demonstrated to inhibit MCTs, inducing a decrease in cell proliferation, migration and invasion, increasing cell death [109-112]. However, it also acts on the anion exchanger AE1 [57,113].

To overcome this problem about inhibitors non-specificity, AstraZeneca developed a new class of specific and high-affinity inhibitors of MCT1 [114,115]. ARC155858 is a specific inhibitor to MCT1 tested in rat erythrocytes, *Xenopus* oocytes and human breast cancer cell lines [115,116], but even though it binds with higher affinity to MCT1, this inhibitor also acts on the MCT2 isoform [116]. Posteriorly, it has been developed other more powerful MCT1 inhibitor, AZD3965. This compound has shown anticancer effects in a variety of cancer cell lines [115,117], as well as in treatment of tumors *in vivo*, being in phase I/II clinical trials in the UK for patients with prostate cancer and diffuse large-cell B lymphoma [110,115]. On the other hand, there are evidences that MCT1 inhibition combined with MCT4 depletion has been more effective for some aggressive cancers treatment [118-121]. However, there is no available a specific inhibitor for MCT4 to date [118].

Lonidamine (LDN) is an anti-tumor drug that inhibits respiration, as well as aerobic and anaerobic glycolysis in Ehrlich ascites [122]. However, recent studies have been demonstrated that LDN also

inhibits lactate efflux from cancer cells, through inhibition of MCT1, MCT2 and MCT4, as well as pyruvate uptake into the mitochondria, inhibiting mitochondrial pyruvate carrier (MPC) [123,124].

1.3.2.5. MCT1 and 4: role in cancer and potential target for therapy

Highly glycolytic cells utilize MCTs to export lactate, as well as protons, having MCT1 and MCT4 an important dual role, in intracellular pH homeostasis and in the transport of this metabolite, assuring the continuation of glycolysis in the cell. There is evidence for the upregulation of these MCTs in several cancers such as colorectal, lung, glioblastoma, cervical and breast, being involved in lactate transport across the plasma membrane [77,125-131]. However, MCT1/MCT4 presented a differential distribution even within the same tumor, suggesting distinct roles in lactate transport [85]. MCT1 can be involved in both efflux and uptake of lactate, depending of lactate concentration gradient [70]. Sonveaux et al. shown that MCT1 is more expressed on oxygenated tumor cells in different tumors, being crucial to lactate uptake, which serves as fuel for oxidative metabolism in these cells [40]. In contrast, MCT4 is involved on lactate efflux and is a direct target of HIF-1 α , being upregulated in hypoxic tumor cells that present a high glycolytic metabolism and poor vascularization [132,133]. These differences agree with the notion of metabolic cooperation, as already described above (**Figure 5**). However, others researches have demonstrated that MCT1 expression can be present in tumor cells under hypoxia and larger distance from the vessels. This suggests that MCT1 can play a role in lactate transport also in hypoxic areas [134], assisting MCT4, depending of substrate concentration and pH [56]. Therefore, the cooperation between MCT1 and MCT4 to regulate lactate and acidosis levels is essential to tumor cells adaptation and, in this way, they contribute for tumor progression, as well as to resistance to chemotherapy. In the other hand, this symbiosis has suggested MCTs inhibition as a new potential targets for cancer therapy (**Figure 9**) [109,110].

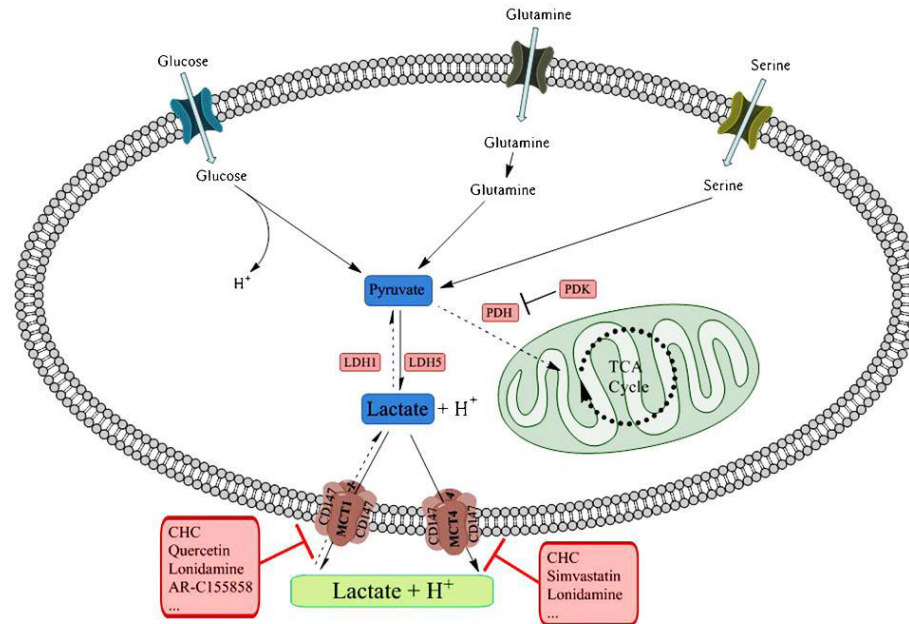


Figure 9. MCT1 and MCT4 as potential anticancer targets. The metabolic pathways results in lactate production and its transport across the plasma membrane (continuous arrows). Discontinuous lines indicate lactate uptake and flow inside oxidative cancer cells. The lactate membranes transporters are viewed as target for the inhibition strategies. CHC: α -cyano-4-hydroxycinnamic acid; LDH: lactate dehydrogenase; MCT: monocarboxylate transporter; PDH: pyruvate dehydrogenase; PDK1: pyruvate dehydrogenase kinase 1. Adapted from [77].

1.4. Tumor metabolism as a target for anticancer therapy

Altered metabolism is a biochemical pattern of cancer cells characterized by a favored dependence on glycolysis for energy production, even though it is less efficient than oxidative phosphorylation. As already mentioned, cancer cells overtake this disadvantage adjusting the activity of a set of intermediate molecules and signaling pathways that in a direct or indirect way have a central role in the upregulation of the glycolysis pathway, being an attractive target for therapeutic intervention, as shown **Figure 10** [135].

Metabolic inhibitors can have membrane transporters as target. One example are the MCTs inhibitors, already referred. Other membrane transporters involved in the metabolic phenotype of cancer cells belong to the GLUT family, responsible by glucose uptake. Some GLUTs isoforms are overexpressed

in almost all cancer types, contributing to increased glucose consumption, which in turn facilitates a higher glycolysis rate [136]. Phloretin, WZB117 and Fasentin are examples of GLUTs inhibitors with anticancer effect in different cancer types as it has been shown *in vitro* and *in vivo* assays [137-139]. Besides membrane transporters, different intracellular proteins can be also targets of metabolic inhibitors. The enzymes HKII and phosphofructo kinase (PFK) are examples of such targets. HKII is responsible to convert glucose in glucose-6-phosphate, the first step both of glycolysis and in some cancer cells is associated to mitochondrial membrane through the voltage dependent anion channel (VDAC) having privileged access to the ATP generated there [140]. LDN was firstly referred as being a MCTs inhibitor, but is also an inhibitor of HKII, and its pharmacokinetic studies have been tested in phase II and III clinical trials [141]. 2-deoxyglucose (2-DG) is other inhibitor of HKII, being responsible to convert 2-DG into to deoxyglucose-6-phosphate, a molecule that cannot be further metabolized, blocking glycolysis pathway [142]. Some researchers have shown that 2-DG induced Akt phosphorylation, which is an intermediate of pro-survival pathways and is associated to chemo- and radiotherapy resistance [142-145]. However, 2-DG in combination with others anticancer agents enhances chemotherapy/radiotherapy in cell lines and animal models, being in phase I/II of clinical trials [144,146-147]. Glyceraldehyde 3-phosphate dehydrogenase (GAPDH) is other target to antitumor drugs as is crucial to produce NADH, which is involved in the regulation of intracellular ROS levels, besides being an intermediate of the glycolytic pathway. Consequently, the inhibition of GAPDH lead to cell death by blocking the production of energy and promoting oxidative stress [135]. 3BP is a promising glycolytic inhibitor, which will be described later in this topic, which has as target both HK II and GAPDH [148,149]. LDH, which has been associated to poor prognosis in cancer diseases, converts pyruvate into lactate, the last step of glycolysis. Silencing LDH by siRNA or its inhibition by a small-molecule inhibitor, FX11, induces tumor cell death by depleting intracellular ATP levels [150].

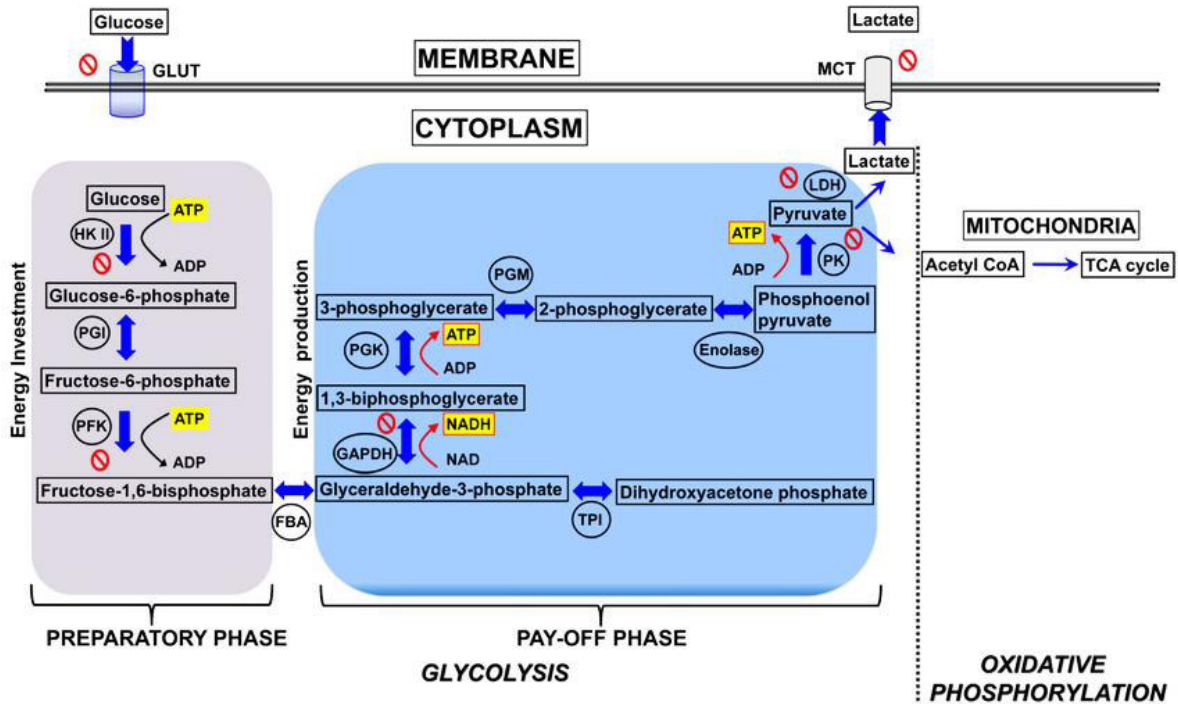


Figure 10. Glycolysis as potential target for anticancer therapy. In diagram are demonstrated two phases of glucose metabolism (glycolysis and oxidative phosphorylation) and the molecular targets used as potential therapeutic drug strategies. The enzymes involved in reactions are abbreviated, black arrows show energy consumption, the red arrows indicate the energy release, and the red encircled represented the block symbol and shows the targets for drug development [135].

These inhibitors have specific targets from glucose uptake, passing through enzymes responsible for converting it into lactate, or it is export from the cell to extracellular space. Therefore, the block of any of these pathway steps, will lead to energy and biosynthetic precursors depletion, as well as oxidative stress, inducing cell death. On the other hand, although these inhibitors have a promising antitumor potential, the cytotoxicity for healthy cells remain a challenge for the reason that these targets end up being ubiquitously expressed in all cells. In this way, the concept for anti-cancer agent combination, selective targeting and delivery appear as new challenges for therapeutic efficacy.

1.4.1. 3-Bromopyruvate

3BP is a small alkylating molecule, pyruvate derivative and analog of lactate. It is capable of reacting with thiol groups (-SH) and hydroxyl groups (-OH) of proteins leading to their loss of functionality. 3BP has shown great ability to inhibit tumor glycolysis by the depletion of intracellular ATP [151], leading to different mechanisms of activation of cell death [152-156]. Additionally, 3BP acts as a cytotoxic agent in several tumor lines, including colorectal, pancreas, breast cancer and glioblastoma, among others [152-158].

3BP treatment causes energy depletion by inhibition of glycolytic enzymes as HK II, responsible by catalyzing the first irreversible step of glycolysis. HKII is frequently over expressed in solid tumors and its inhibition could disrupt energy balance, leading to cell death [148,159]. GAPDH is other glycolytic enzyme targeted by 3BP. GAPDH is a multifunctional enzyme involved in multiple biosynthetic pathways, and in this way, its inhibition can lead to cell death by energy and biosynthetic precursors depletion [160-162]. 3BP is also capable of increasing intracellular ROS, leading to mitochondrial dysregulation. These alterations in cellular redox induce cell apoptosis by cytochrome C release, after mitochondrial membrane potential loss [163-165]. In this way, the redox signaling in cancer cells can be targeted by 3BP to anticancer therapy [166]. **Figure 11** represents the possible mechanism of 3BP action. Different reports evidenced that 3BP is transported into the cell by MCTs [167]. Once into the tumor cells, the 3BP depletes cell ATP production by the inhibition of both glycolysis and oxidative phosphorylation [167]. In fact, some researches demonstrated that tumors reduced in size after treatment with 3BP. In rat model, hepatocellular carcinoma cells were xenografted into two different locations of animals. After tumor development, the animals were treated with 3BP, which eradicated the advanced tumor, demonstrating the potential anticancer effect of 3BP [167-169]. In translational study, a patient with fibrolamellar hepatocellular carcinoma (FLC) was treated with a specially formulated 3BP and, despite ending up dying, he was able to survive a much longer period than expected, and with better quality of life [170].

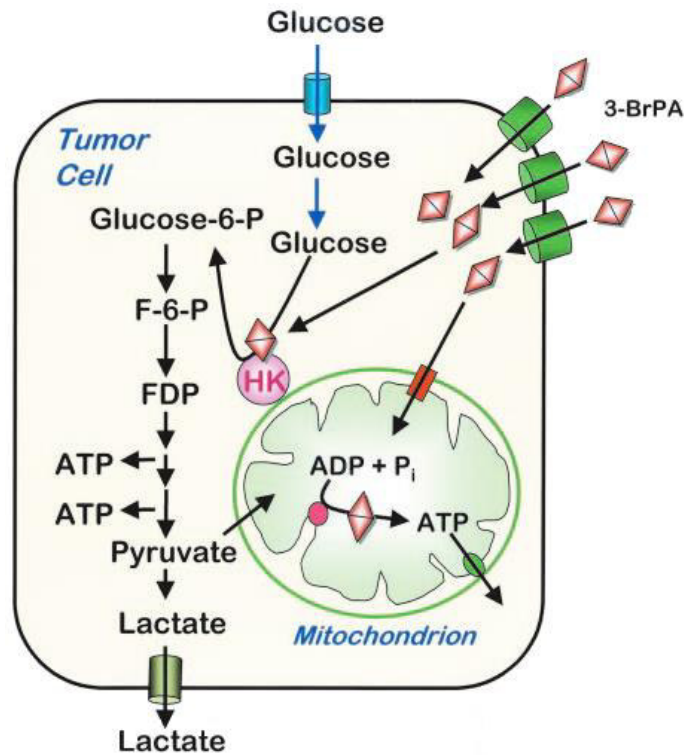


Figure 11. Mechanism of 3BP action. The 3BP was transported inside to cancer cell and inhibited ATP production by glycolysis, inhibiting mitochondrial bound hexokinase and oxidative phosphorylation depleting energy supply. Adapted from [167].

1.5. Colorectal Cancer

Colorectal cancer (CRC), also known as bowel cancer, is a neoplasia that develops from colon or rectum, being one of the most common malignancies in the Western World. Globally, there are 14.1 million new cancer cases, wherein 1.36 million are colorectal cancers that lead to more than half a million death annually, being the third most frequent cancer in men and the second most frequent in women, after lung and prostate, and breast cancer, respectively [171-174]. Both incidence and mortality rates differ around the world, in which the developed countries present high CRC incidence rates, due to western diet and lifestyle, while countries that have more limited resources present high CRC mortality rates [172].

The risk factors for CRC are obesity, sedentary lifestyle, heavy alcohol consumption, smoking, high consumption of red or processed meat and very low intake of fruit and vegetables. Besides these

factors, old age also increases the risk of colorectal cancer, being recommended a CRC screening for individuals over 50 years. Even though, some studies have demonstrated an increased incidence of CRC in the 40 – 44 years group, suggesting the screening beginning at age 40 [175-178]. Individuals with a personal history of adenoma, colon cancer, and inflammatory bowel disease, familiar history of CRC or polyps and inherited syndromes are high-risk groups, whose must be actively screened and, in cases of inherited syndromes referred for genetic counselling [179,180]. However, the most frequent type of CRC is sporadic or non-hereditary from somatic mutations and linked mostly to environmental causes [174].

Most CRC start as a polyp that consists a cell growth in the inner lining of the bowel and grows toward the center. Most polyps are not malignant and only the called adenomas can become cancer. The adenocarcinoma is the most frequent and, since the polyps/adenomas formation to a malignant/metastasizing phenotype, a gradual progression occurs, based on the acquisition of mutations set over time that result on the deregulated cell proliferation, unrepair of DNA damage, cell “immortality”, angiogenesis and invasion (**Figure 12**) [181-186]. Chromosomal and microsatellite instability contribute to mutations in the tumor suppressor genes such as APC and p53 and in oncogenes such as RAS protein family, as well as in inactivation of genes responsible for DNA nucleotide mismatch repair [173,187].

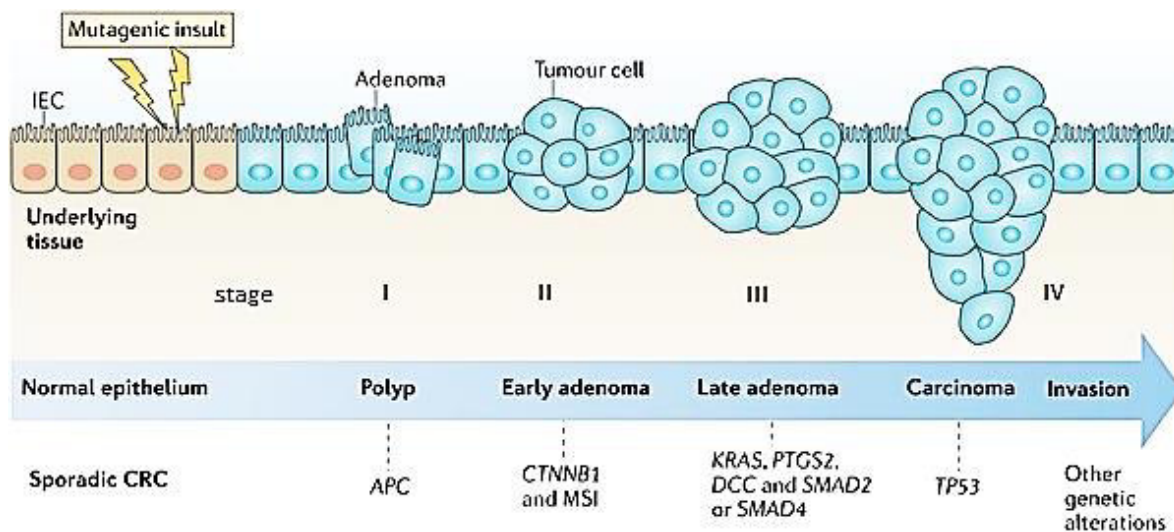


Figure 12. Colorectal carcinogenesis from normal epithelium to CRC. Genetic alterations involved in CRC development, microsatellite instability (MSI), activation of the oncogene KRAS, activation of cyclooxygenase 2

(COX2; encoded by PTGS2), and mutation and loss of heterozygosity (LOH) of TP53, adenomatous polyposis coli (APC), deleted in colon cancer (DCC) and SMAD4. Adapted from [186].

Both the early identification of adenomas and premalignant lesions are important for survival patient, as well as in the selection of the therapeutic approach. It is grouped between stages I to IV according with to the American Joint Cancer Committee (AJCC)/ Union for International Cancer Control (UICC) TNM classification. This provides a detailed description of the tumor size and if it has spread to lymph nodes or to another part of your body. Once the colon cancer is diagnosed, the surgery can be realized to remove the pre-malignant lesions or polyps and depending of the type and stage of tumor, the chemotherapy may be administered as adjuvant [188,189]. The chemotherapeutic options for this type of cancer may be mainly divided in two groups. The cytotoxic classical chemotherapy and targeted therapy (5-fluorouracil, Capecitabine, Irinotecan and Oxaliplatin), acting on cells that divide rapidly or interfering specifically in tumor development and growth, respectively. The other group includes monoclonal antibodies against the epidermal growth factor receptor (Cetuximab and Panitumumab), inhibitors of the vascular endothelial growth factor (Bevacizumab and Aflibercept) and small-molecule inhibitor of intracellular kinases signaling cascade (Regorafenib) [190]. 5-fluorouracil (5-FU) is the classical chemotherapeutic agent most used in conventional therapy of CRC, acting in thymidylate synthase (TS), an enzyme responsible to DNA synthesis [191]. However, after long-term treatment, cancer cells become more resistant, being necessary new therapeutic strategies [192,193].

1.5.1. Relevance of short-chain fatty acid in colorectal cancer

Recently, there are researches that reveal that extrinsic factors as diet, age, stress and medication can change composition of intestinal microbiota can contribute to CRC carcinogenesis [79,194]. Intestinal microbes ferment the carbohydrates and proteins that are not absorbed in gut during digestion, producing short-chain fatty acids (SCFA). The SCFAs, such as butyrate, have a central role in colon homeostasis, as well as a protective effect [194]. Besides inhibit pathogenic microorganisms and increase nutrients absorption by lower luminal pH, they serve as a source of energy for colonocytes and at the same time contributes to colon motility, inflammation reduction and apoptosis increase,

inhibiting tumor cell progression [106,194-196]. As already referred, the butyrate has a regulator role over transporter proteins expression, the MCTs, of which is its substrate [83,84]. However, as tumor colonocytes present mainly glycolytic phenotype, the butyrate accumulates into the cells, increasing its capacity as histone deacetylases (HDAC) inhibitor to inhibit cell proliferation and stimulate apoptosis [197,198]. In this way, it is important to understand the role of SCFAs in gut, which could be a new strategy to prevention and treatment of CRC [199,200].

1.6. Rationale and aim

MCTs play a vital role in the glycolytic metabolism, exporting lactate by a proton symport mechanism. Some evidence points MCTs as potential targets for anticancer therapy. MCTs activity inhibition leads to disruption in glycolytic cell metabolism, induces cell death and decreases cell invasion, revealing the importance of MCT activity in intracellular pH homeostasis and tumor aggressiveness [72]. Furthermore, MCTs overexpression in cancer cells can be used to mediate the uptake of anticancer compounds that are MCTs substrates.

The 3BP is an analogous of lactate with anti-tumor properties. Its uptake occurs via MCTs, being a glycolytic inhibitor with targets already identified, including HK II, succinate dehydrogenase and GAPDH. However, its mechanism of action is not well understood. Different studies have demonstrated that environmental conditions like pHe value or the presence of short-chain carboxylic acids influence 3BP toxicity, probably through the alteration of MCTs activity [84,114].

The work plan presented aims to characterize 3BP effect in different CRC cancer cell lines and to clarify the mechanism of regulation of MCT1 and MCT4 expression in different conditions, correlating 3BP toxic effect to the expression of MCTs. These parameters were evaluated at different conditions, including different pHe, glucose starvation or hypoxia. The role of monocarboxylic acids like butyrate or lactate in the regulation of MCTs expression and in the sensitivity of cells to 3BP was also assessed.

Chapter 2

Material and Methods

2.1. Cell Lines and Cell Culture

In the present study, three human colorectal adenocarcinoma (CRC) cell lines were used, namely HCT-15, HT-29 and Caco-2, which were obtained from American Type Culture Collection (ATCC). All cell lines were maintained in Dulbecco's Modified Eagle's Medium (DMEM, Lonza), supplemented with 10% Fetal Bovine Serum (FBS; Gibco™, Invitrogen Corporation) and 1 % penicillin/streptomycin solution (Sigma- Aldrich). The cells were grown in a humidified incubator at 37 °C and 5 % CO₂ (Water Jacketed CO₂ Incubators, Shel Lab). When cells reached approximately 80 % confluence, it has been made a subculture (passage) to ensure that the cells were healthy and in the exponential phase of growth. The subculture was made twice a week with a dilution ratio of 1:8, 1:6 and 1:5 for HCT-15, HT-29 and Caco-2, respectively.

To perform cellular assays, sub-confluent cells were gently washed with phosphate-buffer saline (PBS) and then detached with trypsin (Gibco™, Invitrogen Corporation) at 37 °C for 2 to 4 min, approximately. Trypsin was inactivated with DMEM 10 % FBS and the cells were re-suspended in this fresh medium. 20 µl of this cell suspension were collected for cell counting, in a polypropylene tube containing 20 µl of Trypan Blue (Sigma- Aldrich), being the cells counted in a *Neubauer* chamber, and the cell density calculated. The cells were then diluted in fresh medium, in the proper density for the assay.

2.2. Preparation of Monocarboxylic Acids

2.2.1. 3-Bromopyruvate

3-Bromopyruvate (3BP) (Sigma-Aldrich) was prepared by freshly dissolving into cold PBS, being after that filter-sterilized (0.22 µm). Working solutions were prepared from stock solutions (20 or 2 mM), making the appropriate dilutions in DMEM 10 % FBS. The volume of 3BP plus PBS was constant and corresponded to 10 % of the total volume, being the 3BP used in the appropriate volume to the desired concentration and PBS used to make up the total volume.

2.2.2. Butyrate, acetate and lactate

The carboxylic acids were prepared in PBS to a final concentration of 1 M at pH 7.2. These solutions were sterilized by autoclave and stored for a maximum of one month at 4 °C. To perform the assay, working solutions were freshly prepared from the stock (1 M), using the appropriate volume to dilute in DMEM. The volume of the carboxylic acid plus PBS was constant and corresponded to 10 % of the total volume, being the carboxylic acid used in the appropriate volume to the desired concentration and PBS used to make up the total volume. To ensure that pH medium was not modified with the acid addition, the pH of the culture medium was measured after this addition. Butyrate and lactate were obtained from Sigma-Aldrich and acetate was obtained from Merck.

2.3. Determination of Cell Viability by the Sulforhodamine B assay

Cell viability was evaluated by the sulforhodamine B (SRB) assay, which is a method that estimates the total biomass of the cell culture, based in the staining of cellular proteins with this dye. After cell treatment in the appropriate conditions, 50 % trichloroacetic acid (TCA) (25 µL) was added to fix the cells, being the cells incubated during 1 h at 4 °C. Then, the plates were rinsed 5 times with distilled water to remove TCA and were air-dried. Cells were then stained with 0.4 % sulforhodamine B solution (50 µl, TOX-6, Sigma-Aldrich) for 30 min and, after that, plates were rinsed 5 times with 1 % acetic acid, until the unincorporated dye was removed. After the plates were dried, the incorporated sulforhodamine was solubilized in 10 mM Tris Base solution (100 µl, Sigma-Aldrich). Spectrophotometric measurement was performed at 540 nm (Tecan infiniteM200 plate reader).

The percentage of cell viability was determined by comparing the average of the optical density (OD) of the cell suspensions, in triplicate, of treated versus untreated cells. Untreated cells corresponded to 100 % viable cells. The IC₅₀ values were estimated from at least three independent experiments using GraphPad Prism 5 Software, applying a sigmoidal dose-response non-linear regression, after logarithmic transformation.

2.4. Determination of the appropriate cell density

The appropriate cell density determination is important to ensure that cells are in exponential growth phase during the whole experience. For each cell line, cells were plated in 96-well plates using different densities of the cell suspension (0 to 4.0×10^5 viable cells/mL) and incubated overnight to promote cell adhesion. After that, the medium was replaced by fresh medium and the cells were incubated during the corresponding time of the experiments to be performed. The cell viability was evaluated by SRB assay and the results are the means of triplicates of at least three independent experiments.

2.5. Determination of 3BP IC_{50}

To determine the response of CRC cell lines (HCT-15, Caco-2 and HT-29) to 3BP, the IC_{50} value (drug concentration that corresponds to 50 % of cell viability/growth inhibition) was determined either in basal conditions or in the different conditions to assay: hypoxia, starvation, different extracellular pH (pHe) and pre-treatment with monocarboxylic acids.

Cells were plated into 96-well plates, at a density of 7.5×10^3 cells per well (100 μ L) in the case of the HCT-15 cell line and 10×10^3 cells per well (100 μ L) in Caco-2 and HT-29 cell lines. To determine 3BP effect in cell viability, cells were left to adhere overnight in DMEM 10 % FBS, and after this period, the medium was removed and the cells were incubated in DMEM 10 % FBS containing 3BP, during 16 h at 37 °C. The range of 3BP concentrations used was between 10-300 μ M, 20-1000 μ M and 50-500 μ M for HCT-15, Caco-2 and HT-29 cell lines, respectively. Untreated cells were used as control.

HCT-15 cell line was selected to determine the effect of the conditions above mentioned in 3BP cytotoxicity. The times of incubation in the different conditions to be assayed were the following: 16 h to assess the effect of pHe, 24 h in hypoxia, starvation and in the pre-treatment with butyrate and 48 h in the pre-treatment with lactate and acetate. After the corresponding time, cells were treated with 3BP during 16 h, as referred above. The respective controls were made incubating the cells in basal conditions during the same period of time, and treating after that time with 3BP for 16 h. Cell viability was then determined by the SRB assay and the IC_{50} calculated. The following sections detail the experimental protocols used in the assayed conditions.

2.5.1. Extracellular pH

HCT-15 cell line was exposed to different extracellular pH (pHe) simultaneously with the 3BP treatment. DMEM with L-glutamine and without sodium bicarbonate (NaHCO_3) (Biochrom) was supplemented with 10 % FBS and 1 % penicillin/streptomycin solution. To keep the desired pH, DMEM was buffered with 4-(2-hydroxyethyl)-1-piperazineethanesulfonic acid (HEPES, Sigma-Aldrich), for a final concentration of 25 mM in the medium, and the pH was adjusted at the desired value. Cells were treated with 3BP in the range of appropriate concentrations, in medium with pH adjusted to 7.4 (physiological pH) or 6.6 (usually present in the tumor microenvironment), during 16 h at 37 °C.

2.5.2. Hypoxia

In *in vitro* studies, the hypoxia induction can be performed using hypoxic chambers or chemical compounds, which leads to the “chemically induced hypoxia”. In the present study, hypoxia induction was performed using cobalt chloride (CoCl_2 , Panreac) which works as oxygen sensor, inhibiting prolyl hydroxylase domain (PHD) and inducing HIF-1 α stabilization, thus avoiding the HIF-1 α degradation in the presence of oxygen [201,202].

CoCl_2 was dissolved into dimethylsulfoxide (DMSO, Sigma-Aldrich) to a 160mM stock solution, filter-sterilized (0.22 μm) in aseptic, from which intermediate concentrations were prepared into DMSO (2mM-100mM) and stored at -20 °C until used. Working solutions were freshly prepared in culture medium without FBS containing 1 % penicillin/streptomycin solution and of DMSO in a concentration did not exceed 1 %.

To determinate the hypoxia effect in cell viability, the HCT-15 cells were first treated with CoCl_2 (0, 20, 50, 750, 100, 200, 500 and 1,000 μM) and the cells were then maintained under standard culture conditions for 24 h [203,204]. Cell viability was evaluated by the SRB assay, as described above. The concentration of 200 μM of CoCl_2 was chosen to assess the effect of hypoxia in 3BP cytotoxicity, because at higher concentrations, there was decrease in cell viability. For that, HCT-15 cells were seeded in 96-well plates at the appropriate cell density and incubated overnight. After cell adhesion, cells were incubated with 200 μM CoCl_2 for 24 h. After this, the medium was removed, and after

washing, cells were treated with 3BP in the appropriate range of concentrations, during 16 h at 37 °C. Control conditions were performed with 1 % DMSO in DMEM without FBS and without CoCl₂.

2.5.3. Glucose Starvation

HCT-15 cells were seeded in 96-well plates at the appropriate cell density. After overnight adhesion, the medium was replaced by DMEM medium without glucose (Gibco™), supplemented with 10 % FBS and 1 % penicillin/streptomycin solution. Cells were incubated in this glucose-free medium 24 h, and after this time the medium was replaced by medium containing 3BP in the appropriate range of concentrations and cells were incubated for 16 h at 37 °C. Untreated cells were used as control.

2.5.4. Pre-treatment with monocarboxylic acids

For the pre-treatment with monocarboxylic acids, cells were incubated 24 or 48 h in DMEM 10 % FBS containing the carboxylic acids (butyrate, lactate or acetate), in a range of concentrations between 10-70 mM, before the treatment with 3BP. Briefly, HCT-15 cells were seeded in 96-well plates at the appropriate cell density and incubated overnight. After cell adhesion, cells were exposed to the different carboxylic acids in the appropriate concentrations, during 24 or 48 h at 37 °C. After the period of incubation, the medium containing the acids was removed, cells were washed twice with PBS and treated with IC₅₀ of 3BP. As control, the cells were incubated with carboxylic acids during the same time, followed by 16 h of incubation in DMEM medium without 3BP or the carboxylic acid. Cell viability was evaluated by the SRB assay, as described above, considering 100 % viability the cells not exposed to any treatment.

To determine the influence the different carboxylic acids in 3BP IC₅₀, cells were pre-treated to a fixed concentration of the acid (10 mM for the three acids or 40, 50 and 20 mM of butyrate, lactate and acetate, respectively) during 24 or 48 h, followed by incubation in medium containing 3BP in the same range of concentrations previously used in the determination of 3BP IC₅₀ value. As control, cells were incubated during the same period of time in medium without monocarboxylic acids, replacing the respective volume by PBS (**Figure 13**).

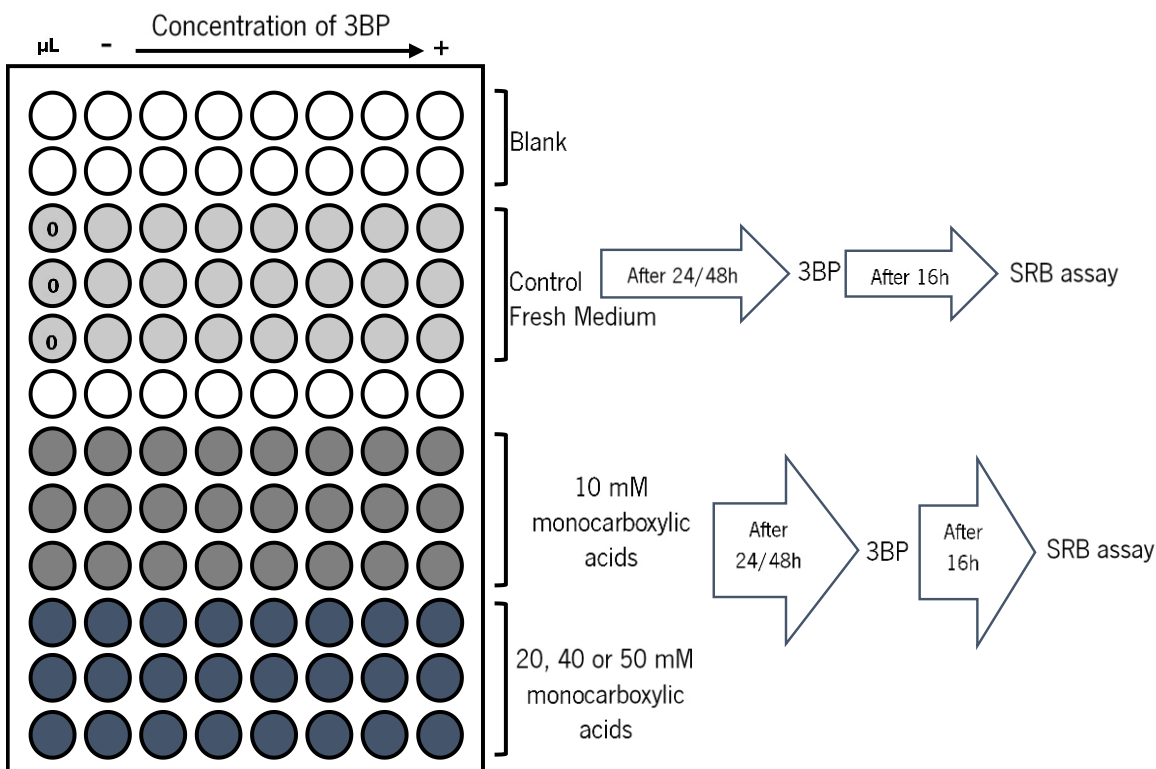


Figure 13. Representative scheme of the 96-well plate for the assays described above showing the pre-treatment with the monocarboxylic acids followed by 3BP treatment in the appropriate range of concentrations. Cells were incubated 24 or 48 h with 10 mM for the three acids or 40, 50 and 20 mM of butyrate, lactate and acetate, respectively, followed by the treatment with 3BP for 16 h at 37 °C. The cells not exposed to any treatment (0) correspond to 100 % of viable cells and blank correspond to wells with only culture medium, without cells.

2.6. Metabolic profile determination

The effect of 3BP on cell metabolism was assessed by analyzing extracellular glucose and lactate levels in the medium of cells treated with IC_{50} and $\frac{1}{2} IC_{50}$ concentrations of 3BP. The effect of hypoxia, different pH_e and glucose starvation on cell metabolism was also evaluated, treating the cells as mentioned below and measuring glucose and lactate levels in the medium.

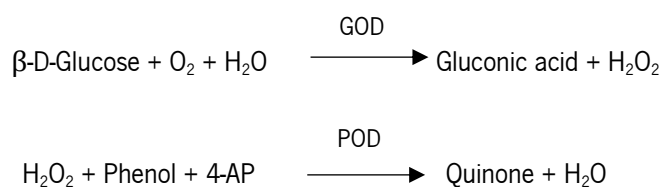
Cells of HCT-15, HT-29 and Caco-2 cell lines were seeded in 96-well plates at the appropriate cell density and incubated overnight. After cell adhesion, cells were incubated with the respective IC_{50} or $\frac{1}{2} IC_{50}$ of 3BP during 16 h at 37 °C.

For hypoxia, different pHe and starvation conditions, HCT-15 cells were seeded in 96-well plates at the appropriate cell density and incubated overnight to adhere. After that, cells were incubated with 200 μM CoCl_2 or glucose-free medium for the hypoxia or starvation condition, respectively, and incubated for 24 h at 37 °C.

Cell culture medium (150 μl) was collected after the respective treatment and stored at -20 °C until glucose and lactate quantification. The metabolites were measured by spectrophotometry at 505 nm, according to manufacturer's instructions and normalized for the total biomass. The total protein content, expressed as total biomass, was assessed using the SRB assay, as described above. The results are representative of at least, three independent experiments, each one in triplicate. Extracellular glucose and lactate levels were expressed as μg of metabolite/total biomass.

2.6.1. Extracellular Glucose Quantification

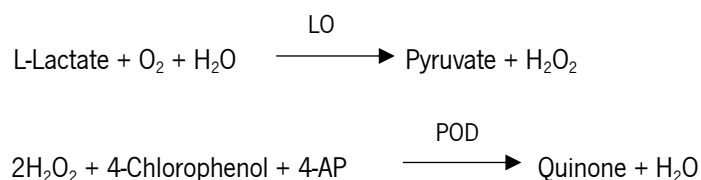
Extracellular glucose was assessed by an enzymatic colorimetric kit (Spinreact) based on the enzymatic oxidation of glucose to gluconic acid by glucose oxidase (GOD). A chromogenic oxygen acceptor, phenol, 4 – aminophenazone (4-AP) in the presence of peroxidase (POD), detects the formed hydrogen peroxide (H_2O_2) of the glucose oxidation. The intensity of the color formed is proportional to the glucose concentration in the sample:



200 μl of working solution was mixed with 2 μl of each sample (previously diluted in the ratio of 1:10). Blank was performing by adding 200 μl of working solution only. The mixture was gently mixed and incubated for 20 min at room temperature. The absorbance was read at 505 nm in a microplate reader (Tecan infiniteM200).

2.6.2. Extracellular Lactate Quantification

The extracellular lactate levels were assessed by using a colorimetric kit (Spinreact), where lactate is oxidized by lactate oxidase (LO) to pyruvate and H_2O_2 . Then, H_2O_2 is metabolized by POD and converted to quinone. The intensity of the red color is directly proportional to the lactate concentration in the sample:



200 μl of working solution was mixed with 2 μl of each sample. Blank contained 200 μl of working solution alone. The mixture was homogenized and incubated for 10 min at room temperature. The absorbance was read at 505 nm in a microplate reader (Tecan infiniteM200).

2.7. Wound-healing assay

The cell migration of the cancer cells in the different conditions assayed was assessed by the wound-healing assay, which mimics cell migration during wound healing in *in vivo*. This method has been employed by researchers for years to estimate cell migration rate of different cells and culture conditions in *in vitro*. The principle is to create a cell-free area (wound) in a cell confluent monolayer with a pipette tip. The "healing" of the "wound" is achieved by cell migration. After creating the wound, the images were then captured at regular intervals for 24 h period [205].

The cells were plated in 6-well plates at a density of 7.5×10^4 cells/well (1500 μl) for HCT-15 and 10×10^4 cells/well (1500 μl) for HT-29 and Caco-2, and allowed to attach overnight at 37 °C in a 5 % CO_2 humidified atmosphere (Water Jacketed CO_2 Incubators, Shel Lab), until reaching total confluence. Then, two wounds were created in the confluent cells by manual scratching with a pipette tip. Cells were gently washed once with PBS and treated with respective IC_{50} and $\frac{1}{2} IC_{50}$ of 3BP, glucose-free medium or $CoCl_2$. The cell-free areas were photographed in specific sites (two sites for each wound)

at 100X magnification using a Nikon Eclipse TE 2000-U inverted microscope equipped with digital camera system at 0, 12 and 24 h.

The migration distance (5 measures by wound) was calculated with QWound software (version 1.01) and percentage of cell migration relative to time zero of control (untreated cells) was evaluated using GraphPad Prism 5 Software. At least three independent experiments were conducted.

2.8. MCT1 and MCT4 expression assessment

Quantitative real-time polymerase chain reaction (qRT-PCR) and Western-blot assays were performed to measure the expression of MCT1 and MCT4 proteins in the different conditions assayed (basal conditions, 3BP treatment, monocarboxylic acids treatment, hypoxia, starvation and exposure to different pH), being the cell localization of these proteins determined by immunofluorescence assays.

2.8.1. RNA isolation and analysis

The cell lines were seeded in 6-well plates at the appropriate cell density, and maintained under optimal growth conditions until they reached about 70 % - 80 % confluence. Then, 500 μ l of NZYol from Nzytech was added for isolate the total RNA. After promoting cell lysis by NZYol, the suspensions were transferred to RNase-free tube and incubated at room temperature (RT) during 5 min to allow the complete dissociation of nucleoproteins. 200 μ l of chloroform were added to the lysates to allow the protein precipitation and the lysates were incubated further 5 min at RT and centrifuged at 14,000 rpm for 15 min at 4 °C. Upon centrifugation, the aqueous phase was collected into new RNase-free tubes and 500 μ l isopropanol were added. After carefully mixing and a 5 min-incubation at RT, the mixtures were centrifuged at 14,000 rpm for 10 min at 4 °C, being possible to observe a white pellet in this phase, corresponding to RNA. After discarding the supernatant, the pellets were washed with 500 μ l of 75 % v/v ethanol, vortexed and centrifuged at 7500 g for 5 min at 4 °C. The supernatant was discarded and the pellets were air-dried for about 5-10 min. Then, RNA was resuspended in 50 μ l of water with diethylpyrocarbonate (DEPC, Sigma-Aldrich) and stored at -20 °C (for periods shorter than one month) or -80 °C (for periods longer than one month). All the solutions utilized in this protocol were prepared in water with DEPC.

The concentration/purity and integrity/contamination with genomic DNA of the isolated RNA were evaluated using NanoDrop 2000 Spectrophotometer of the Thermo Scientific (OD260 and OD260/280nm ratio) and by electrophoresis (1.4 % (w/v) RNase-free agarose gel in Tris-acetate-EDTA (TAE)), respectively. The isolated RNA was used to measure *SLC16A1* and *SLC16A3* genes expression by qRT-PCR, which codify for MCT1 and MCT4 proteins, respectively.

2.8.2. Real-Time Quantitative Polymerase Chain Reaction

Primers Design

SLC16A3 primers sequences used in this work were previously described in the literature [206], being the *SLC16A1* and Actin designed in this work, and their specificity checked in the Primer-Blast program of NCBI (<https://www.ncbi.nlm.nih.gov/tools/primer-blast/>). Primers were designed on exon-intron junctions to amplify fragments of the target genes with sizes ranging from 80 to 200 bp. The forward and reverse primer sequences used in this work for qRT-PCR are presented in **Table 3**. The primers were purchased to STABvida, being reconstituted in nuclease-free water to a final concentration of 100 μ M. Before their use in qRT-PCR experiments, a PCR was done with the isolated RNA to assess the presence of contaminating genomic DNA amplification for each primer pair. Then, another PCR was run to check primer specificity and annealing temperatures. As control positive, plasmids containing *SLC16A1* and *SLC16A3* complementary DNA (cDNA) were used.

Table 3. Sequences of forward and reverse primers, corresponding to *SLC16A1*, *SLC16A3* and *actin* genes, used for amplification of the cDNAs and size estimated for the respective amplicon.

Gene	Forward Primer	Reverse Primer	Amplified Sequence Length
<i>SLC16A1</i> (MCT1)	5'-tctgtgtctatgctggattctt-3'	5'-ttgagccgacctaaaagtgg-3'	172
<i>SLC16A3</i> (MCT4)	5'-atcctgggcttcattgacat-3'	5'-atggagaagctgaagagga-3'	101
<i>ACTIN</i>	5'-aatctggcaccacaccttcta-3'	5'-atagcacagcctggatagcaa-3'	170

Complementary DNA synthesis

Before performing qRT-PCR, it was necessary to synthesize the cDNA from the isolated RNA through a reverse transcriptase-mediated reaction. cDNA was prepared using the NZY First-Strand cDNA Synthesis Kit according to manufacturer's instructions, being 1 µg of total RNA used as template. Each reaction was composed of 10 µl NZYRT 2x Master Mix, 2 µl NZYRT Enzyme Mix, a volume of RNA template equivalent to 1 µg RNA and DEPC-treated H₂O to a final volume of 20 µl. cDNA synthesis reaction was initiated by 10 min incubation at 25 °C, followed by 30 min at 50 °C and an inactivation step at 85 °C for 5 min and then put shortly on ice. Finally, 1 µL NZY RNase H (E. coli) was added, and the mixture was incubated at 37 °C for 20 min and heated at 85 °C for 5 min for the enzyme inactivation. The resulting cDNA samples were stored at -20 °C until use.

Quantitative Real-Time Polymerase Chain Reaction assay

Quantitative Real-time-PCR (qRT-PCR) is a technique for quantify gene expression levels, which use a fluorophore like SYBRgreen (iQ™ SYBR® Green Supermix kit, Bio-Rad Laboratories) that binds to DNA double-stranded emitting fluorescence. For each qRT-PCR run, a mix contained 0.2 µl of each primer at 10 µM, 10 µl of iQ SYBR Green Supermix, 4 µl cDNA and 5.6 µl of ultrapure H₂O in a final volume of 20 µl. Three different controls were performed in the assays: no reverse transcriptase control (NRT) that use isolated RNA as template to detect contamination by genomic DNA; non-template control (NTC) to evaluate reagent contaminations (ultrapure H₂O was place instead of cDNA); loading control with the housekeeping gene actin, which is expressed constitutively.

Primers efficiency were also tested, using appropriate dilutions of the cDNA. Serial dilutions of the cDNA (10^{-1} , 10^{-10} and 10^{-100}) were done in RNase-free water for standard curve, plotting threshold cycle (Ct) (cycle where the threshold detection of the fluorescence signal was reached) against the corresponding logarithm of the template concentration. For the experiments of qRT-PCR, each dilution was assayed in duplicate for all primers pairs (MCT1, MCT4 and Housekeeping-Actin), being at least three independent experiences made for all situations assayed.

The thermal cycling conditions consisted in an initial denaturation step at 95.0 °C for 3 min followed by 39 amplification cycles, each comprising denaturation (95.0 °C for 20 s), annealing (59.0 °C for

30 s) and extension (72.0 °C for 30 s). Fluorescent data were acquired during each extension step. The melting curve was obtained by analyze of temperatures between 65.0 to 95.0 °C, with increments of 0.5 °C for 5 s. The cycle conditions were run in a C1000™ Thermal Cycler, interfaced to a CFX96™ Real-Time PCR Detection System and data were acquired and analyzed by CFX Manager™ Software, version 1.0 (Bio-Rad Laboratories). Actin housekeeping gene amplification was used as a reference gene for normalization of gene expression levels and to determinate the ΔCT .

2.8.3. Protein extraction and quantification

After the appropriate treatment to the cells, the medium of cell culture was removed and the plates containing the cells were placed on ice and washed with cold PBS. 200 μL of Lyse Buffer¹ supplemented with Protease inhibitor cocktail (Sigma-Aldrich) were added to the cells and the mixture transferred to an eppendorf tube after scraping. Then, the suspension was incubated for 15 min on ice (vortexing occasionally) and centrifuged at 13,000 rpm for 15 min at 4 °C. The pellet was discarded and total protein extract (supernatant) was collected and stored at -80 °C until use.

Protein concentration was determinate using the BCA™ Protein Assay Kit (Thermo Scientific) according to the manufacturer's instructions.

2.8.4. Western Blotting

Western blotting, also known as immunoblotting is a technique used for the detection and analysis of proteins. The method is based on the formation of a labelled antibody-protein complex via specific binding of antibodies to proteins separated by gel electrophoresis and transferred to a nitrocellulose membrane. This antibody-protein complex is detected by a detection system allowing a quantitative analysis of protein expression.

Each protein sample was separated on 10 % polyacrylamide gel by SDS-PAGE (200 V for 60 min) and transferred (110 mA for 75 min) onto a nitrocellulose membrane (Amersham Biosciences) in transfer buffer², using a semidry system (TE70 ECL Semi-dry, Transfer Unit, Amersham Biosciences).

¹ 150 mM NaCl, 5 mM EDTA, 1 % Triton X-100, 50 mM Tris-HCL pH 7,5.

² Glycine 192 mM, Tris basis 25 mM, methanol 20 % at adjusted pH 8.3 with HCL 37 %.

Membranes were blocked with 5 % milk in TBS/0.1 % Tween 20 (Tris-buffer saline Tween 20 (TBS-T)) for 1 h at room temperature. After incubation (overnight at 4 °C) with the primary polyclonal antibodies (see **Table 4**), the membranes were washed 3x5 min with 1 % milk in TBS-T and incubated 60 min with the horseradish peroxidase (HRP)-conjugated secondary antibody solutions (anti-rabbit IgG, 1:1500 (Sigma-Aldrich); anti-mouse IgG, 1:1500 (Vector)) at room temperature. After washing 2x5 min with TBS-T and 1x5 min with TBS, the bound antibodies were visualized by immunoreactive bands, using the Enhanced Chemiluminescence (ECL) method. Equal parts of ECL A (10 mL of 100mM Tris, 90 mM Coumaric acid (Sigma-Aldrich) and 250 mM luminol (Fluka)) and ECL B (10 mL of Tris 100 mM pH 8.5 and 30 % (v/v) Hydrogen peroxide) solutions were mixed and each blot was immersed in the resulting ECL solution for 4 min. Membranes were placed in a photo cartridge (Hypercassette™, Amersham Biosciences), exposed to autoradiographic film (Kodak BioMax Light Film) in the darkroom for various times and manually developed. The developed films were air dried at RT and the protein content was estimated measuring the density of each band and normalizing to α -tubulin content with the software Image J.

Table 4. Primary antibodies used in the present study.

Protein	Primary Antibody	
	Dilution	Company
MCT1	1:200	Santa Cruz Biotechnology (sc-365501)
MCT4	1:500	Santa Cruz Biotechnology (sc-50329)
α-Tubulin	1:500	Abcam (ab15246)

2.8.5. Immunofluorescence

Immunofluorescence is a technique that utilizes fluorescent-labeled antibodies to detect specific target antigens allowing to detect the localization of a specific protein.

Cells were seeded in 6-well plates containing glass coverslips, in the appropriate conditions. Before using the glass coverslips, they were treated with poly-L-Lysine to promote cell adhesion and sterilized with 70 % and 96 % ethanol. After cell treatment, the culture medium was removed and the cells

washed with PBS and incubated with methanol at -20 °C for 20 min allowing cell fixation and permeabilization. Then, coverslips were washed twice with PBS and blocked with 5 % BSA (Bio-Rad) in PBS/0.1 % Tween 20 (PBS-T) for 30 min at RT. After blocking, cells were washed 3x5 min with PBST and incubated with anti-MCT-1 (1:250, Santa Cruz Biotechnology) or anti-MCT-4 (1:100, Santa Cruz Biotechnology) diluted in 5 % BSA in PBS-T, overnight. After incubation with primary antibody, coverslips were washed 3x5 min with PBS-T and incubated with fluorescence anti-mouse (for MCT-1, 1:1500, Alexa Fluor® 488) and fluorescence anti-rabbit (for MCT-4, 1:1500, Alexa Fluor® 488) secondary antibodies for 1 h at RT. Finally, the coverslips were washed 3x5 min with PBS-T, mounted on Vectashield Mounting Medium with DAPI, and immediately observed under the fluorescence microscope (ZEISS LSM 800 with Airyscan). Three coverslips were prepared for each experimental condition and representative images are shown in the results.

2.9. Statistical Analysis

Statistical analysis was performed with the Graph Pad Prism 5 software. The results are presented as normalized means \pm SD, at least three independent experiments. Statistical significance was assessed by the t-test considering p values <0.05 as statistically significant for a confidence level of 95 %.

Chapter 3
Results

3.1. 3-Bromopyruvate effect different colorectal cancer cell lines: evaluation of viability, metabolism and cell migration.

This work aimed to evaluate the cytotoxic effect of the alkylating compound 3-bromopyruvate (3BP) in different colorectal cancer cell lines (HCT-15, HT-29 and Caco-2). Before such evaluation, the adequate cell seeding density was determined for each cell line, to ensure that cells were at exponential growth phase during the whole assay. The values chosen to the cell seeding were 7.5×10^3 viable cells for HCT-15 and 10×10^3 viable cells for HT-29 and Caco-2, for the SRB assay (data not show).

The cell lines were incubated in the presence of different concentrations of 3BP for 16 h and the cell viability and the respective IC_{50} were assessed by SRB assay. In all cell lines, it was observed that 3BP decreased the cell viability in a dose-dependent manner (**Figure 14**). However, it is evident that the three cell lines presented different sensitivity to 3BP, being HCT-15 the most sensitive cell line, presenting an IC_{50} value considerably lower than the Caco-2 and HT-29 that presented IC_{50} values higher than 200 μ M (**Table 5**).

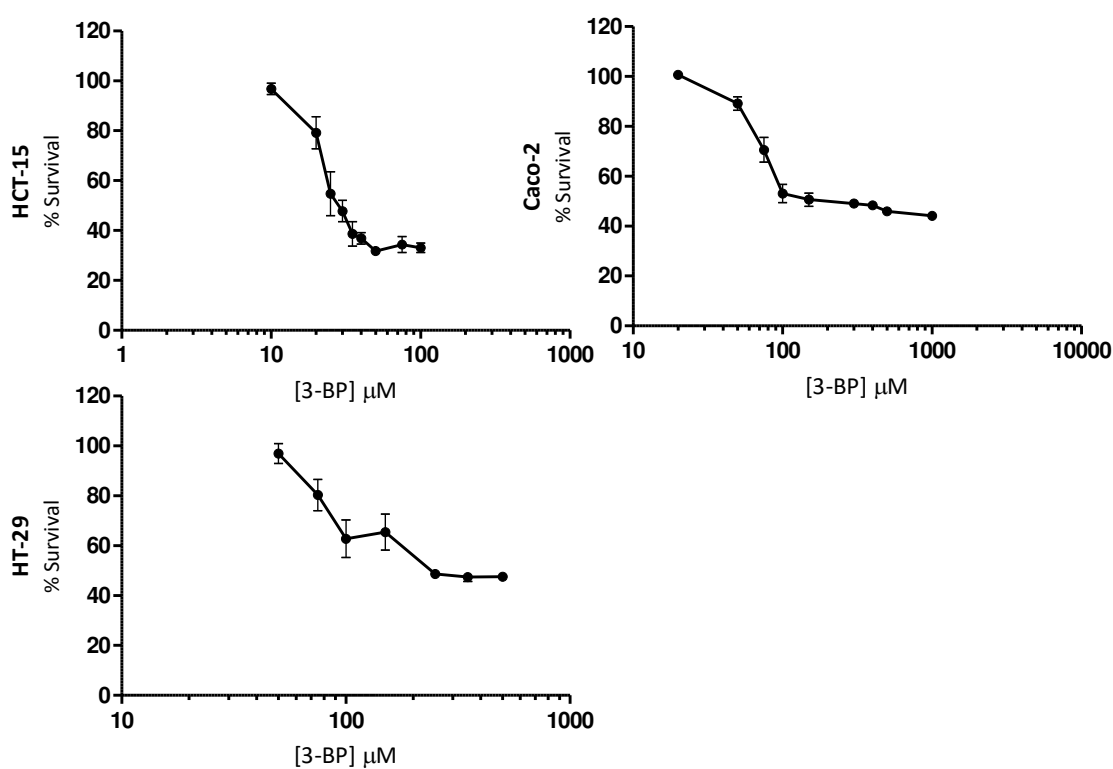


Figure 14. Effect of 3BP on HCT-15, Caco-2 and HT-29 cell survival assessed by the SRB assay after 16 h of exposure to the compound. The values plotted in the graphs correspond the mean of triplicates from at least three independent experiments.

Table 5. IC₅₀ values for 3BP for the cell lines HCT-15, Caco-2 and HT-29 determined by SRB assays. Results are expressed as mean ± SD of triplicates from at least three independent experiments.

Cell Lines	HCT-15	Caco-2	HT-29
Determined IC₅₀ value	31.76 μM	234.15 μM	263.67 μM
SD ±	6.78	18.78	74.89

In order to understand if this effect on cell viability was due to metabolism disturbance, glucose and lactate levels present in cell culture medium were measured, using colorimetric kits. HCT-15, HT-29 and Caco-2 cells were treated 16 h with the respective ½ IC₅₀ and IC₅₀ values of 3BP. After this, extracellular glucose and lactate were determined and normalized to the total biomass. As control, untreated cells were used (**Figure 15**).

This metabolism assay showed that HCT-15 cells are the most glycolytic ones, since these cells presented higher extracellular lactate levels than HT-29 and Caco-2 in basal conditions. Concerning 3BP effect in metabolism, it was observed for HCT-15 cells that treatment with the corresponding IC₅₀ of 3BP, but not with the ½ IC₅₀, resulted in a significant decrease of extracellular lactate levels and increase of extracellular glucose levels, compared to the control (**Figure 15 A and B**). In HT-29 and Caco-2, 3BP induced a significant increase in extracellular glucose levels for ½ IC₅₀ and IC₅₀ values, as well as a decrease in extracellular lactate levels (**Figure 15 A and B**).

Thus, analyzing the results obtained for the different cell lines metabolism in response to 3BP treatment, it was verified that all cell lines responded to the treatment, decreasing glucose consumption and lactate production, a behavior in agreement with the anti-glycolytic effect of the 3BP.

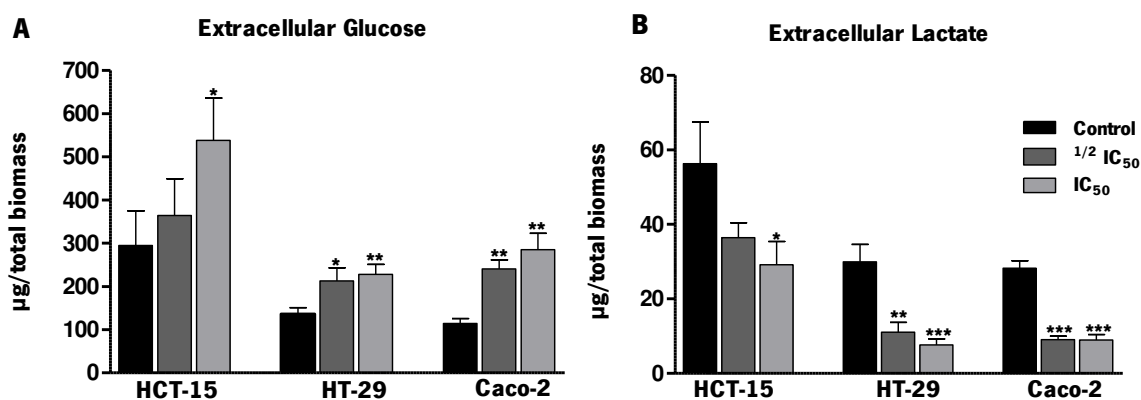


Figure 15. Effect of 3BP in metabolic profile of HCT-15, HT-29 and Caco-2 cell lines. Cells were incubated in the presence of the $\frac{1}{2}$ IC₅₀ (dark gray bars) and IC₅₀ (light gray) of 3BP for 16 h. After this time, extracellular glucose (**A**) and lactate (**B**) were quantified by colorimetric kits and normalized for the total biomass, determined by the SRB assay. Untreated cells were used as control (black bars). Results are presented as mean \pm SD of at least three independent experiments. Significantly different between groups: *P < 0.05; **P < 0.01; ***P < 0.001.

To study the effect of 3BP on cell migration, the wound-healing assay was performed, mimicking *in vitro* the cell migration that occur *in vivo*. The different CRC cell lines were treated for 24 h with the respective $\frac{1}{2}$ IC₅₀ and IC₅₀ values of 3BP. Images of the cells were registered at different times (0, 12 and 24 h).

The effect of 3BP on the migration capacity of HCT-15 (**Figure 16**), Caco-2 (**Figure 17**) and HT-29 (**Figure 18**) cell lines was evaluated. Untreated HCT-15 cells exhibited the highest cell migration capacity, especially at 24 h as shown in **Figure 16 A**. The treatment with 3BP decreased cell migration capacity, being this inhibition more evident at 24 h than at 12 h for both concentrations. At 24 h, cell migration capacity was 53%, 39% and 34% for untreated cells (control), $\frac{1}{2}$ IC₅₀ and IC₅₀ of 3BP, respectively (**Figure 16 B**).

Concerning the other cell lines, analyzing the wound representative pictures, they shown that both untreated Caco-2 and HT-29 cells have not a high migration capacity (**Figure 17 A and 18 A**). Nevertheless, it was observed that 3BP affected significantly the migration capacity in these cell lines either at 12 or 24 h at both concentrations used (**Figure 17 B and 18 B**). In Caco-2, this inhibitory

effect of 3BP was more significant at 24 h for $\frac{1}{2}$ IC_{50} and IC_{50} of 3BP, in which cells migrated only 9% and 4%, respectively, whereas untreated cells (control) migrated 21% (**Figure 17 B**). In HT-29 cells, 3BP inhibited significantly cell migration capacity, being observed that cells treated with $\frac{1}{2}$ IC_{50} of 3BP migrated 8% and 17% at 12 and 24 h, respectively, whereas untreated cells migrated 19% and 27% in same periods of time. However, it is worthy to refer that it was not possible to evaluate the effect of 3BP in the concentration corresponding to the IC_{50} after 12 h and 24 h of treatment, due to loss of cell viability impairing the mathematical treatment of the results (**Figure 18 B**).

Thus, analyzing the results obtained for all cell lines, it was observed that 3BP inhibited the cell migration capacity, a characteristic associated to tumor aggressiveness and metastasis development.

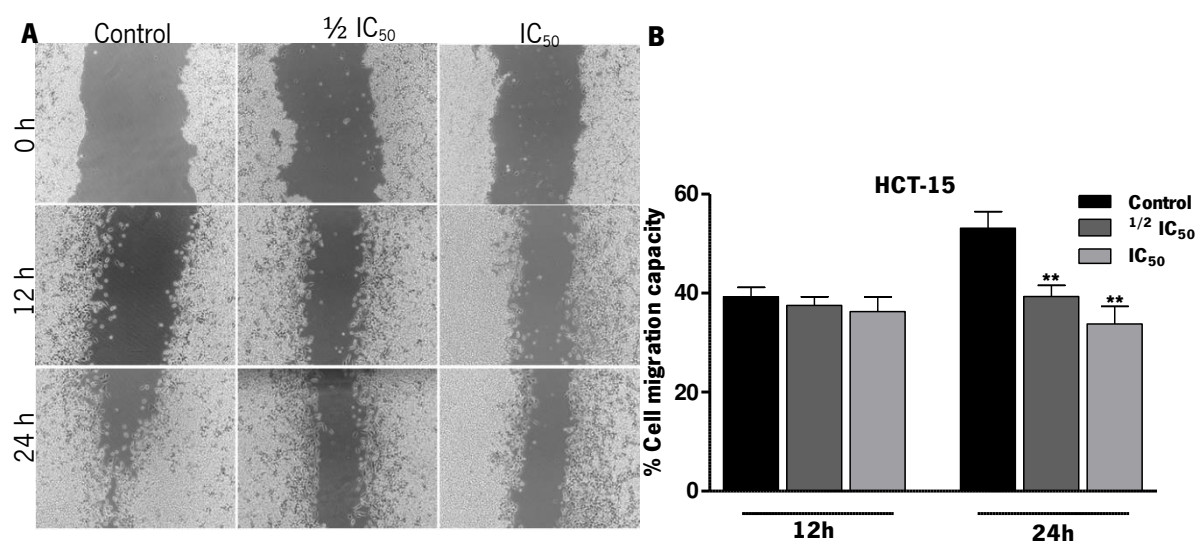


Figure 16. Inhibitory effect of 3BP on cell migration capacity of HCT-15 cell line. **A)** Representative pictures of the migratory capacity of HCT-15 cells treated with 3BP in the concentrations of $\frac{1}{2}IC_{50}$, IC_{50} and 0 μ M (control). **B)** Percentage of cell migration in untreated cells (black bars) or in cells treated with $\frac{1}{2}IC_{50}$ (dark gray bars) and IC_{50} (light gray bars) of 3BP for 12 and 24h. Results represent the mean \pm SD of at least three independent experiments. Significantly different between groups: **P < 0.01.

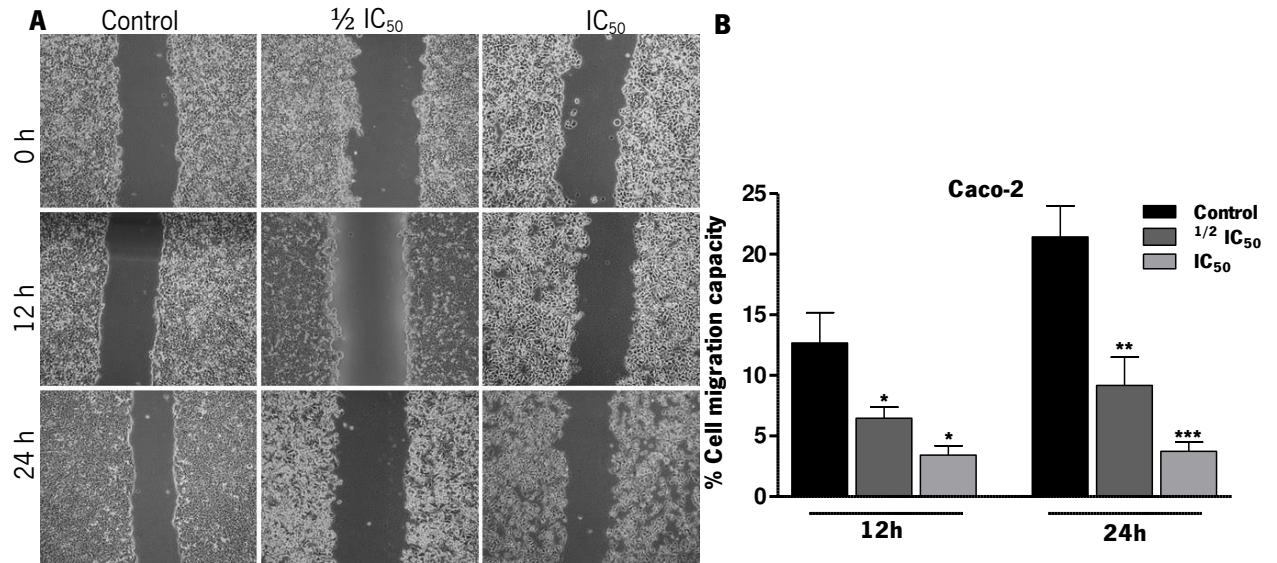


Figure 17. Inhibitory effect of 3BP on cell migration capacity of Caco-2 cell line. **A)** Representative pictures of the migratory capacity of Caco-2 cells treated with 3BP in the concentrations of $\frac{1}{2}IC_{50}$, IC_{50} and $0 \mu M$ (control). **B)** Percentage of cell migration in untreated cells (black bars) or in cells treated with $\frac{1}{2}IC_{50}$ (dark gray bars) and IC_{50} (light gray bars) of 3BP for 12 and 24 h. Results represent the mean \pm SD of at least three independent experiments. Significantly different between groups: * $P < 0.05$; ** $P < 0.01$; *** $P < 0.001$.

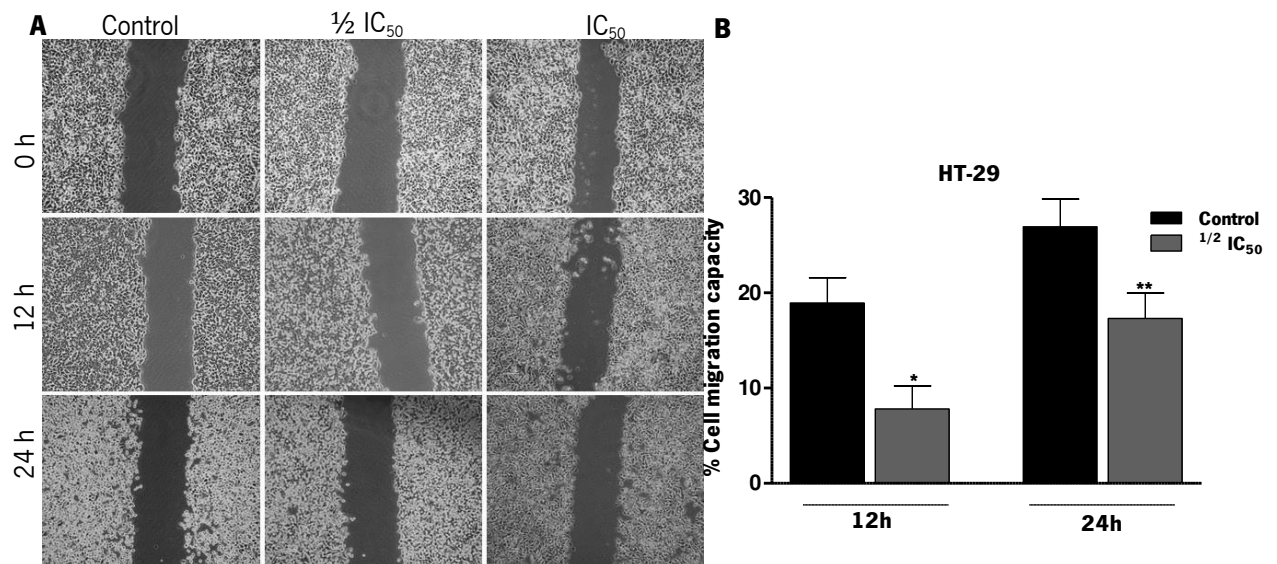


Figure 18. Inhibitory effect of 3BP on cell migration capacity of HT-29 cell line. **A)** Representative pictures of the migratory capacity of HT-29 cells treated with 3BP in the concentrations of $\frac{1}{2}IC_{50}$, IC_{50} and $0 \mu M$ (control). **B)** Percentage of cell migration in untreated cells (black bars) or in cells treated with $\frac{1}{2}IC_{50}$ (dark gray bars) of

3BP for 12 and 24 h. Results represent the mean \pm SD of at least three independent experiments. Significantly different between groups: *P < 0.05; **P < 0.01; ***P < 0.001.

3.1.1. Assessment of MCT1 and MCT4 expression in CRC cell lines.

In this study, MCT1 and MCT4 expression was evaluated by quantitative (Western Blot and qRT-PCR) and qualitative (Immunofluorescence) assays.

The qRT-PCR was performed using mRNA samples of the different CRC cell lines to assess the expression of the genes *SLC16A1* and *SLC16A3* coding for MCT1 and MCT4 protein, respectively. The qRT-PCR assays showed that the different cell lines expressed both genes, but expression levels were different between them. HCT-15 presented the highest levels of expression either for *SLC16A1* or *SLC16A3* (**Figure 19**). Nevertheless, mRNA levels do not always correlate with protein expression levels. In this way, Western Blot assay was performed to quantify MCTs protein. As shown in **Figure 20**, all cell lines expressed MCT1, being once again observed that HCT-15 was the cell line that presented highest basal expression levels of MCT1, followed by HT-29 and Caco-2 cell lines (**Figure 20 A and B**). Concerning MCT4, no conclusive results were obtained in Western Blot and optimization conditions have still to be established. As the uptake of 3BP is most probably mediated by MCTs [114], the different expression of these transporters can be responsible for the differences observed in cell sensitivity to 3BP.

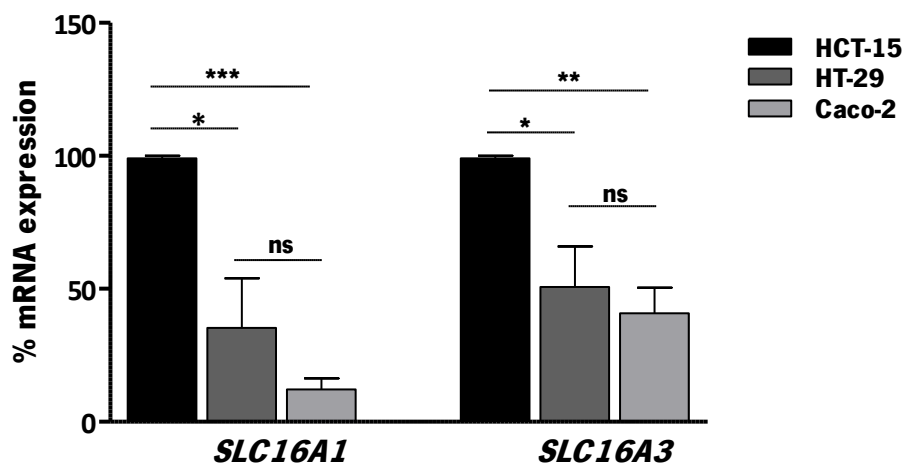


Figure 19. Expression levels of *SLC16A1* and *SLC1A3* genes in HCT-15, HT-29 and Caco-2 cell lines determined by qRT-PCR. Actin was used as housekeeping gene. The cell line with highest expression of each gene was used as reference. Results are representative of three independent experiments. Significantly different between groups: * $P < 0.05$; ** $P < 0.01$; *** $P < 0.001$. **ns**: no statistically significant.

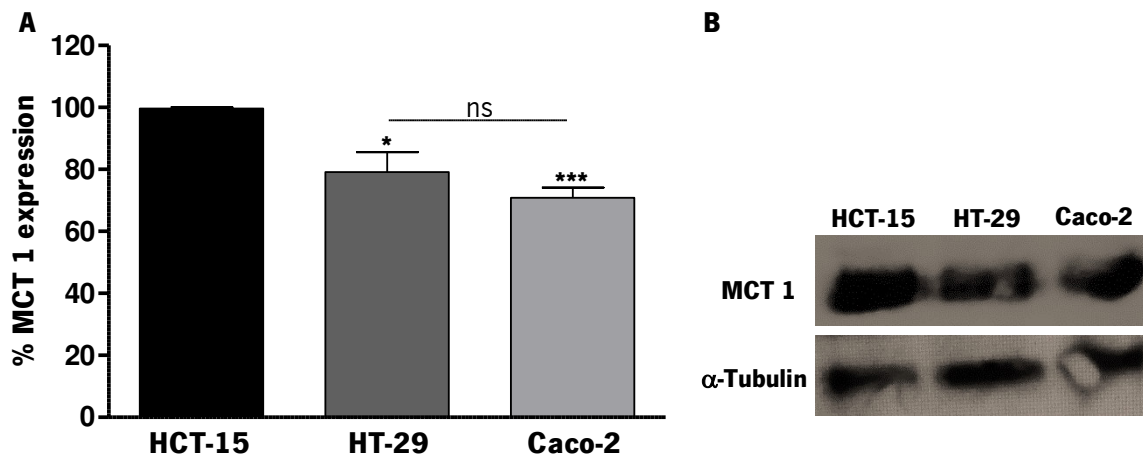


Figure 20. MCT 1 expression analysis in HCT-15, HT-29 and Caco-2 cell lines assessed by Western-blot. The cell line presenting higher expression of MCT 1 was used as reference. **A)** Levels of protein expression relative to the control cells and normalized to α -tubulin. The results are presented as mean \pm SD of two independent experiments. **B)** Representative results of MCT 1 protein expression. Significantly different between groups: * $P < 0.05$; *** $P < 0.001$; **ns**: no statistically significant.

MCTs exert their functions of transporters at plasma membrane. As so, their cell localization has been evaluated by immunofluorescence. The analysis of representative pictures using both MCT1 and MCT4 antibodies showed that these proteins are present in all cell lines. In HCT-15 cells, MCT1 was localized essentially at plasma membrane, although some residual expression was also observed in nucleus. Concerning Caco-2 and HT-29 cells, MCT1 was also localized in nucleus and plasma membrane, but in the last case only in the junctions between cells. In these two cell lines, MCT1 also appeared in the cytoplasm. Concerning MCT4, it was present mainly in plasma membrane for Caco-2 and HT-29 cell lines and, once again, in junction between cells. In HCT-15 cells, MCT4 was localized in both cytoplasm and plasma membrane (**Figure 21**).

Transport function of both MCT1 and MCT4 is associated with their correct traffic to plasma membrane. The present study showed that HCT-15, the most sensitive cell line to 3BP, presented the proper location for both MCTs, according to their transporter function. On the other side, in Caco-2 and HT-29 cell lines, the most resistant cells, MCTs were essentially in the junctions between cells.

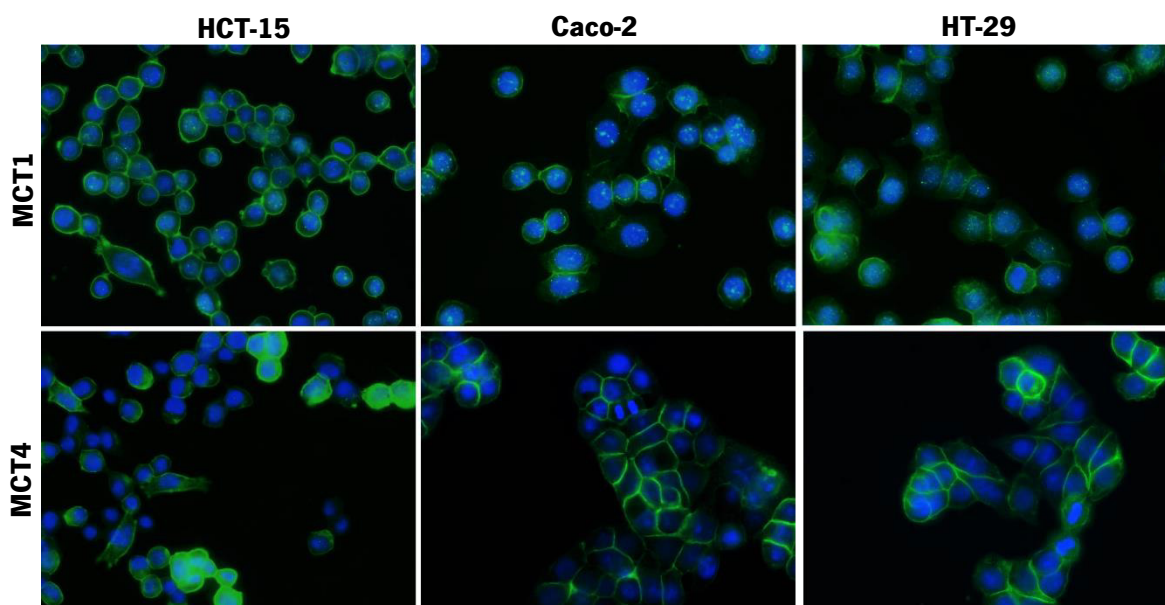


Figure 21. MCT1 and MCT4 cellular localization in HCT-15, Caco-2 and HT-29 cell lines. Representative images of immunofluorescence are shown at 400x magnification.

3.2. Effect of tumor microenvironment in MCTs expression and cell sensitivity to 3BP

3.2.1. Hypoxia

As HCT-15 was the most responsive cell line to 3BP, it was the one chosen for the following assays. Concerning the effect of hypoxia, HCT-15 cells were incubated with CoCl_2 to simulate this condition. CoCl_2 is responsible for HIF-1 α stabilization, inducing chemically hypoxia. After the period of incubation, the extracellular glucose and lactate, as well as cell biomass were determined. HCT-15 cells showed a significant increase of extracellular lactate levels under hypoxia compared to normoxia (control). The glucose concentration in the culture medium increased, but not significantly when

compared to control (**Figure 22**). Thus, the results indicate that cells treated with CoCl_2 increased their glycolytic phenotype.

Hypoxia is a characteristic of malignant cancers, being associated to aggressiveness and therapy resistance. As previously referred, hypoxia induces a metabolic switch in cell tumors through deregulation of several metabolic enzymes, contributing to increased glycolytic rates. Therefore, the results presented here are in accordance with the expected behavior under hypoxic conditions.

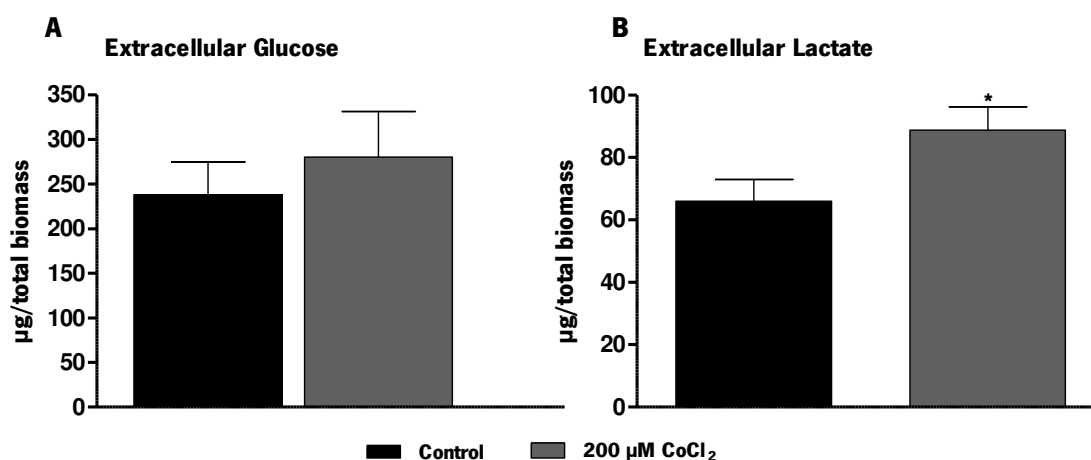


Figure 22. Effect of hypoxia in metabolic profile of HCT-15 cells. Hypoxia was chemically induced by incubating the cells in the presence of 200 μM CoCl_2 for 24 h (gray bars). After this time, the medium was collected and extracellular glucose (**A**) and lactate (**B**) were quantified by colorimetric kits and normalized for the total biomass, determined by the SRB assay. Untreated cells were used as control (black bars). Results are presented as mean \pm SD of at least three independent experiments. Significantly different between groups: * $P < 0.05$.

HCT-15 cells migration capacity was evaluated by the wound-healing assay, being observed a lower migratory capacity under hypoxic conditions when compared to cells grown in normoxia (**Figure 23**). Normoxic cells migrated 38% and 47% at 12 and 24 h, respectively, whereas hypoxic cells migrated only 30% and 36% over the same period of time, respectively. As HCT-15 cells presented a glycolytic phenotype in hypoxia, it would be expected that these cells present higher motile capacity. In these conditions, higher levels of lactate are produced, what induces environmental acidification, a characteristic associated with aggressiveness tumors [207]. Nevertheless, in the present study, the

cells had less motile capacity. It is worthy to mention that the medium used in the assays was buffered, and so the influence of proton efflux could be masked.

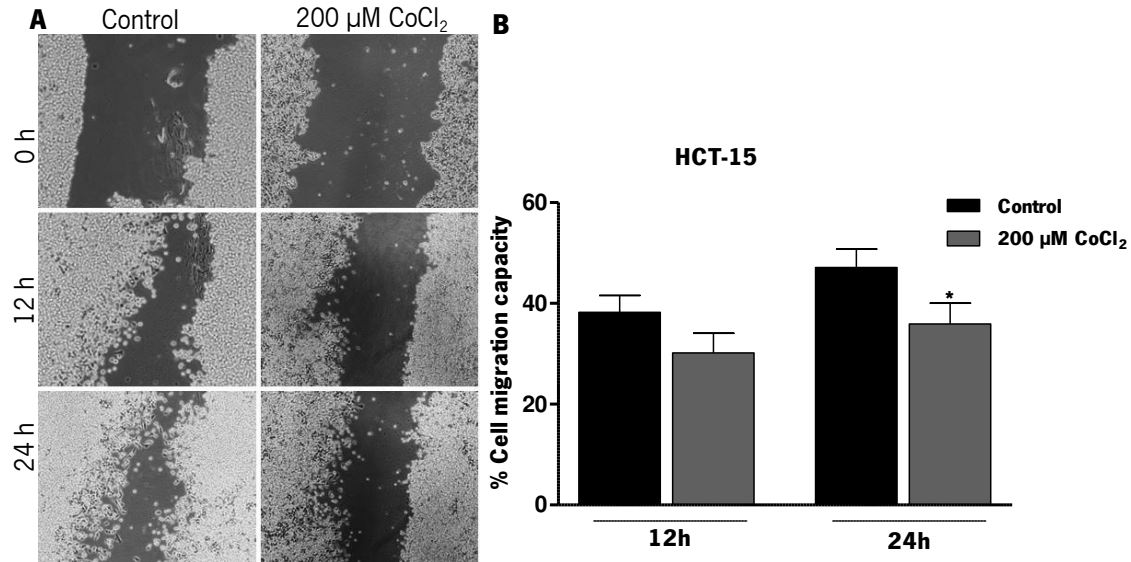


Figure 23. Effect of hypoxia on cell migration capacity of HCT-15 cell line. **A)** Representative pictures of the migratory capacity of HCT-15 cells treated with 200 μ M CoCl_2 . **B)** Percentage of cell migration in untreated cells (black bars) and hypoxic cells with 200 μ M CoCl_2 (gray bars) for 12 and 24 h. Results represent the mean \pm SD of at least three independent experiments. Significantly different between groups: * $P < 0.05$.

The qRT-PCR was performed to assess the expression of the genes *SLC16A1* and *SLC16A3* (coding for MCT1 and MCT4, respectively) on hypoxia, induced by CoCl_2 . Analysis of qRT-PCR results showed that both genes were expressed, but it was evident a significant increase of *SLC16A3* gene expression levels in hypoxia, whereas *SLC16A1* maintained its expression (**Figure 24**). HIF-1 is involved in environmental adaption of tumor cells to hypoxia, enhancing glycolysis and consequently, lactate production and efflux. These results are in accordance with the glycolytic phenotype presented by HCT-15 cells, as cells need to export the lactate produced by glycolysis, mainly through MCT4. The *HIF-1 α* gene was assessed to assure that hypoxia was induced, being verified a significant increase of its expression in hypoxia (**Figure 24**). However, these results should be validated by Western Blot to confirm these differences at protein level.

MCTs localization was assessed by immunofluorescence. MCT1 was localized essentially at plasma membrane in both normoxia (control) and hypoxia. However, in hypoxic cells MCT1 expression was also observed in nucleus. MCT4 was found in the cytoplasm and cell membrane in some cells under normoxia, being the fluorescence more intense in hypoxia in plasma membrane and cytoplasm, where it was also observed a residual fluorescence in the nucleus (**Figure 25**).

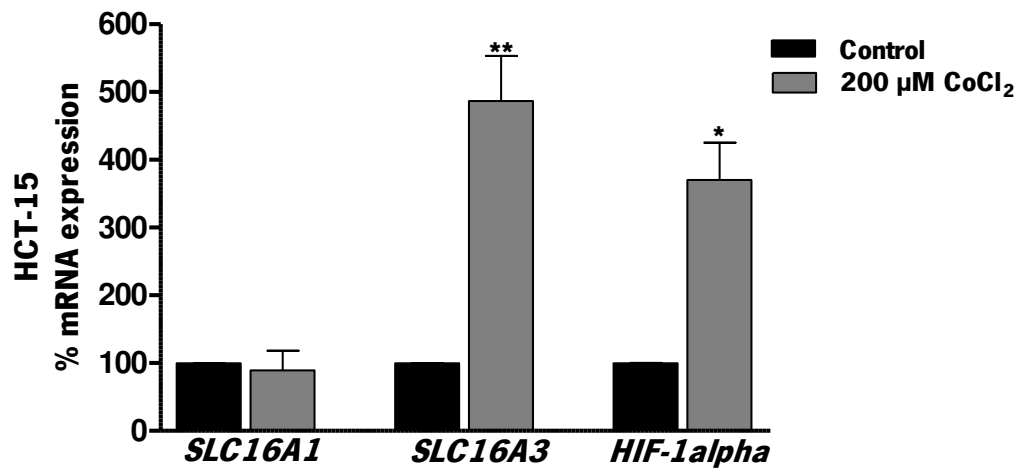


Figure 24. Effect of hypoxia in the expression levels of *SLC16A1*, *SLC1A3* and *HIF-1* genes in HCT-15 cells determined by qRT-PCR. Hypoxia was chemically induced by incubating the cells in the presence of 200 μM CoCl₂ for 24 h (gray bars) and untreated cells (black bars) were used as reference. Actin was used as housekeeping gene. Results are representative of three independent experiments. Significantly different between groups: *P < 0.05; **P < 0.01.

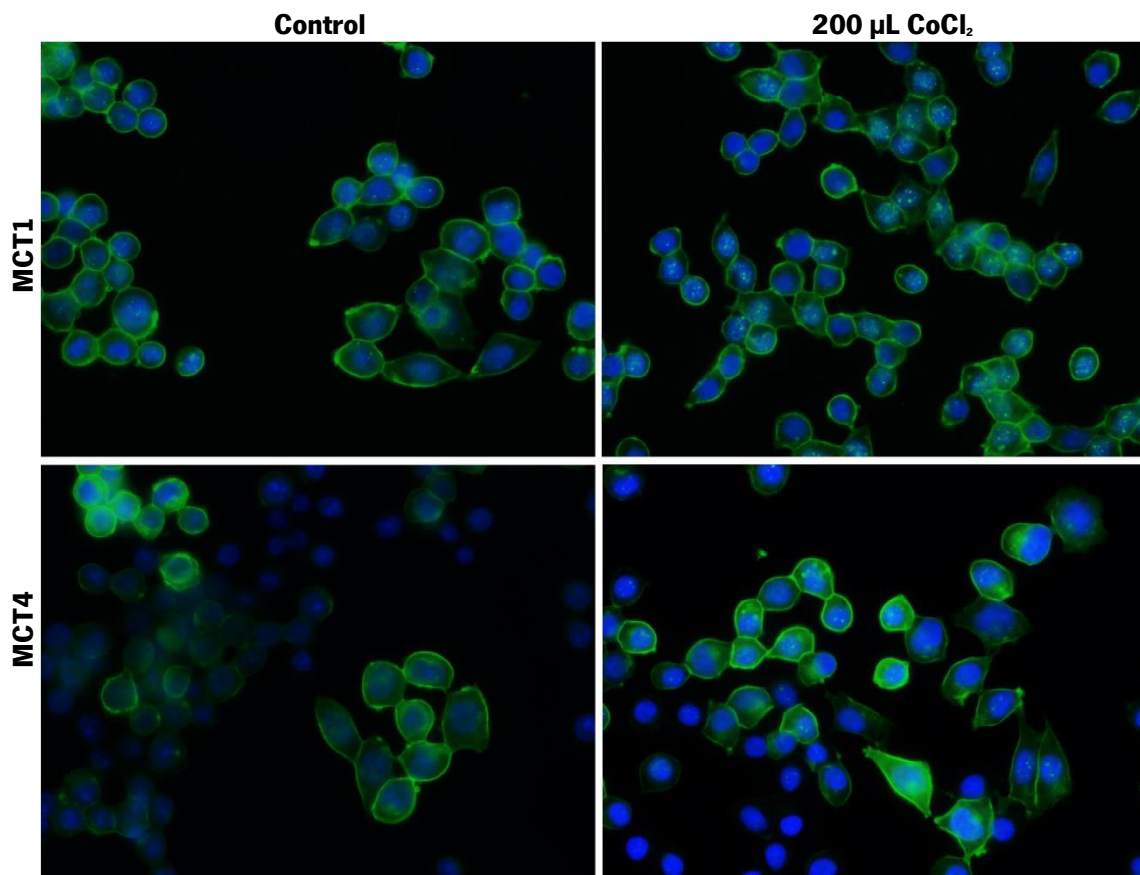


Figure 25. Effect of hypoxia on MCT1 and MCT4 cellular localization of HCT-15 cell line. Cells were incubated with CoCl₂ (200 μL) or fresh medium (control) for 24 h. Representative images of immunofluorescence are shown at 400x magnification.

To also analyze the influence of hypoxia in 3BP cytotoxic effect, HCT-15 cells were incubated for 24 h with CoCl₂ and then treated with different concentrations of 3BP for 16 h. Cell viability and the respective 3BP IC₅₀ were assessed by SRB assay. As shown in **Figure 26**, 3BP was significantly less cytotoxic in hypoxia than in normoxia, with IC₅₀ of $80.66 \pm 4.54 \mu\text{M}$ and $37.23 \pm 9.18 \mu\text{M}$, respectively. According to the results obtained for MCTs expression, it would be expected a higher toxicity of 3BP under hypoxic conditions, due to the increased expression of MCT4, a transporter of the compound. However, HCT-15 cells were more resistant to 3BP in hypoxia, indicating that other factors should influence its toxicity.

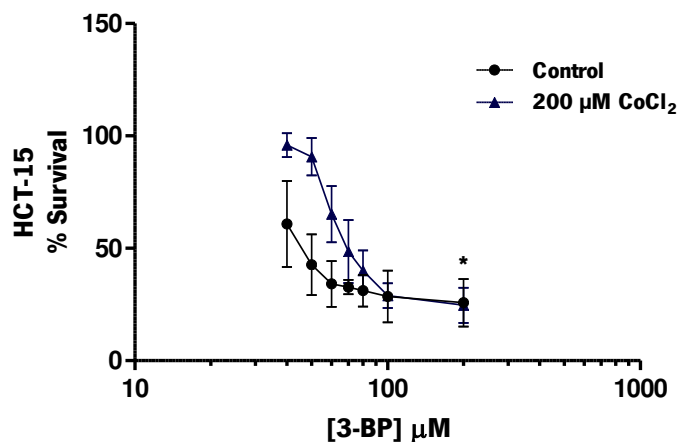


Figure 26. Effect of hypoxia on cell viability of HCT-15 cells treated with 3BP, assessed by SRB assay. Hypoxia was chemically induced by incubating the cells in the presence of 200 μM CoCl_2 (\blacktriangle) or with fresh medium as control (\bullet) for 24 h followed by treatment with 3BP for 16 h. The values plotted in the graphs correspond the mean \pm SD of triplicates from at least three independent experiments. Significantly different between groups: * $P < 0.05$.

3.2.2. Extracellular pH

Extracellular pH was other environment factor studied in this work to see its effect in cell metabolism, cell migration, MCTs expression and 3BP toxicity. HCT-15 cells were incubated for 24 h with medium buffered at pH 6.6 and 7.4 that are representative of tumor microenvironment and physiological pHe, respectively. In order to understand the influence of pHe in cell metabolism, glucose and lactate levels present in cell culture medium were measured at these different pHes and normalized to total biomass. It was observed that HCT-15 cells showed a significant decrease of extracellular lactate levels and a significant increase of the glucose levels in culture medium at pH 6.6 compared to pH 7.4 (control) (**Figure 27**).

As previous referred, the environmental acidification is a consequence of the glycolytic phenotype presented by tumor cells, originating an increased proton efflux, coupled to lactate transport. In the present work, the acidic pHe was induced by buffering the medium mimicking the pHe present in tumor microenvironment, which can have influence on the cellular metabolism itself. In fact, it was

observed that HCT-15 cells were less glycolytic at lower pHe, most probably because the acidic pHe inhibits glycolysis, promoting a decrease in the glycolytic rate.

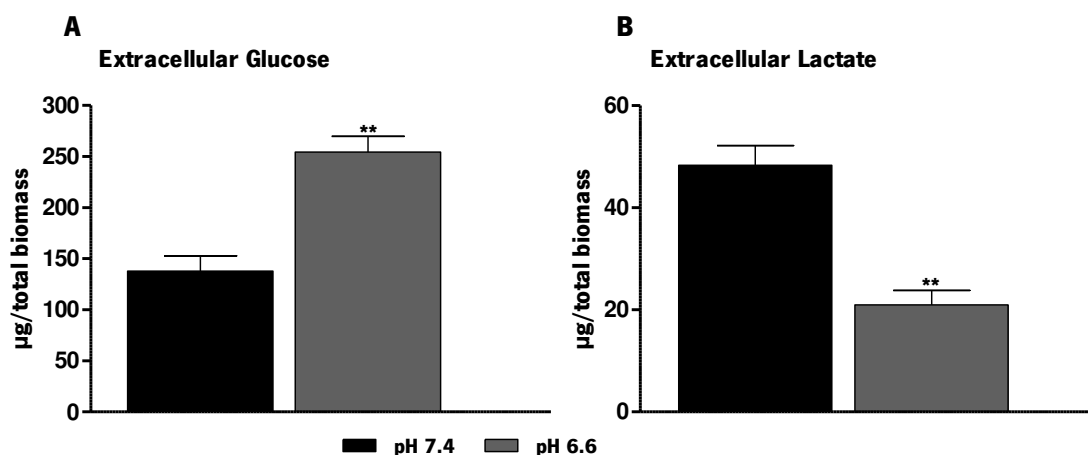


Figure 27. Effect of extracellular pH in metabolic profile of HCT-15 cell line. Cells were incubated with medium buffered with HEPES at pH 6.6 (gray bars) and 7.4 (black bars) for 24 h. After this time, the medium was collected and extracellular glucose (**A**) and lactate (**B**) were quantified by colorimetric kits and normalized for the total biomass, determined by the SRB assay. Cells incubated at pHe 7.4 were used as control (black bars). Results are presented as mean \pm SD of at least three independent experiments. Significantly different between groups: * $P < 0.05$.

Concerning the effect of pHe in the migratory capacity, it was observed that after exposition at different pHe for 24 h, HCT-15 cells presented similar migratory capacity at both pHe 6.6 and 7.4 (**Figure 28 A**). This result was observed at either 12 or 24 h, in which the cells migrated 25% and 45%, respectively, compared to pHe 7.4 that migrated 23% and 42%, respectively (**Figure 28 B**). It is described that an acidic environment contributes to a migratory and invasive phenotype [38]. However, this effect was not evident for this cell line.

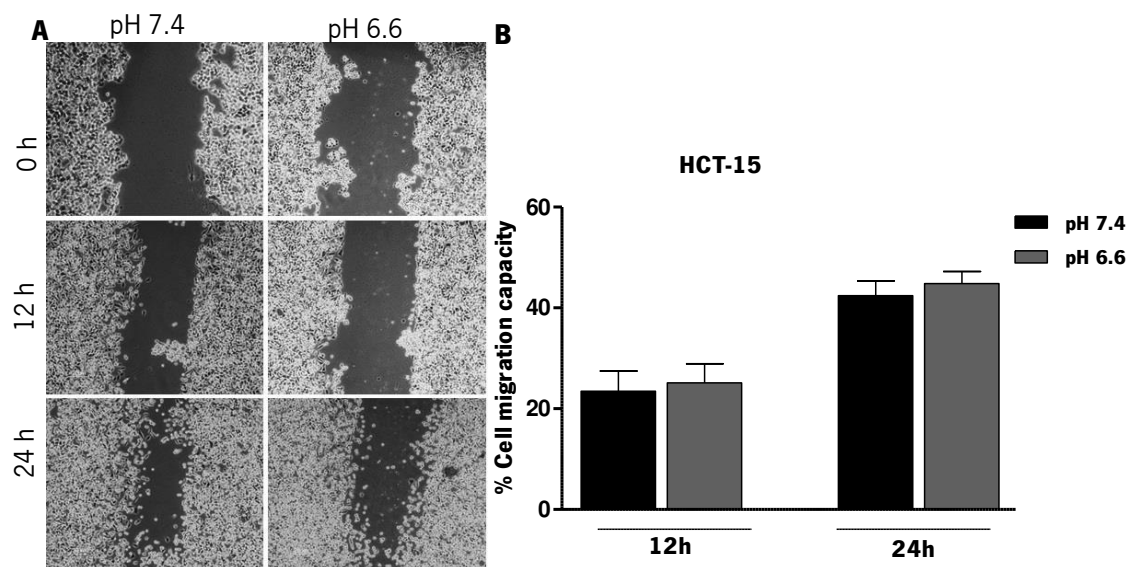


Figure 28. Effect of extracellular pH on cell migration capacity of HCT-15 cells. **A)** Representative pictures of the migratory capacity of HCT-15 cells incubated with medium buffered with HEPES at pHe 6.6 and 7.4. **B)** Percentage of cell migration at pHe 7.4 (black bars) and 6.6 (gray bars) for 12 and 24 h. Results represent the mean \pm SD of at least three independent experiments.

The analysis of MCT1 and MCT4 gene expression demonstrated that the *SLC16A1* (MCT1) gene levels decreased at lower pHe compared to the control, while *SLC16A3* (MCT4) gene levels remains similar to the control (**Figure 29**). The analysis of protein localization by immunofluorescence showed that MCT1 was mainly localized in both plasma membrane and cytoplasm at pH 7.4, whereas at pH 6.6 MCT1 was localized mainly in cell membrane. Concerning MCT4, it seems that pHe did not influence its cellular localization, being localized at cytoplasm and plasma membrane at both pHe (**Figure 30**).

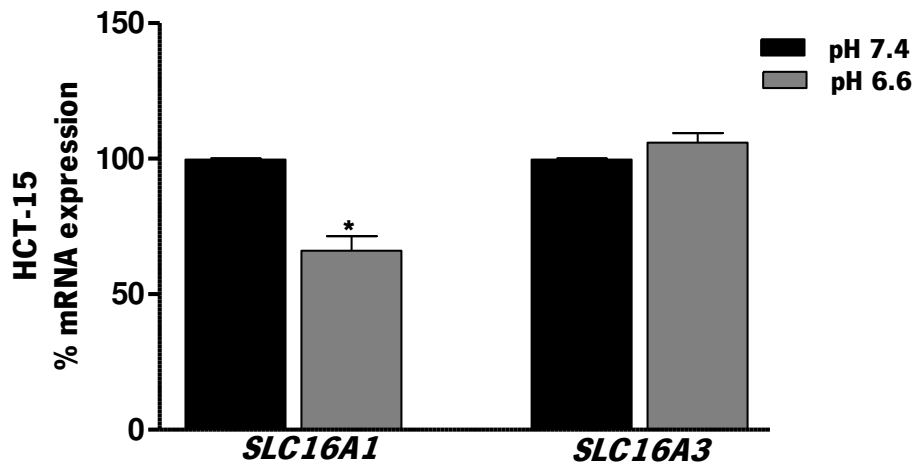


Figure 29. Effect of extracellular pH in the expression levels of *SLC16A1* and *SLC16A3* genes in HCT-15 cells determined by qRT-PCR. Gray bars represent cells incubated with medium buffered with HEPES at pH 6.6 and black bars represent cells incubated with medium buffered with HEPES at pH 7.4 that were used as reference. Actin was used as housekeeping gene. Results are representative of three independent experiments. Significantly different between groups: *P < 0.05.

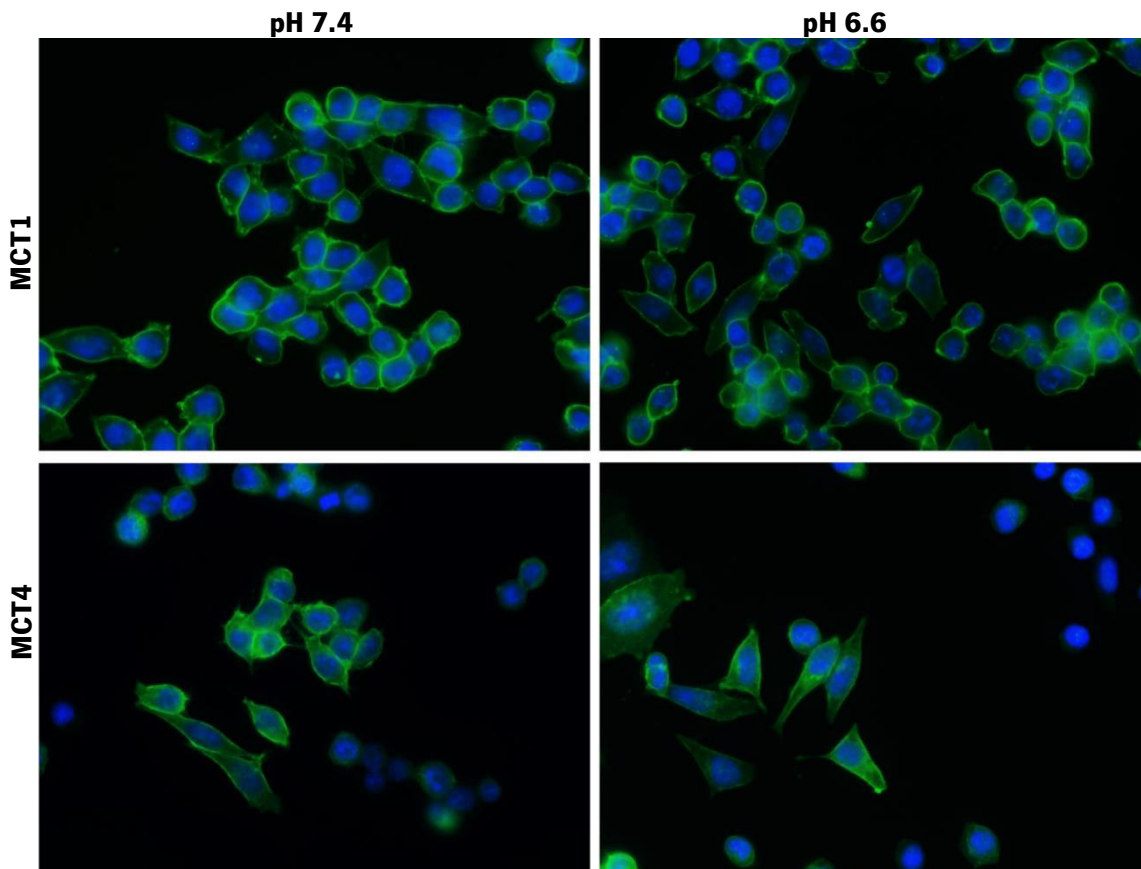


Figure 30. Effect of extracellular pH on MCT1 and MCT4 cellular localization of HCT-15 cell line. Cells were incubated with medium buffered with HEPES at pH 7.4 or 6.6. Representative images of immunofluorescence are shown at 400x magnification.

The effect of pH on 3BP cytotoxic effect was also analyzed. Cells were incubated for 16 h at different concentrations of 3BP in medium buffered with HEPES at the different pHs (6.6 and 7.4). The cell viability and the respective IC_{50} of 3BP were assessed by SRB assay. As shown in **Figure 31**, 3BP was more cytotoxic at pH 6.6 than pH 7.4, with IC_{50} of $10.86 \pm 3.63 \mu\text{M}$ and $16.54 \pm 1.29 \mu\text{M}$, respectively. Analysis of cell sensitivity to 3BP indicated that although the difference was not significant, HCT-15 cells were more sensitive to 3BP at low pH compared to physiological pH. Although a decreased expression of the *SLC16A1* gene (MCT1) was observed, suggesting that pH may play another role in the action of 3BP.

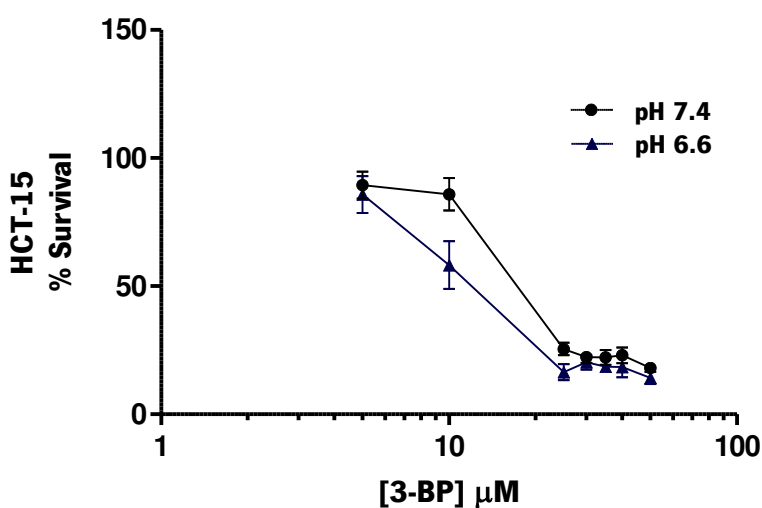


Figure 31. Effect of extracellular pH on cell viability of HCT-15 cells treated with 3BP, assessed by SRB assay. Cells were incubated with a range of 3BP concentration prepared in medium buffered with HEPES at pH 7.4 (●) and 6.6 (▲) for 16 h. The values plotted in the graphs correspond the mean \pm SD of triplicates from at least three independent experiments.

3.2.3. Glucose Starvation

The role of glucose deprivation in cell metabolism and behavior of HCT-15 cell line was also evaluated. Cells were incubated for 24 h in glucose-free medium and, after this period, extracellular glucose and lactate levels were determined using colorimetric kits and were normalized for total biomass. As control, cells incubated for the same period in medium with glucose were used. By the analysis of metabolic profile, it can be observed that HCT-15 cells, even without glucose, produced lactate (**Figure 32**), demonstrating that cells might rely the metabolism on other nutrients present in the medium as energy source. However, and as predicted, HCT-15 cells decreased the extracellular lactate levels in free-glucose medium, when compared to control. The concentration of nutrients available during tumor growth is unstable and tumor cells may be subjected to long period of nutrients starvation. Glucose is the preferential nutrient used by tumor cells, being their first choice of carbon source, but there are others metabolic pathways beyond glycolysis that tumor cells may resort to obtain energy supply.

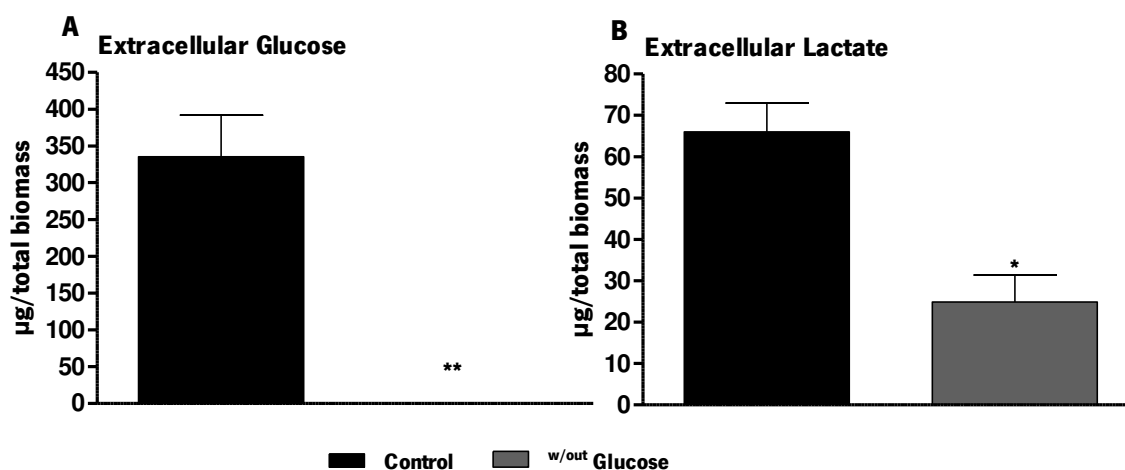


Figure 32. Effect of glucose starvation in metabolic profile of HCT-15 cell line. Cells were incubated with glucose-free medium for 24 h (gray bars). After this time, the medium was collected and extracellular glucose (**A**) and lactate (**B**) were quantified by colorimetric kits normalized for total biomass, determined by the SRB assay. Cells incubated in medium with glucose were used as control (black bars). Results are presented as mean \pm SD of at least three independent experiments. Significantly different between groups: * $P < 0.05$; ** $P < 0.01$.

The effect of starvation on cell migration capacity was also analyzed. It was observed that HCT-15 cells also presented lower migratory capacity when incubated with glucose-free medium (**Figure 33 A**). Untreated cells migrated 40% and 49% at 12 and 24 h, respectively, while in starved cells, the percentage of cell migration capacity was 27% and 29% for the same corresponding time (**Figure 33 B**). Indeed, it was expected that cells were less motile in starvation, since the main energy source was unavailable.

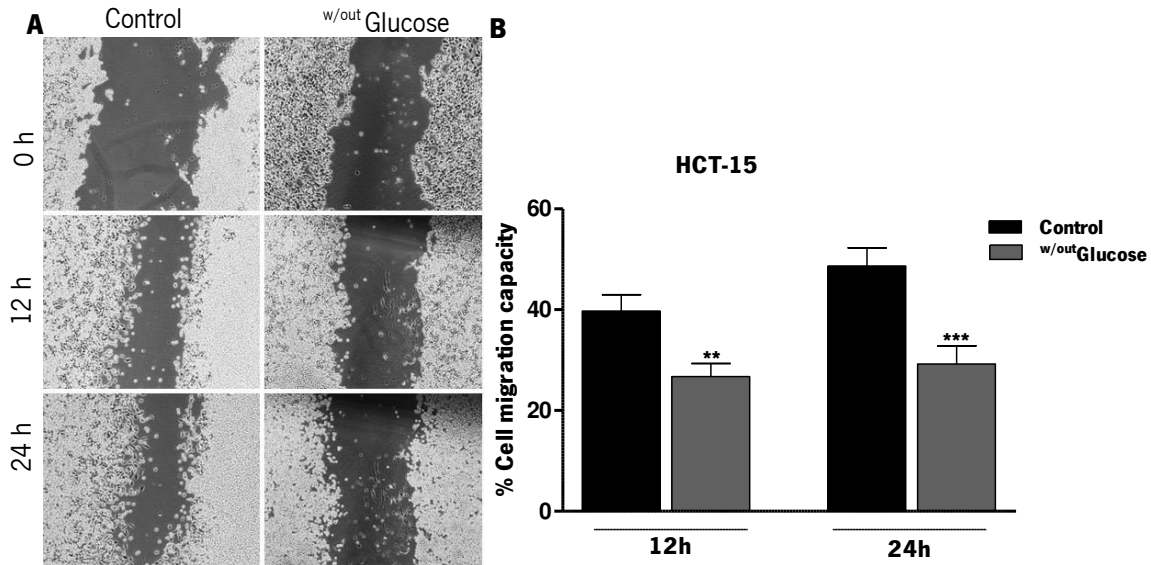


Figure 33. Effect of glucose starvation on cell migration capacity of HCT-15 cell line. **A)** Representative pictures of the migratory capacity of HCT-15 cells incubated with glucose-free medium and complete medium (control). **B)** Percentage of cell migration in cells incubated with complete medium (black bars) and glucose-free medium (gray bars) for 12 and 24 h. Results represent the mean \pm SD of at least three independent experiments. Significantly different between groups: ** $P < 0.01$; *** $P < 0.001$.

qRT-PCR was performed in mRNA samples of HCT-15 to assess the influence of glucose starvation in the expression of the genes *SLC16A1* and *SLC16A3* coding for MCT1 and MCT4, respectively. Cells were grown in glucose-free medium for 24 h and after this time total RNA was extracted. As control, RNA samples of HCT-15 cells grown in normal medium with glucose were used. It can be observed that both genes were overexpressed in starvation conditions (**Figure 34**). When representative pictures of immunofluorescence were analyzed, it was possible to observe that MCT1 was localized predominantly in plasma membrane and cytoplasm in both control and glucose-free condition. MCT4

was also localized in cytoplasm and cell membrane, although in starvation conditions, the fluorescence was slightly more intense in cytoplasm compared to control (**Figure 35**).

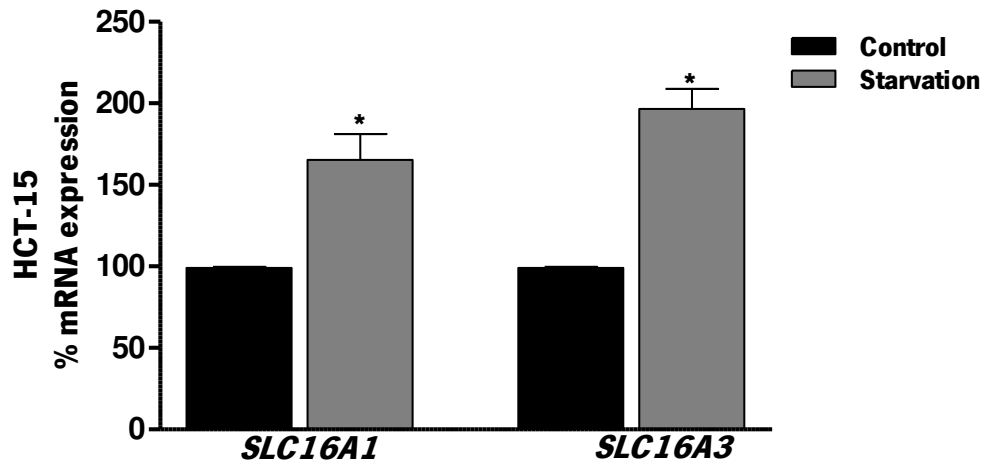


Figure 34. Effect of glucose starvation in the expression levels of *SLC16A1* and *SLC16A3* genes in HCT-15 cells (gray bars) determined by qRT-PCR. Cells grown in medium with glucose (black bars) were used as reference. Actin was used as housekeeping gene. Results are representative of three independent experiments. Significantly different between groups: *P < 0.05.

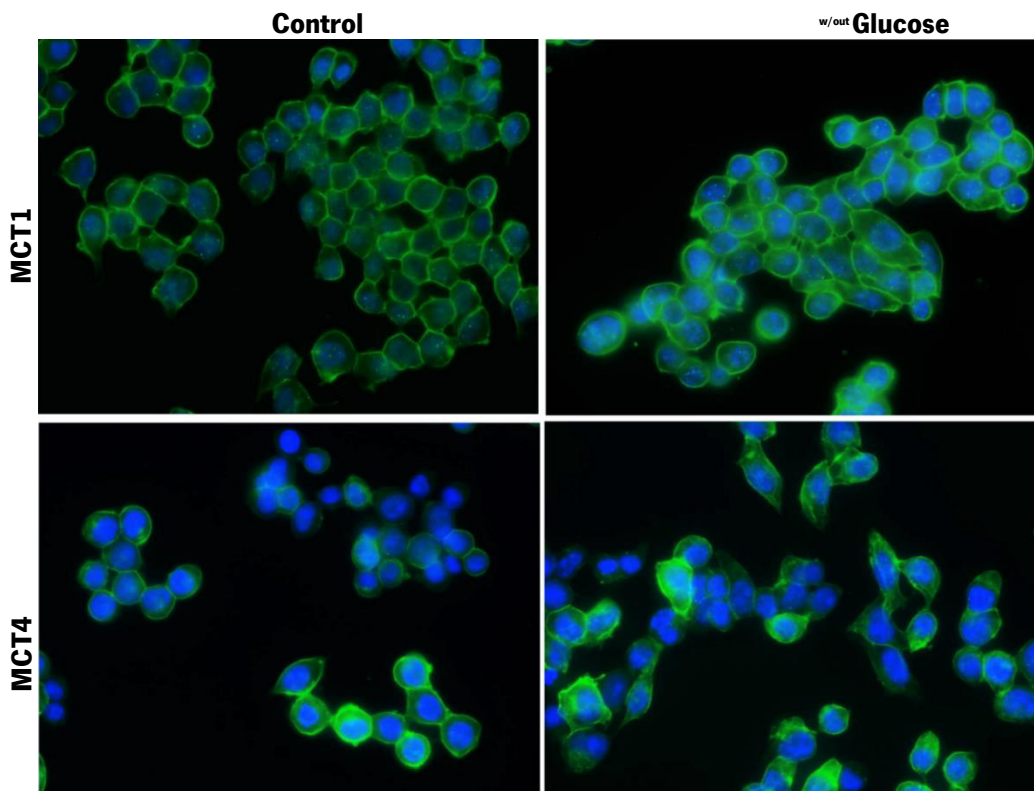


Figure 35. Effect of glucose starvation on MCT1 and MCT4 cellular localization of HCT-15 cell line. Cells were incubated with complete medium (control) or glucose-free medium for 24 h. Representative images of immunofluorescence are shown at 400x magnification.

Concerning the effect of glucose starvation in cell viability upon exposure of the cells to 3BP, it was observed that HCT-15 cells were significantly more resistant to 3BP, when in glucose starvation, although higher expression of MCTs were observed in these conditions. As shown in **Figure 36**, 3BP was less cytotoxic in glucose starvation than in control condition, being IC_{50} of $51.87 \pm 7.90 \mu\text{M}$ and $28.75 \pm 4.22 \mu\text{M}$, respectively. As already mentioned, tumor cells adapted their metabolism to overcome these adversities, regulating enzymes and transporters involved in the different metabolic pathways. In this case, only the expression of MCTs was evaluated, indicating that others factor beyond MCTs can be involved either in 3BP action mechanism. However, additional tests will be required to validate this hypothesis.

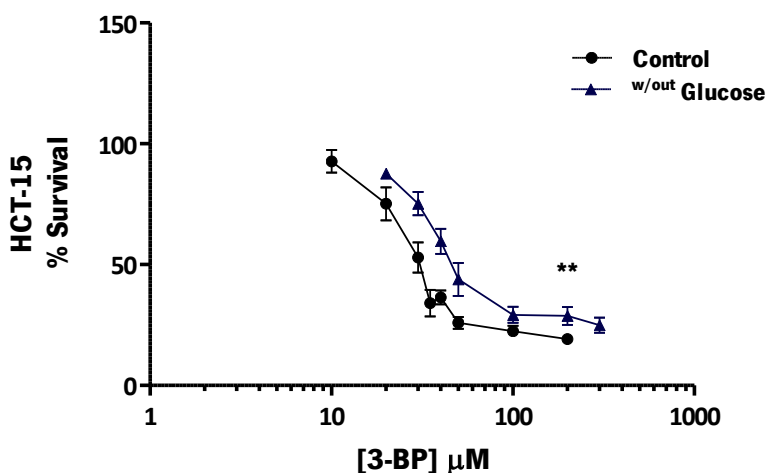


Figure 36. Effect of glucose starvation on cell viability of HCT-15 cell line, assessed by SRB assay. Cells were incubated with free-glucose medium (●) or fresh medium (▲) for 24 h followed by treatment with 3BP for 16 h. The values plotted in the graphs correspond the mean \pm SD of triplicates from at least three independent experiments. Significantly different between groups: ** $P < 0.01$.

3.3. Influence of the short-chain fatty acids in 3-bromopyruvate cytotoxicity and monocarboxylate transporters expression in HCT-15 cell line.

Short-chain fatty acids (SCFA) are produced by intestinal microbiota during fermentation, having a protective role in colon and may be used by colonocytes as fuel. Its transport into the cells occur through (S)MCTs that are also reported to be involved in the transport of 3BP [114]. Additionally, it has been report that the butyrate induces MCTs expression and is able to increase cell sensitivity to 3BP in breast cancer cells [84]. In the present work, it was evaluated the effect of different SCFAs usually present in the intestinal tract, including butyrate, lactate and acetate on MCT1 and MCT4 expression, as well as their influence in cytotoxic effect of 3BP in HCT-15 cell line.

3.3.1 Cells pre-treated with short-chain fatty acids

To evaluate the influence of SCFA in 3BP cytotoxic activity in cancer cells, HCT-15 cells were incubated in the presence of a range of concentration of the different SCFAs during 24 and 48 h, being afterward incubated with the respective IC_{50} of 3BP for 16 h. As control, a similar assay was performed but without 3BP treatment to verify if, the SCFAs were by themselves affecting cell survival.

The analysis of SCFAs effect on cell viability (**Figure 37**, black bars), assessed by the SRB assay, demonstrated that the three SCFAs presented different effects according with acid concentration and incubation time. The lactate and acetate were not cytotoxic compared to untreated cells with exception of highest concentrations at 48 h (**Figure 37 B and C**). In contrast, butyrate, at 24 h decreased significantly cell viability at different concentrations. At 48 h, butyrate decreased about 50% cell viability even at the lower concentration used (**Figure 37 A**). When cells were incubated with IC_{50} value of 3BP after pre-treatment with different SCFAs (**Figure 37**, gray bars), the results also varied in dose- and time-dependent manner. Both lactate and acetate did not increased 3BP cytotoxic effect at 24 h compared to control. At 48 h, the 3BP effect was enhanced significantly in cells treated from 20 mM of acetate up and in cells treated with the highest concentrations of lactate (above 50 mM). Cells treated with butyrate 10 mM for 24 h presented a significant decrease in cell viability after treatment with IC_{50} value of 3BP compared to control, which correspond to cells treated only with the IC_{50} value

of 3BP. At 48 h, a significant decrease of cell viability was observed for all concentrations of butyrate compared to control.

These results indicated that the minimum butyrate concentration and incubation time (between the conditions assayed) needed to affect 3BP effect was 10 mM at 24 h. For lactate and acetate, it was necessary 48 h incubation to enhance the effect of 3BP, as the cell viability decreased significantly with 50 mM and 20 mM of lactate and acetate acid treatment, respectively.

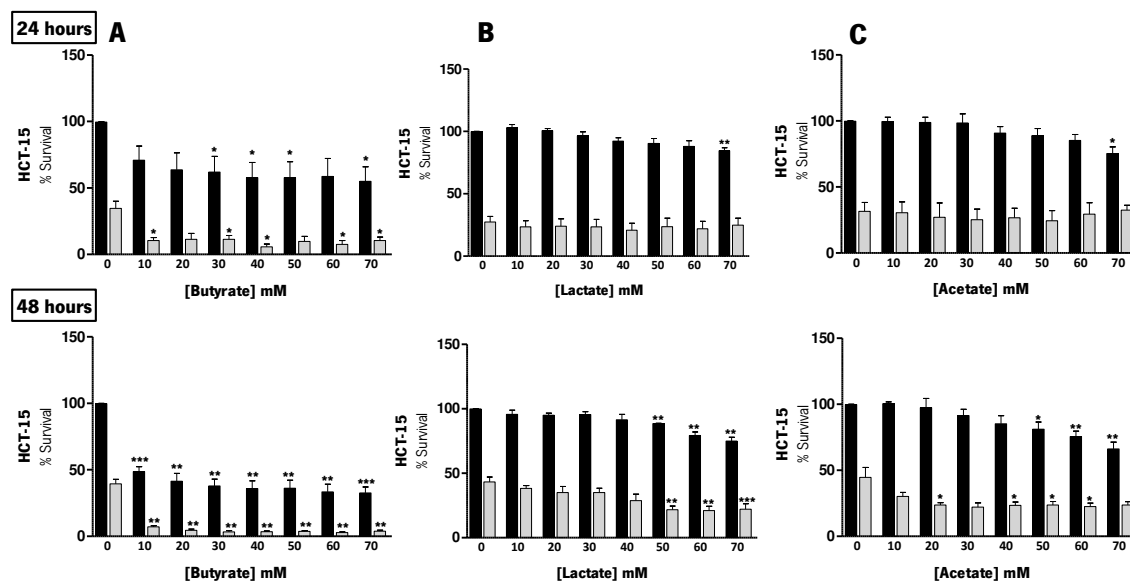


Figure 37. Cell viability, evaluated by the SRB assay, of HCT-15 cells incubated during 24 h and 48 h in medium containing butyrate (A), lactate (B) or acetate (C) in a range of concentrations (up to 70 mM), followed by 16 h incubation in medium with (gray bars) or without 3BP (black bars) using the IC_{50} previously determined. Results are the mean \pm SD of triplicates of at least three independent experiments. Significantly different between groups: * $P < 0.05$, ** $P < 0.01$, *** $P < 0.001$, significantly different from the respective untreated cells.

After the determination of incubation time and concentration of SCFAs that did not induce cell death, but potentiate 3BP effect, HCT-15 cells were incubated with two-fixed concentration of each SCFAs for 24 h and 48 h accordingly. Cells were pre-treated with 10 mM of each SCFAs and 40 mM, 50 mM and 20 mM of butyrate, lactate and acetate, respectively, and incubated for 24 h with butyrate and 48 h with lactate and acetate. After this pre-treatment, cells were incubated in the presence of different concentrations of 3BP for 16 h and the cell viability and the respective IC_{50} were assessed by SRB assay.

In HCT-15 cells pre-treated or not with SCFAs, it was observed that 3BP decreased the cell viability in a dose- and time-dependent manner (**Figure 38**). However, only butyrate and acetate enhanced 3BP effect, decreasing significantly its IC_{50} value for both concentrations assayed. Concerning lactate, the IC_{50} value of 3BP was approximately the same IC_{50} determined for cells without SCFA pre-treatment (**Table 6**).

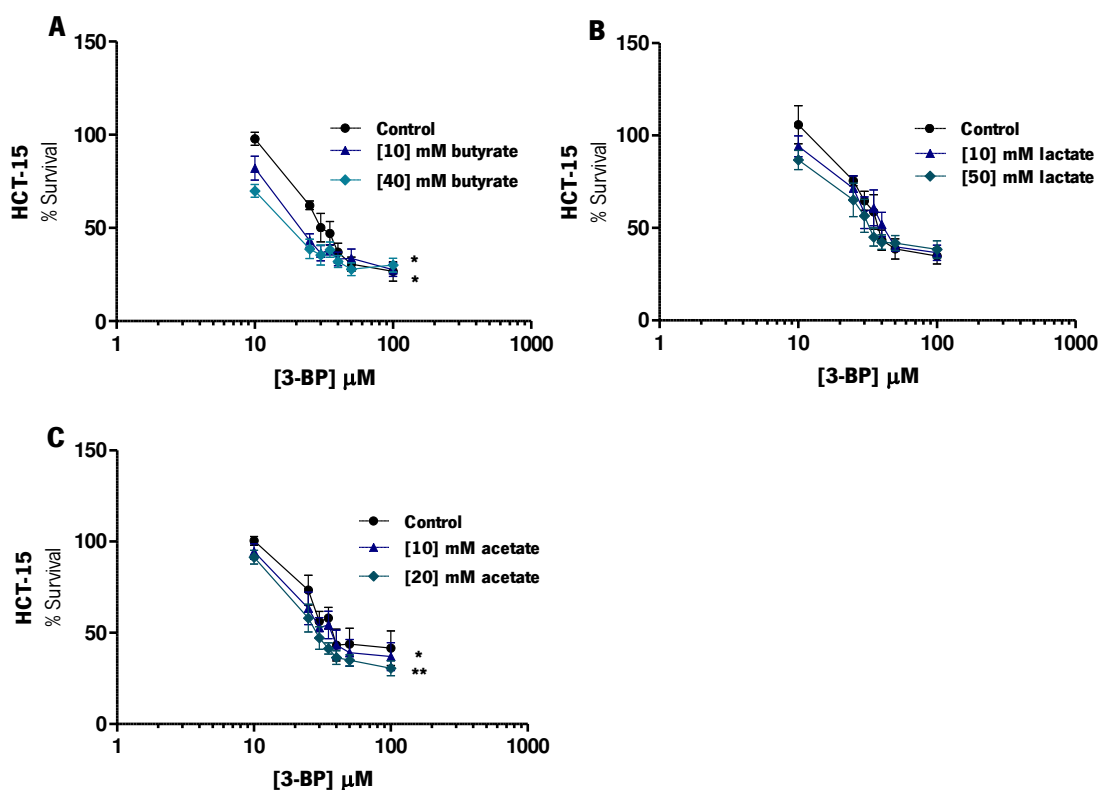


Figure 38. Effect of short-chain fatty acids on cell sensitivity of HCT-15 cells to 3BP, assessed by SRB assay. Cells were incubated with 10 mM (▲) and 40 mM (◆) of butyrate (**A**) for 24 h and with 10 mM (▲) and 50 mM (◆) of lactate (**B**) or 10 mM (▲) and 20 mM (◆) of acetate (**C**) for 48 h, followed by treatment with range of concentration of 3BP (up to 1000 μ M) for 16 h. Results are the mean \pm SD of triplicates of at least three independent experiments. Significantly different between groups: *P < 0.05, **P < 0.01, significantly different from the respective cells not subjected to pre-treatment with SCFA (●).

Table 6. IC₅₀ values for 3BP for the cell line HCT-15 after pre-incubation with concentration of each short-chain fatty acids assessed by SRB assays. Results are expressed as mean ± SD of triplicates from at least three independent experiments.

Cell Line	HCT-15								
	24 h Butyrate (μM)			48 h Lactate (μM)			48 h Acetate (μM)		
Conditions	Control	[10]	[40]	Control	[10]	[50]	Control	[10]	[20]
Determined									
IC₅₀ value (μM)	31.10	21.92	17.60	45.34	44.09	39.81	35.36	29,97	26,72
SD ±	7.50	4.73	5.22	12.79	11.30	15.67	9.85	10,18	5,61

3.1.2. Assessment of MCT1 and MCT4 expression

Since HCT-15 cells presented high sensitivity to 3BP after incubation with butyrate and acetate, the expression of genes *SLC16A1* and *SLC16A3* coding for MCT1 and MCT4, respectively, were evaluated by qRT-PCR, with the purpose of understand if this cytotoxic effect of 3BP was due to some alteration in the expression levels of MCTs. Cells were grown in medium with a fixed concentration, previously referred, for each SCFA during 24 h (butyrate) and 48 h (lactate and acetate), and total RNA was extracted. As control, HCT-15 cells grown in medium without any SCFA and total RNA was also extracted. Analyses of real-time assays showed that *SLC16A3* gene was overexpressed significantly when incubated with butyrate and acetate (**Figure 39 A and C**). In contrast, *SLC16A1* gene presented a decrease of expression when incubated with butyrate and remained its expression constant when incubated with acetate, compared to control (**Figure 39 A and C**). Concerning lactate, *SLC16A1* was overexpressed, but *SCL16A3* presented expression levels similar to control (**Figure 39 B**). However, to validate these results, Western Blot assays should be performed.

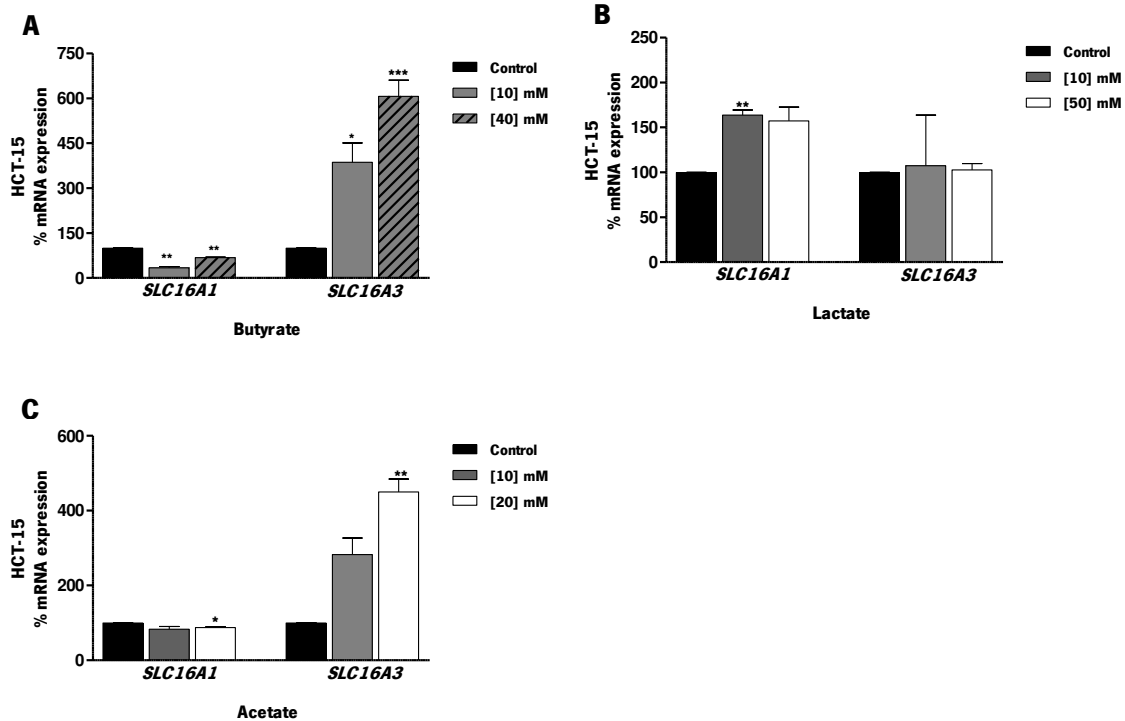


Figure 39. Effect of short-chain fatty acids in the expression levels of *SLC16A1* and *SLC16A3* genes in HCT-15 cells determined by qRT-PCR. Cells were incubated 24 h with 10 (gray bars) and 40 mM (gray diagonal bars) of butyrate (**A**) and 48 h with 10 (gray bars) and 50 mM (gray diagonal bars) of lactate (**B**) or 10 (gray bars) and 20 mM (gray diagonal bars) of acetate (**C**). The untreated cells (black bars) were used as reference. Actin was used as housekeeping gene. Results are representative of three independent experiments. Significantly different between groups: * $P < 0.05$, ** $P < 0.01$, *** $P < 0.001$.

The cellular localization of MCT1 and MCT4 was assessed by immunofluorescence and the analyses of representative pictures showed that in untreated cells (control), both proteins were localized either in plasma membrane or cytoplasm and, in some cells, MCT1 was found in nucleus (**Figure 40, 41 and 42**). After a period of incubation for 24 h with 10 and 40 mM of butyrate, MCT1 relocated almost totally in the plasma membrane, although some protein was still found in nucleus (**Figure 40**). It was also observed that for the highest concentration of butyrate, MCT1 localized mainly in nucleus. Concerning MCT4, cells presented higher intensity of fluorescence in plasma membrane and cytoplasm at both of butyrate concentrations used (10 and 40 mM) (**Figure 40**).

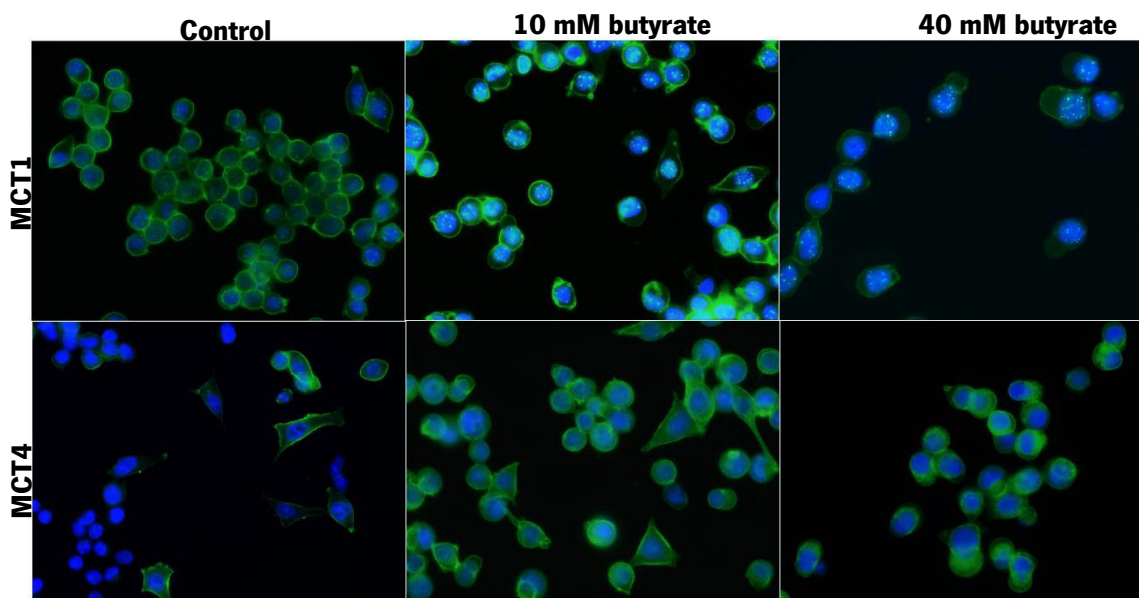


Figure 40. Effect of butyrate on MCT1 and MCT4 cellular localization of HCT-15 cell line. Cells were incubated with butyrate (10 and 40 mM) or with fresh medium (control) for 24 h. Representative images of immunofluorescence are shown at 400x magnification.

It was also observed that cells treated with 10 mM and 50 mM of lactate during 48 h, presented both MCT1 and MCT4 localized in plasma membrane and cytoplasm and did not present differences comparing to the control (**Figure 41**). Concerning acetate, MCT1 was also localized in cell membrane, cytoplasm and nucleus and did not present any variation comparing to the control. However, MCT4 was more intense in cytoplasm and plasma membrane in cells treated with 20 mM of acetate during 48 h comparing to the control and with cells treated with 10 mM of acetate (**Figure 42**). Thus, overall these results suggest that MCT4 should have a higher involvement on 3BP toxic effect. However, additional tests will be required to validate these results.

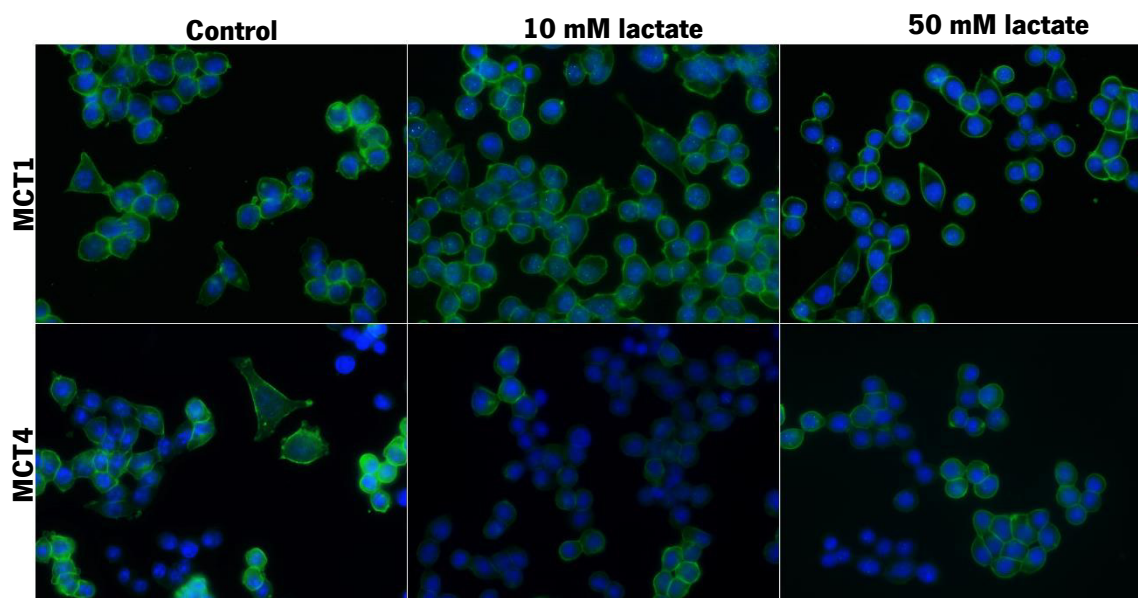


Figure 41. Effect of lactate on MCT1 and MCT4 cellular localization of HCT-15 cell line. Cells were incubated with lactate (10 and 50 mM) or with fresh medium (control) for 48 h. Representative images of immunofluorescence are shown at 400x magnification.

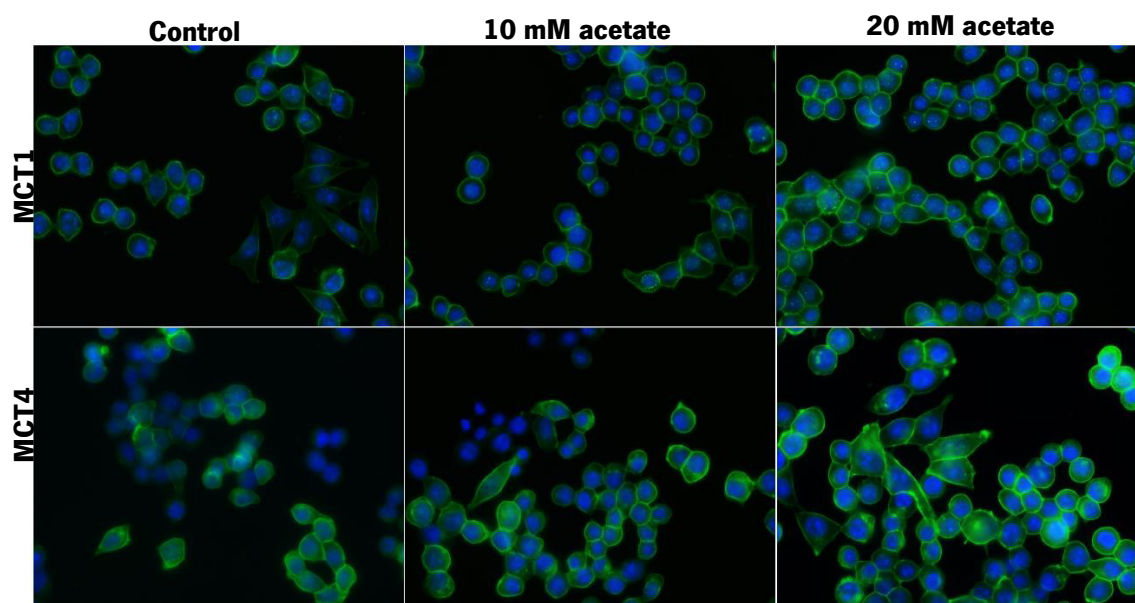


Figure 42. Effect of acetate on MCT1 and MCT4 cellular localization of HCT-15 cell line. Cells were incubated with acetate (10 and 20 mM) or fresh medium (control) for 48 h. Representative images of immunofluorescence are shown at 400x magnification.

Chapter 4
Discussion

Discussion

The cellular energetic deregulation is an hallmark of cancer, as tumor cells present predominantly a glycolytic profile with increased glucose consumption and lactate production, even under aerobic conditions (Warburg effect) [3,9]. This glycolytic phenotype is deeply correlated with tumor microenvironment, because the abnormal cell proliferation can lead to lack of oxygen and nutrients for long periods inducing hypoxic and starving stress. However, tumor cells are able to regulate enzymes and transporter proteins that allow them to take advantage of these adverse conditions. Therefore, this metabolic flexibility is important for the maintenance of the glycolytic profile of tumor cells, which consequently leads to environmental acidification due the high rate of lactate production and in this way contribute to an invasive and metastatic phenotype. Additionally, these characteristics are responsible by poor outcomes and resistance to radio- and chemotherapy observed. In case of colorectal cancer (CRC), the recurrence rates after treatments are 40-60% in the first three years, independently of the tumor stage [208,209]. Thus, in the last years, the tumor metabolism and microenvironment have been objects of an intensive investigation, aiming at discovering and understanding the mechanisms of action of new and specific anti-tumor compounds.

Transporters (GLUTs and MCTs) and glycolytic enzymes (HKII and GAPDH) are upregulated in tumor cells, being a target in the development of new anticancer therapies. 3-bromopyruvate (3BP) is an alkylating chemical compound with anticancer properties that acts as glycolytic inhibitor, able to cause rapid toxicity to different tumor cells [170-173]. Its uptake into the cells occurs via MCTs that are upregulated in several types of cancer. The high levels of expression of MCTs in colon carcinoma has been associated with tumor aggressiveness [125]. However, little is known about the influence of MCTs on cellular response to 3BP in CRC, as well as the influence of the tumor microenvironment in this response.

The work developed in this thesis aimed to understand the role of MCTs expression in the sensitivity to 3BP in different CRC cell lines. Furthermore, this work also aimed evaluated the influence of tumor microenvironment on MCT expression and consequently in the glycolytic pattern and cell response to 3BP.

The colorectal cancer cell line with greater expression of MCTs was the most sensitive to 3-bromopyruvate.

3BP presented cytotoxic effect in the three CRC cell lines (HCT-15, HT-29 and Caco-2) assayed. A decrease of cell viability in a 3BP dose-dependent manner was observed, being evident however that the three cell lines presented different sensitivities to treatment. HCT-15 was the most sensitive cell line, presenting an IC_{50} considerably lower than the Caco-2 and HT-29. In agreement with its anti-glycolytic effect, the treatment with 3BP also led to a decrease in both glucose consumption and lactate production in all cell lines. 3BP main target is HKII, responsible for the first step of intracellular glucose metabolism [140]. HKII is the predominant hexokinase isoform found in cancer cells, where it is overexpressed and associated to mitochondria [148]. It has been reported that HKII expression can be correlated with cell sensitivity to 3BP. In 2008, Kim and co-workers demonstrated this correlation in hepatoma cells, where the cell line with highest levels of HKII expression was the most sensitive to 3BP [164]. However, these results are controversial and others researches have demonstrated the opposite [210]. Ho *et al* (2016) reported that the 3BP effect is independent of HKII expression in colorectal cancer cell lines with HKII knockdown [211]. Thus, other proteins should be also involved in 3BP toxicity, and these can include other 3BP targets like GADPH, succinate dehydrogenase and vacuolar ATPase [212]. Concerning efflux pumps (like for example the ABC-transporter glycoprotein P), although it is well described that their expression can be one of the major causes of the multidrug resistance (MDR) phenotype and increased resistance in cancer to certain chemotherapeutic drugs [213], it is not probable that they are the main reason of cancer cells resistance to 3BP. For the activity of these pumps, the ATP generated through cancer cells metabolism is essential, and enhances drug efflux activity [214]. However, 3BP is a glycolytic inhibitor that cause ATP depletion, decreasing ABC transporter activity and drug efflux. Furthermore, it was already demonstrated, using the *Saccharomyces cerevisiae* model, that 3BP is not substrate of the tested drug-efflux pumps belonging to the ABC family [214-216].

MCTs, more specifically MCT1 and MCT4, have an important role in the tumor metabolism, being upregulated in tumor cells [55], and thus, they can have a central role in cell sensitivity to 3BP, since its uptake occurs through these proteins. In fact, HCT-15, the cell line more glycolytic and sensitives

to 3BP, presented higher MCT1 and MCT4 expression levels than other cell lines, as well as a proper cell localization. These proteins need to be properly located at the cell membrane to exert their right function [99,100]. By immunofluorescence assays, it was possible to perform a qualitative analysis of MCT1 and MCT4 localization. Both proteins were localized in the plasma membrane. However, in the cell lines more resistant (Caco-2 and HT-29) to 3BP, MCT1 and MCT4 appeared essentially in junctions between cells, whereas in HCT-15 cells they are localized around plasma membrane. In addition, MCT1 was also localized in cytoplasm and nucleus in Caco-2 and HT-29. Although it was not possible to associate this result with right protein function, it is described in literature that these proteins require an accessory protein, CD147 [101]. Halestrap and co-workers reported a MCT1 and MCT4 accumulation in the perinuclear region (characteristic of the Golgi apparatus) and when co-expressed with CD147 both proteins were correctly in plasma membrane, indicating the relevance of this chaperone for MCTs localization and function [57,101]. In this work, MCT4 was not found in nucleus in any cell line. However, other factors can be involved in right function and localization of MCTs like the glycosylation status of CD147 [103,217].

The cell migration and invasion capacity are characteristics associated with a malignant phenotype, in which cancer cells are able to become motile, moving from primary tumor to a different location metastasizing other tissues. Some researchers have demonstrated the migratory, invasive and metastatic potential of different CRC cell lines *in vitro* and *in vivo* models [218-220]. The results obtained by the wound-healing assay, showed that HCT-15 had higher migration ability than HT-29 and Caco-2 in basal conditions. Although the cell line with higher motile capacity is the one with the highest level of MCTs expression, complementary assays are necessary to confirm that increased migration is due to the upregulation of MCTs. Nevertheless, 3BP inhibited cell migration capacity in all cell lines, being more efficient after 24 h of treatment. As already mentioned, 3BP inhibits glycolysis depleting the energy production and consequently cell proliferation and motility [221].

Tumor microenvironment affected MCT1 and MCT4 expression in HCT-15 cells.

Hypoxia is characterized by oxygen supply deprivation and, in the case of cancer, can be due to rapid tumor growth. This continuous growth and proliferation in a hypoxic environment is supported by

metabolic alterations of cancer cells [25,222] and, as expected, HCT-15 cells were more glycolytic in hypoxia (chemically induced) than normoxia. Hypoxia leads to increased levels of the transcription factor, HIF-1, which is responsible to upregulate genes involved in this environment adaptation including GLUT-1, HKII, PDK-1 or LDH and, in this way, enhances glucose uptake and glycolysis [218]. On the other hand, MCT4 is upregulated by HIF-1, as it contains a HRE present in promoter region [90]. MCT4 promotes the efflux of the lactate/H⁺, maintaining pHi homeostasis in hypoxic tumor cells that present a high glycolytic metabolism [30,132-133]. Although the results must be confirmed by Western blotting assays, the evaluation of the expression levels of *SLC16A1* and *SLC16A3* genes demonstrated an overexpression of *SLC16A3* (MCT4), in contrast to *SLC16A1* (MCT1), where no variations were observed. Additionally, in immunofluorescence assays, it was observed a more intense fluorescence of MCT4 under hypoxia in either plasma membrane or cytoplasm, probably due to its overexpression verified by qRT-PCR analysis. However, additional assays are required to support this hypothesis.

Concerning cell migration, and in contrast to what was expected, cells under hypoxia presented lower migration capacity compared to cells grown in normoxia. HCT-15 produced more lactate in hypoxia than normoxia, being this metabolite associated to environment acidification and according to what is described in literature, the acidic pHe induce cell migration and invasion of tumor cells [37,38]. Thus, it was expected that cells in hypoxia had a higher migratory capacity. These contradictory results are probably due to the cell line type or by the fact, the medium used in this assay was buffered, avoiding such acidification of the medium.

Regarding the cytotoxic effect of 3BP, Xu and co-workers reported that HCT116 colorectal cancer cells grown under hypoxic conditions were more sensitive to 3BP than in normoxia [223]. However, in present work, HCT-15 became more resistant in hypoxia. Analysis of MCTs expression suggests that MCT4 is not the main one involved in the cytotoxicity of 3BP in these conditions, being important to mention that this result needs to be validated by Western blot and that other facts such as CD147 can influence the activity of both MCTs. On the other hand, in the present study, the hypoxic culture condition was created chemically by incubating cells with CoCl₂. The CoCl₂ treatment induced HIF-1 α expression by blocking of HIF-1 α VHL complex binding and thereby preventing the degradation of HIF-1 α [201]. Thus, this compound can be influence genes expression involved in resistance to 3BP.

However, it is necessary to compare the expression of the glycolytic proteins in hypoxia induced by CoCl_2 and by a hypoxic chamber.

Several studies of the acidosis effects on the phenotypes of various tumor cell models have demonstrated that acidity enhances cell invasion, aggressiveness and resistance to chemotherapy [30,47]. However, little is known about acidity of extracellular pH (pHe) on cell metabolism. In the present work, HCT-15 cells at pHe 6.6 presented cell migratory capacity similar to pHe 7.4, but regarding the metabolic profile, HCT-15 cells were less glycolytic under acidic pHe. Ippolito and co-workers demonstrated in neuroendocrine prostate cancer model that pHe changes nutrient uptake and metabolism in PNEC cells, presenting a 8.3-fold decrease in glucose levels and an increase of 9.5-fold in lactate levels in media at pH 8.5 relative to pH 6.5, in agreement to what is also observed in this work. It was also demonstrated that the lactate produced came essentially from glycolysis [224].

To sustain a glycolytic phenotype, cancer cells rely not only on changes in the expression level of glycolytic enzymes and transporters, but also on pumps and other proteins that regulate intracellular pH including H^+ pumps and exchangers (ATPase, NHE), transporters that facilitate protons efflux (CA, and HCO_3^- transporters (**Figure 4**) [225]. Herein, it was evaluated the expression of MCT1 and MCT4 under acidic pH, once these proteins are proton-lactate symporters and at same time are vehicle to 3BP uptake. Despite MCT1-coding gene *SLC16A1* expression had decreased at pH 6.6, the localization was in plasma membrane like as it happens at pHe 7.4. MCT4 had similar gene expression levels and protein localization at both pHes. Although MCT1 presented lower expression levels at 6.6, HCT-15 cells were slightly more sensitive to 3BP at acidic pHe than physiological pHe (7.4). It has been already reported an increased toxicity of 3BP at acidic pH in breast cancer lines [114]. However, this cytotoxicity is due not to a change in the expression of MCTs, but to the mechanism of uptake into the cell via MCT coupled with a proton [226].

The concentration of several nutrients available during tumor growth is also unstable, subjecting tumor cells to periods of nutrients starvation. Although glucose is the preferential substrate, cancer cells can reprogram their metabolism and use other substrates like glutamine or lactate [23,24,40]. To elucidate

the effect of glucose starvation on cell metabolism, migratory capacity and sensitivity to 3BP, HCT-15 cells were incubated in glucose-free medium. Cells became less glycolytic as expected, as estimated by extracellular lactate levels, presented lower migratory capacity and became more resistant to 3BP. Ippolito *et al.* reported that cells at physiological pH with glucose deprivation were enabled to reprogram their metabolism, producing lactate from glutamine [224], which is present in the culture medium used in this assay. Concerning MCTs, they play an essential role in the metabolic homeostasis of the tumor microenvironment, maintaining glycolytic phenotype and pH_i homeostasis [39], but little is known about the effect of glucose availability in MCTs expression, although it was already reported that hyperglycemia enhanced MCT1 expression in brain [227]. However, based on qRT-PCR and immunofluorescence results, both *SLC16A1* and *SLC16A3* genes were overexpressed and the proteins fluorescence was more intense in cytoplasm in glucose starvation in HCT-15 cell line. It would be also expected that cells in these conditions turned out to be more sensitive to 3BP, but the opposite happened. It was reported in human colorectal cells that limiting glucose led to decrease of HKII and, consequently an increase of cell resistance to 3BP [211]. Indeed, this could justify such results and low lactate levels were observed in starved cells. However, it is necessary additional experiments to verify HKII and MCTs expression and correlate this to cell sensitivity to 3BP.

Influence of the short-chain fatty acids in 3-bromopyruvate cytotoxicity and monocarboxylate transporters expression in HCT-15 cell line.

In CRC, the intestinal microbiota composition has an important role in colon homeostasis, being its change associated to CRC carcinogenesis. The intestinal bacteria are responsible to produce SCFAs as result of fermentative metabolism and these metabolites have been described as having cell protective effect [194]. In the present work, it was explored the role of SCFAs, including butyrate, acetate and lactate, in MCTs regulation and consequently in cell sensitivity to 3BP. The treatment with butyrate sensitized HCT-15 cells to 3BP, and an increased expression of *SLC16A3* (MCT4) was observed. In contrast, *SLC16A1* (MCT1) expression decreased, but the protein localization was mainly in plasma membrane, where it can exerts its function correctly. It was described that butyrate induced overexpression of MCT1 in tumor colonocytes [83,228]. In the present work, the cell line used was

different. In the same conditions, the acetate also induced significant change both in *SLC16A3* expression and in cell sensitivity. The same did not happen with lactate, where no changes in cytotoxicity effect were observed.

Based on these results, both butyrate and acetate appear to play an important role in the regulation of MCT4 and cell sensitivity. Although MCT4 has not a diversity of substrates as large as MCT1 and it is associated with lactate efflux due to its distribution in high glycolytic tissues and its high K_m , the hypothesis that 3BP can enter the cell via MCT4 should not be discarded. Previous results from our lab demonstrated in breast cancer cell lines that 3BP cytotoxicity was correlated with MCT4 and CD147 overexpression and MCT1 re-localization in plasma membrane after butyrate treatment [84]. It was also demonstrated in same model that the increase of 3BP cytotoxicity was due not only to overexpression of MCTs but also to by an increase in the affinity for 3BP uptake, as well as high glycosylation of CD147 stimulated by butyrate [114]. Such results demonstrated the importance of the chaperone CD147 that can play a fundamental role in the activity and proper cell localization of MCTs, being necessary evaluate the its role in CRC cell lines used in this work.

Concerning acetate treatment, MCT1 expression remained similar after treatment with acetate, whereas MCT4 was overexpressed, being localized in both plasma membrane and cytoplasm. Additionally, the HCT-15 cells were significantly more sensitive to 3BP after treatment with acetate, suggesting that this may be related to the expression of MCT4 and possibly MCT1. It has been previously demonstrated that acetate induced overexpression and re-localization of MCT1, as well as MCT4 and CD147 global overexpression in CRC cell lines, verifying that 3BP potentiated acetate-induced apoptosis. It was also demonstrated that acetate was transported through sodium dependent monocarboxylate transporter (SMCT) 1 [229]. The SMCT1 is coded by *SLC5A8* gene, and has been classified as tumor suppressor, being expressed in normal colon, but silenced in colon cancer. This transporter also has SCFA as substrates, including butyrate and acetate [62]. As known, butyrate is a HDAC inhibitor, inhibiting cell proliferation and stimulate apoptosis selectively in tumor cells [197,198], which may justify the silencing of the gene in tumor cells. However, concerning HCT-15, the cell line used in present work, it was observed SMCT1 expression [229]. This finding may explain the effect of both butyrate and acetate in cell sensitivity to 3BP. However, these issues are poorly understood and need further investigation.

Chapter 5

Final Remarks and Future Perspectives

As previously discussed, the preference of tumor cells by glycolysis to satisfy their energy requirements has been already known for decades, being considered in recent years as a signature of tumor cells. The metabolic reprogramming is considered a therapeutic target, in which several drugs have been tested in preclinical studies with promising results. An example is 3BP, a glycolytic inhibitor with the capability to target both glycolytic enzymes and ATP production in mitochondria. In this context, MCTs plays an essential role not just by conveniently performing the co-transport of lactate with protons to the extracellular milieu, but they may be the “weakness”, as they are the gateway to 3BP, due to their overexpression in various cancers.

In the present work, we demonstrated that HCT-15 cell line presented a higher basal expression of MCTs than Caco-2 and HT-29 and subsequent increased glycolytic profile and motile capacity and sensitivity to 3BP. We also observed that HCT-15 presented increased resistance under hypoxia and glucose starvation conditions, although an increase in MCT expression levels under these conditions has been observed. In addition, HCT-15 cells were slightly more sensitive to 3BP at acidic pH, but this may be not associated to MCTs expression. However, increased toxicity of 3BP after treatment with butyrate and acetate seems to correlate with increased expression of MCT4, demonstrating that this transporters proteins can be an important part of the mechanism of action of 3BP. However, other factors can be also involved that justify the different sensitivities to 3BP in different conditions.

Future Perspectives

All these findings raise many questions to be carried out in the future to complement this work.

To complement the results obtained in CRC cell lines, it would be important to evaluate MCTs protein levels in all the conditions studied in the present work, as well as others metabolic markers including HKII, GAPDH, LDH, GLUTs, CAIX, PDH, PDK and correlate with the effect of 3BP, glycolytic phenotype and aggressiveness.

Additional studies for MCT1 and MCT4 activity inhibition, with MCTs down-regulation or specific inhibitors (developed by AstraZeneca), will be important to confirm if MCTs inhibition increases resistance of CRC cells to 3BP. In addition, it will be important to perform expression, localization and inhibition studies of CD147, a chaperone involved in correct activity of MCTs.

Additionally, there are recent reports the SCFAs increased cytotoxic effect of 3BP through overexpression of MCTs. However, it will be important to evaluate the cell expression and localization of SMCT1 protein as well as its involvement in the transport of these SCFAs and of 3BP.

Microenvironment affected both cell sensitivity and MCTs expression. Concerning MCT4, it was more expressed with SCFAs treatment and apparently correlated with 3BP toxic effect, but under hypoxic conditions, where also observed a MCT4 overexpression, cells were more resistance. Indeed, it would be interesting to combine these conditions to understand what kind of regulation occurs at the level of MCT4.

Finally, the evaluation of both MCTs regulation and 3BP toxic effect in different conditions, it should be also tested using other models *in vitro* and other antitumor compounds. These assays should be tested on non-tumor cell lines to evaluate possible side effects, which may be extended to *in vivo* assays.

References

References

- [1] DeBerardinis, R.J. and Chande, I.N.S. (2016). Fundamentals of cancer metabolism. *Oncology*. 2, 1-18.
- [2] Heiden G.V., Cantley L.C. and Thompson C.B. (2009). Understanding the Warburg effect: the metabolic requirements of cell proliferation. *Science*. 324, 1029-33.
- [3] Warburg, O. (1956) On the Origin of Cancer Cells. *Science*. 123, 309-314.
- [4] DeBerardinis, R.J., *et al.* (2008). The biology of cancer: metabolic reprogramming fuels cell growth and proliferation. *Cell Metabolism*. 7, 11-20.
- [5] Greaves, M., and Maley, C. C. (2012). Clonal evolution in cancer. *Nature*. 481, 306-313.
- [6] Yan, H., *et al.* (2009). Mutant Metabolic Enzymes Are at the Origin of Gliomas. *Cancer Res*. 69, 9157-9159.
- [7] Nigro, J.M., *et al.* (1989). Mutations in the p53 gene occur in diverse human tumour types. *Nature*. 342, 705-708.
- [8] Hanahan, D., and Weinberg, R. A. (2000). The hallmarks of cancer. *Cell*. 100, 57-70.
- [9] Hanahan, D., and Weinberg, R. A. (2011). Hallmarks of cancer: the next generation. *Cell*. 144, 646-674.
- [10] Gonçalves, V.M., Baltazar, F. and Reis, R. (2015) Brain Tumor Metabolism - Unraveling Its Role in Finding New Therapeutic Targets. In T. Lichtor (Eds), *Molecular Considerations and Evolving Surgical Management Issues in the Treatment of Patients with a Brain Tumor*, Dr. Terry Lichtor (Ed.), InTech, DOI: 10.5772/59606. Available from: <http://www.intechopen.com/books/molecular-considerations-and-evolving-surgical-management-issues-in-the-treatment-of-patients-with-a-brain-tumor/brain-tumor-metabolism-unraveling-its-role-in-finding-new-therapeutic-targets>.
- [11] Warburg, O. (1956) On respiratory impairment in cancer cells. *Science*. 124, 269-270.
- [12] Astuti, D. *et al.* (2001) Gene Mutations in the Succinate Dehydrogenase Subunit SDHB Cause Susceptibility to Familial Pheochromocytoma and to Familial Paraganglioma. *American Society of Human Genetics*. 69, 49-54.
- [13] Fantin, V.R., St-Pierre, J. and Leder, P. (2006) Attenuation of LDH-A expression uncovers a link between glycolysis, mitochondrial physiology, and tumor maintenance. *Cancer Cell*. 9, 425-434.
- [14] Seyfried, T.N. and Shelton, L.M. (2010) Cancer as a metabolic disease. *Nutrition and Metabolism*. 7, 1-22.
- [15] Kroemer, G. and Pouyssegur, J. (2008) Tumor Cell Metabolism: Cancer's Achilles' Heel. *Cancer Cell*. 13, 472-482.
- [16] Darleen, C.N. *et al.* (2015) Introduction to the molecular basis of cancer metabolism and the Warburg effect. *Mol Biol Rep*. 42, 819-823.
- [17] Yen, T.C. *et al.* (2004) ¹⁸F-FDG Uptake in Squamous Cell Carcinoma of the Cervix Is Correlated with Glucose Transporter 1 Expression. *The Journal of Nuclear Medicine*. 45, 22-29.
- [18] Potter, M., Newport, E. and Morten, K. J. (2016). The Warburg effect: 80 years on. *Biochemical Society Transactions*. 44, 1499-1505.
- [19] Hensley, C.T. *et al.* (2013) Glutamine and cancer: cell biology, physiology, and clinical opportunities. *The Journal of Clinical Investigation*. 123, 3678-84.
- [20] Qing G, *et al.* (2012) ATF4 regulates MYC-mediated neuroblastoma cell death upon glutamine deprivation. *Cancer Cell*. 2, 631-644.
- [21] Reitzer, L.J. *et al.* (1979). Evidence that glutamine, not sugar, is the major energy source for cultured HeLa cells. *J Biol Chem*. 254, 2669-76.
- [22] DeBerardinis, R.J. *et al.* (2007). Beyond aerobic glycolysis: Transformed cells can engage in glutamine metabolism that exceeds the requirement for protein and nucleotide synthesis. *Proc Natl Acad Sci U S A*. 104, 19345-50.
- [23] Shanware, N. P. *et al.* (2011). Glutamine: pleiotropic roles in tumor growth and stress resistance. *J Mol Med*. 89, 229-236.
- [24] Son, J. *et al.* (2013). Glutamine supports pancreatic cancer growth through a KRAS-regulated metabolic pathway. doi:10.1038/nature12040.

References

- [25] Xia, Y. *et al.* (2012). Recent advances in hypoxia-inducible factor (HIF)-1 inhibitors. *European Journal of Medicinal Chemistry*. 49, 24-40.
- [26] Muz, B. *et al.* (2014). Hypoxia promotes stem cell-like phenotype in multiple myeloma cells. *Blood Cancer Journal*. 4, e262; doi:10.1038/bcj.2014.82
- [27] Swietach, P. *et al.* (2007). Regulation of tumor pH and the role of carbonic anhydrase 9. *Cancer Metastasis Rev*. 26, 299-310.
- [28] Porporato, P.E. *et al.* (2011). Anticancer targets in the glycolytic metabolism of tumors: a comprehensive review. *Front Pharmacol*. 2, 49.
- [29] Swietach, P. *et al.* (2014). The chemistry, physiology and pathology of pH in cancer. *Phil. Trans. R. Soc. B* 369: 20130099.
- [30] Damaghi, M., Wojtkowiak, J.W. and Gillies, R.J. (2013). pH sensing and regulation in cancer. *Frontiers in Physiology*. 4, 1-10.
- [31] Ziello, J. E. *et al.* (2007). Hypoxia-Inducible Factor (HIF)-1 Regulatory Pathway and its Potential for Therapeutic Intervention in Malignancy and Ischemia. *Yale Journal of Biology and Medicine*. 80, 51-60.
- [32] Semenza, G.L. (2003). Targeting HIF-1 for cancer therapy. *Nature Reviews*. 3, 721-732.
- [33] Masson, N. and Ratcliffe, P.J. (2014). Hypoxia signaling pathways in cancer metabolism: the importance of co-selecting interconnected physiological pathways. *Cancer & Metabolism*. 2, 1-17.
- [34] Sermeus, A. and Michiels, C. (2011). Reciprocal influence of the p53 and the hypoxic pathways. *Cell Death Dis*. 2:e164.
- [35] Pore, N. *et al.* (2006). Akt1 activation can augment hypoxia-inducible factor-1alpha expression by increasing protein translation through a mammalian target of rapamycin-independent pathway. *Mol Cancer Res*. 4, 471-479.
- [36] Flugel, D. *et al.* (2007). Glycogen synthase kinase 3 phosphorylates hypoxia-inducible factor 1alpha and mediates its destabilization in a VHL-independent manner. *Mol Cell Bio*. 27, 3253-65.
- [37] Goetze, K. *et al.* (2011). Lactate enhances motility of tumor cells and inhibits monocyte migration and cytokine release. *International Journal of Oncology*. 39, 453-463.
- [38] Kato, Y. *et al.* (2013). Acidic extracellular microenvironment and cancer. *Cancer Cell International*. 13, 1-8.
- [39] Nakajima, E.C. and Houten, B.V. (2013). Metabolic Symbiosis in Cancer: Refocusing the Warburg Lens. *Molecular Carcinogenesis*. 52, 329-37.
- [40] Sonveaux, P. *et al.* (2008) Targeting lactate-fueled respiration selectively kills hypoxic tumor cells in mice. *J Clin Invest*. 118, 3930-42.
- [41] Bonuccelli, G. *et al.* (2010). Ketones and lactate “fuel” tumor growth and metastasis Evidence that epithelial cancer cells use oxidative mitochondrial metabolism. *Cell Cycle*. 9, 3506-14.
- [42] Migneco, G. *et al.* (2010). Glycolytic cancer associated fibroblasts promote breast cancer tumor growth, without a measurable increase in angiogenesis Evidence for stromal-epithelial metabolic coupling. *Cell Cycle*. 9, 2412-22.
- [43] Pavlides, S. *et al.* (2009). The reverse Warburg effect: aerobic glycolysis in cancer associated fibroblasts and the tumor stroma. *Cell Cycle*. 8, 3984-4001.
- [44] Sotgia, F. *et al.* (2011). Understanding the Warburg effect and the prognostic value of stromal caveolin-1 as a marker of a lethal tumor microenvironment. *Breast Cancer Res*. 13,213.
- [45] Yoshida, G.J. (2016). Metabolic reprogramming: the emerging concept and associated therapeutic strategies. *Journal of Experimental & Clinical Cancer Research*. 34:111.
- [46] Kato, Y. *et al.* (2005). Acidic Extracellular pH Induces Matrix Metalloproteinase-9 Expression in Mouse Metastatic Melanoma Cells through the Phospholipase D-Mitogen-activated Protein Kinase Signaling. *The Journal of Biological Chemistry*. 280, 10938-44.

- [47] Romero-Garcia, S. et al. (2016) Lactate Contribution to the Tumor Microenvironment: Mechanisms, effects on immune Cells and Therapeutic Relevance. *Frontiers in Immunology*. 7, 1-11.
- [48] Hirschhaeuser, F., Sattler, U. and Mueller-Klieser, W. (2011). Lactate: A Metabolic Key Player in Cancer. *Cancer Research*. 71, 6921-25.
- [49] Xu, L., Fukumura, D. and Jain, R.K. (2002). Acidic extracellular pH induces vascular endothelial growth factor (VEGF) in human glioblastoma cells via ERK1/2 MAPK signaling pathway: mechanism of low pH-induced VEGF. *J Biol Chem*. 277, 11368-74.
- [50] Yokota, H. et al. (2007). Lactate, choline, and creatine levels measured by vitro 1H-MRS as prognostic parameters in patients with non-small-cell lung cancer. *J Magn Reson Imaging*. 25, 992-9.
- [51] Chang, C.H. et al. (2015). Metabolic Competition in the Tumor Microenvironment Is a Driver of Cancer Progression. *Cell*. 162, 1-13.
- [52] Yamada, Y. et al. (2011). Lactate dehydrogenase, Gleason score and HER-2 overexpression are significant prognostic factors for M1b prostate cancer. 25, 937-944.
- [53] Danner, B.C. et al. (2010). Long-term Survival Is Linked to Serum LDH and Partly to Tumour LDH-5 in NSCLC. *Anticancer Research*. 30, 1347-52.
- [54] Wang, Z.W. et al. (2016) Prognostic value of preoperative serum lactate dehydrogenase levels for resectable gastric cancer and prognostic nomograms. *Oncotarget*. 7, 39945-56.
- [55] Eilertsen, M. et al. (2014). Monocarboxylate Transporters 1–4 in NSCLC: MCT1 Is an Independent Prognostic Marker for Survival. *PLoS ONE*. 9, 1-9.
- [56] Halestrap, A.P. and Price, N.T. (1999). The proton-linked monocarboxylate transporter (MCT) family: structure, function and regulation. *Biochem J*. 343, 281-99.
- [57] Halestrap, A.P (2012) The Monocarboxylate Transporter Family—Structure and Functional Characterization. *IUBMB Life*. 64, 1-9.
- [58] Halestrap, A.P and Wilson, M.C (2012) The Monocarboxylate Transporter Family—Role and Regulation. *IUBMB Life*. 64, 109-119.
- [59] Juel, C. (1997) Lactate-proton cotransport in skeletal muscle. *Physiol Rev*. 77, 321-58.
- [60] Halestrap, A.P and Meredith, D. (2004). The SLC16 gene family—from monocarboxylate transporters (MCTs) to aromatic amino acid transporters and beyond. *Pflugers Arch*. 447, 619-28.
- [61] Morris, M.E. and M.A. Felmler (2008) Overview of the proton-coupled MCT (SLC16A) family of transporters: characterization, function and role in the transport of the drug of abuse γ -hydroxybutyric acid. *AAPS J*. 10, 311-21.
- [62] Ganapathy, V. et al. (2008). Sodium-coupled Monocarboxylate Transporters in Normal Tissues and in Cancer. *The AAPS Journal*. 10, 193-199.
- [63] Philp, N.J., Yoon, H. and Grollman, E.F. (1998). Monocarboxylate transporter MCT1 is located in the apical membrane and MCT3 in the basal membrane of rat RPE. *American Journal of Physiology*. 274, R1824-R1828.
- [64] Klier, M. et al. (2013). Intracellular and Extracellular Carbonic Anhydrases Cooperate Non-enzymatically to Enhance Activity of Monocarboxylate Transporters. *Journal of Biological Chemistry*. 289, 2765-75.
- [65] Halestrap, A.P. (2013). Monocarboxylic Acid Transport. *Comprehensive Physiology*. 3, 1611-43.
- [66] Broer, S. et al. (2003). The loop between helix 4 and helix 5 in the monocarboxylate transporter MCT1 is important for substrate selection and protein stability. *Biochem. J*. 376, 413-422.
- [67] Wilson, M.C. et al. (2009). Studies on the DIDS-binding Site of Monocarboxylate Transporter 1 Suggest a Homology Model of the Open Conformation and a Plausible Translocation Cycle. *Journal of Biological Chemistry*. 284, 20011-21.
- [68] Garcia-Kim, C. et al. (1994). Molecular characterization of a membrane transporter for lactate, pyruvate, other monocarboxylates - implications for the Cori cycle. *Cell*. 76, 865-873.

References

- [69] Carpenter, L. and Halestrap, A. P. (1994) The kinetics, substrate and inhibitor specificity of the lactate transporter of Ehrlich-Lette tumour cells studied with the intracellular pH indicator BCECF. *Biochem. J.* 304, 751-760.
- [70] Merezhinskaya, N. and Fishbein, W.N. (2009) Monocarboxylate transporters: past, present, and future. *Histol Histopathol.* 24, 243-64.
- [71] Enerson, B.E. and Drewes, L.R. (2003) Molecular features, regulation, and function of monocarboxylate transporters: implications for drug delivery. *J Pharm Sci.* 92, 1531-44.
- [72] Kennedy, K.M and Dewhirst, M.W. (2010). Tumor metabolism of lactate: the influence and therapeutic potential for MCT and CD147 regulation. *Future Oncol.* 6, 1-32.
- [73] Deuticke B. *et al.* (1978). Stereoselective, SHdependent transfer of lactate in mammalian erythrocytes. *Biochim. Biophys.* 509: 21-32.
- [74] Dubinsky W.P. and Racker E. (1978). The mechanism of lactate transport in human erythrocytes. *J. Membr. Biol.* 44: 25-36.
- [75] Cuff, M.A. and Shirazi-Beechey, S.P. (2002) The human monocarboxylate transporter, MCT1: genomic organization and promoter analysis. *Biochem Biophys Res Commun.* 292, 1048-56.
- [76] Sepponen, K. *et al.* (2003). Distribution of monocarboxylate transporter isoforms MCT1, MCT2 and MCT4 in porcine muscles. *Acta Physiol Scand.* 177, 79-86.
- [77] Pinheiro, C. *et al.* (2012). Role of monocarboxylate transporters in human cancers: state of the art. *J Bioenerg Biomembr.* 44, 127-139.
- [78] Hashimoto, T. *et al.* (2007). Lactate sensitive transcription factor network in L6 cells: activation of MCT1 and mitochondrial biogenesis. *The FASEB Journal.* 21, 2602-12.
- [79] Ríos-Covián, D. *et al.* (2016) Intestinal Short Chain Fatty Acids and their Link with Diet and Human Health. *Front. Microbiol.* 7, 1-9.
- [80] Cuff, M.A. and Shirazi-Beechey, S.P. (2002) Substrate-induced regulation of the human colonic monocarboxylate transporter, MCT1. *Journal of Physiology.* 539, 361-371.
- [81] Candido, *et al.* (1978) Sodium butyrate inhibits histone deacetylation in cultured cells. *Cell.* 14: 105-13.
- [82] Canani, R.B. *et al.* (2011) Potential beneficial effects of butyrate in intestinal and extraintestinal diseases. *World J Gastroenterol.* 28: 17: 1519-1528.
- [83] Borthakur, A. *et al.* (2008). Regulation of Monocarboxylate Transporter 1 (MCT1) Promoter by Butyrate in Human Intestinal Epithelial Cells: Involvement of NF- κ B Pathway. *J Cell Biochem.* 103, 1452-63.
- [84] Queiros, O. *et al.* (2012). Butyrate activates the monocarboxylate transporter MCT4 expression in breast cancer cells and enhances the antitumor activity of 3- bromopyruvate. *J Bioenerg Biomembr.* 44, 141-53.
- [85] Marchiq, I. and Pouysségur, J. (2015). Hypoxia, cancer metabolism and the therapeutic benefit of targeting lactate/H⁺ symporters. *J Mol Med.* 94,155-171.
- [86] Enoki, T. *et al.* (2003). Exercise training alleviates MCT1 and MCT4 reductions in heart and skeletal muscles of STZ-induced diabetic rats. *J Appl Physiol.* 94, 2433-38.
- [87] Py, G. *et al.* (2001). Impaired sarcolemmal vesicle lactate uptake and skeletal muscle MCT1 and MCT4 expression in obese Zucker rats. *Am J Physiol Endocrinol Metab.* 281, E1308-E1315.
- [88] Hajduch, E. *et al.* (2000). Lactate transport in rat adipocytes: identification of monocarboxylate transporter 1 (MCT1) and its modulation during streptozotocin-induced diabetes. *FEBS Letters.* 479, 89-92.
- [89] Miranda-Gonçalves, V. *et al.* (2016). Hypoxia-mediated upregulation of MCT1 expression supports the glycolytic phenotype of glioblastomas. *Oncotarget.* 7, 46335-53.
- [90] Ullah, M.S, Davies, A.J. and Halestrap, A.P. (2006). The plasma membrane lactate transporter MCT4, but not MCT1, is up-regulated by hypoxia through a HIF-1 α -dependent mechanism. *J Biol Chem.* 281, 9030-7.
- [91] Boidot, R. *et al.* (2012). Regulation of Monocarboxylate Transporter MCT1 Expression by p53 Mediates Inward and Outward Lactate Fluxes in Tumors. *Cancer Res.* 72, 939-948.

- [92] Price, N. T. *et al.* (1998) Cloning and sequencing of four new mammalian monocarboxylate transporter (MCT) homologues confirms the existence of a transporter family with an ancient past. *Biochem. J.* 329, 321-328
- [93] Pinheiro, C. and Baltazar, F. SLC16A3 (solute carrier family 16, member 3 (monocarboxylic acid transporter 4)). *Atlas Genet Cytogenet Oncol Haematol.* 2010; 14(12):1157-1159.
- [94] Jones, R.S and Morris, M.E. (2016) Monocarboxylate Transporters: Therapeutic Targets and Prognostic Factors in Disease. *Clinical Pharmacology & Therapeutics.* 1-10
- [95] Dimmer, K.S. *et al.* (2000). The low-affinity monocarboxylate transporter MCT4 is adapted to the export of lactate in highly glycolytic cells. *Biochem J.* 350, 219-27.
- [96] Hatta, H. *et al.* (2001). Tissue-specific and isoform-specific changes in MCT1 and MCT4 in heart and soleus muscle during a 1-yr period. *Am J Physiol Endocrinol Metab.* 281, E749-E756.
- [97] Fisel, P. *et al.* (2015). DNA Methylation of the SLC16A3 Promoter Regulates Expression of the Human Lactate Transporter MCT4 in Renal Cancer with Consequences for Clinical Outcome. *Clin Cancer Res.* 19, 5170-81.
- [98] Pullen, T. *et al.* (2011). miR-29a and miR-29b Contribute to Pancreatic -Cell-Specific Silencing of Monocarboxylate Transporter 1 (Mct1). *Molecular and Cellular Biology.* 31, 3182-3194.
- [99] Nakai M. *et al.* (2006). Tissue distribution of basigin and monocarboxylate transporter 1 in the adult male mouse: a study using the wild-type and basigin gene knockout mice. *Anat. Rec. Part A.* 288, 527-535.
- [100] Walters, D. K. *et al.* (2013) CD147 regulates the expression of MCT1 and lactate export in multiple myeloma cells. *Cell Cycle.* 12, 3175-3183
- [101] Kirk, P. *et al.* (2000) CD147 is tightly associated with lactate transporters MCT1 and MCT4 and facilitates their cell surface expression. *The EMBO Journal.* 19, 3896-3904.
- [102] Muramatsu, T. (2015). Basigin (CD147), a multifunctional transmembrane glycoprotein with various binding partners. *J. Biochem.* 1-10.
- [103] Grass, G.D. and Toole, B.P. (2016). How, with whom and when: an overview of CD147-mediated regulatory networks influencing matrix metalloproteinase activity. *Biosci. Rep.* 36, 1-16.
- [104] Yoshida, S. *et al.* (2000). Homo-oligomer formation by basigin, an immunoglobulin superfamily member, via its N-terminal immunoglobulin domain. *Eur. J. Biochem.* 267, 4372-80.
- [105] Tang, W., Chang, S.B. and Hemler, M.E. (2004). Links between CD147 Function, Glycosylation, and Caveolin-1. *Molecular Biology of the Cell.* 15, 4043-50.
- [106] Xiong, L., Edwards III, C.K. and Zhou, L. (2014). The biological function and clinical utilization of CD147 in human diseases: a review of the current scientific literature. *Int. J. Mol. Sci.* 15, 17411-41.
- [107] Agrawal, S.M. and Yong, V.W. (2011). The many faces of EMMPRIN – roles in neuroinflammation. *Biochim. Biophys. Acta.* 1812, 213–19.
- [108] Oliveira, A. *et al.* (2012). Co-expression of monocarboxylate transporter 1 (MCT1) and its chaperone (CD147) is associated with low survival in patients with gastrointestinal stromal tumors (GISTs). *J Bioenerg Biomembr.* DOI 10.1007/s10863-012-9408-5.
- [109] Payen, V. *et al.* (2015). Metabolic changes associated with tumor metastasis, part 1: tumor pH, glycolysis and the pentose phosphate pathway. *Cell. Mol. Life Sci.* DOI 10.1007/s00018-015-2098-5.
- [110] McDonald, P.C., Chafe, S.C. and Dehdar, S. (2016). Overcoming Hypoxia-Mediated Tumor Progression: Combinatorial Approaches Targeting pH Regulation, Angiogenesis and Immune Dysfunction. *Frontier.* 4, 1-16.
- [111] Morais-Santos, F. *et al.* (2014). Differential sensitivities to lactate transport inhibitors of breast cancer cell lines. *Endocr Relat Cancer.* 21, 27-38.
- [112] Colen, C.B. *et al.* (2011) Metabolic targeting of lactate efflux by malignant glioma inhibits invasiveness and induces necrosis: an in vivo study. *Neoplasia.* 13, 620-632.
- [113] Halestrap, A. and Denton, R.M. (1974). Specific Inhibition of Pyruvate Transport in Rat Liver Mitochondria and Human Erythrocytes by α -Cyano-4-hydroxycinnamate. *Biochem. J.* 138, 313-316.

References

- [114] Azevedo-Silva, J. *et al.* (2015). The cytotoxicity of 3-bromopyruvate in breast cancer cells depends on extracellular pH. *Biochem. J.* 467, 247-258.
- [115] Bola, B.M. *et al.* (2014). Inhibition of Monocarboxylate Transporter-1 (MCT1) by AZD3965 Enhances Radiosensitivity by Reducing Lactate Transport. *Mol Cancer Ther.* 13, 2805-16.
- [116] Ovens, M.J. *et al.* (2010). AR-C155858 is a potent inhibitor of monocarboxylate transporters MCT1 and MCT2 that binds to an intracellular site involving transmembrane helices 7–10. *Biochem. J.* 425, 523–530.
- [117] Polanski, R. *et al.* (2014). Activity of the monocarboxylate transporter1 inhibitor AZD3965 in small cell lung cancer. *Clin. Cancer Res.* 20, 926-937.
- [118] Doyen, J. *et al.* (2014). Expression of the hypoxia-inducible monocarboxylate transporter MCT4 is increased in triple negative breast cancer and correlates independently with clinical outcome. *Biochemical and Biophysical Research Communication.* 451, 54-61.
- [119] LeFloch, R. *et al.*(2011). CD147 subunit of lactate/H⁺ symporters MCT1 and hypoxia-inducible MCT4 Is critical for energetics and growth of glycolytic tumors. *Proc. Natl. Acad. Sci. U.S.A.* 108, 16663-68.
- [120] Baenke, F. *et al.* (2015). Functional screening identifies MCT4 as a key regulator of breast cancer Cell metabolism and survival. *J. Pathol.* 237, 152-165.
- [121] Baek, G. *et al.* (2014). MCT4 defines a glycolytic subtype of pancreatic cancer with poor Prognosis and unique metabolic dependencies. *Cell Rep.* 9, 2233-49.
- [122] Floridi, A. *et al.* (1981). Effect of Lonidamine on the Energy Metabolism of Ehrlich Ascites Tumor Cells. *Cancer Research.* 41, 4661-66.
- [123] Fang, J. *et al.* (2006). The H⁺-linked monocarboxylate transporter (MCT1/SLC16A1): a potential therapeutic target for high-risk neuroblastoma. *Mol Pharmacol.* 70, 2108-15.
- [124] Nancolas, B. *et al.* (2016). The anti-tumour agent lonidamine is a potent inhibitor of the mitochondrial pyruvate carrier and plasma membrane monocarboxylate transporters. *Biochem J.* 473, 929-936.
- [125] Pinheiro, C. *et al.* (2008). Increased expression of monocarboxylate transporters 1, 2 and 4 in colorectal carcinomas. *Virchows Arch.* 452, 139-146.
- [126] Meijer, T. *et al.* (2012). Differences in metabolism between adeno- and squamous cell non-small cell lung carcinomas: Spatial distribution and prognostic value of GLUT1 and MCT4. *Lung Cancer.* 76, 316-323.
- [127] Choi, S. *et al.* (2014). The MCT4 Gene: A Novel, Potential Target for Therapy of Advanced Prostate Cancer. *Clin Cancer Res.* 22, 2721-33.
- [128] Pinheiro, C. *et al.* (2010). Monocarboxylate transporter 1 is upregulated in basal-like breast carcinoma. *Histopathology In press.* DOI:10.1111/j.1365-2559.2010.03560.x.
- [129] Pinheiro, C. *et al.* (2010). Expression of monocarboxylate transporters 1, 2 and 4 in human tumours and their association with CD147 and CD44. *J Biomed Biotechnol.* Article ID 427694.
- [130] Miranda-Gonçalves, V. *et al.* (2012). Monocarboxylate transporters (MCTs) in gliomas: expression and exploitation as therapeutic targets. *Neuro-Oncology.* 15, 172-188.
- [131] Pinheiro, C. *et al.* (2008). Increasing expression of monocarboxylate transporters 1 and 4 along progression to invasive cervical carcinoma. *Int J Gynec Pathol.* 27, 568-574.
- [132] Sasaki, S. *et al.* (2015). Involvement of Histidine Residue His382 in pH Regulation of MCT4 Activity. *PLOS ONE.* DOI:10.1371/journal.pone.0122738.
- [133] Parks, S. *et al.* (2016). Hypoxia optimises tumour growth by controlling nutrient import and acidic metabolite export. *Molecular Aspects of Medicine.* 47–48, 3-14.
- [134] Rademakers S.E. *et al.* (2011). Metabolic markers in relation to hypoxia; staining patterns and colocalization of pimonidazole, HIF-1 α , CAIX, LDH-5, GLUT-1, MCT1 and MCT4. *BMC Cancer.* 11, 1-10.
- [135] Ganapathy-Kanniappan, S. and Geschwind, J-F. (2013). Tumor glycolysis as a target for cancer therapy: progress and prospects. *Molecular Cancer.* 12, 1-12.
- [136] Medina, R.A. and Owen. G. (2002). Glucose transporters: expression, regulation and cancer. *Biol. Res.* 35, 1-32.

- [137] Wu, C-H. *et al.* (2009). In vitro and in vivo study of phloretin-induced apoptosis in human liver cancer cells involving inhibition of type II glucose transporter. *Int. J. Cancer.* 124, 2210-19.
- [138] Liu, Y. *et al.* (2011). A Small-Molecule Inhibitor of Glucose Transporter 1 Downregulates Glycolysis, Induces Cell-Cycle Arrest, and Inhibits Cancer Cell Growth in Vitro and In Vivo. *Mol Cancer Ther.* 11, 1672-82.
- [139] Wood, T.E. *et al.* (2008). A novel inhibitor of glucose uptake sensitizes cells to FAS-induced cell death. *Mol Cancer Ther.* 7, 3546-55.
- [140] Mathupala, S.P. *et al.* (2009). Hexokinase-2 bound to mitochondria: cancer's stygian link to the "Warburg Effect" and a pivotal target for effective therapy. *Semin Cancer Biol.* 19, 17-24.
- [141] Nath, K. *et al.* (2016). Mechanism of antineoplastic activity of lonidamine. *Biochimica et Biophysica Acta.* 1866, 151-162.
- [142] Kurtoglu, M. *et al.* (2007). Under normoxia, 2-deoxy-D-glucose elicits cell death in select tumor types not by inhibition of glycolysis but by interfering with N-linked glycosylation. *Mol Cancer Ther.* 6, 3049-58.
- [143] Zhong, D. *et al.* (2009). The Glycolytic Inhibitor 2-Deoxyglucose Activates Multiple Prosurvival Pathways through IGF1R. *Journal of Biological Chemistry.* 284, 23225-33.
- [144] Maschek, G. *et al.* (2004). 2-Deoxy-D-glucose Increases the Efficacy of Adriamycin and Paclitaxel in Human Osteosarcoma and Non-Small Cell Lung Cancers In Vivo. *Cancer Research.* 64, 31-34.
- [145] Zhong, D. *et al.* (2008). 2-Deoxyglucose induces Akt phosphorylation via a mechanism independent of LKB1/AMP-activated protein kinase signaling activation or glycolysis inhibition. *Mol Cancer Ther.* 7, 809-817.
- [146] Mohanti, B.K. *et al.* (1996). Improving cancer radiotherapy with 2-deoxy-d-glucose: phase i/ii clinical trials on human cerebral gliomas. *Int. J Radiation Oncology Bid Phy.* 35, 103-111.
- [147] Stein, M. *et al.* (2010). Targeting Tumor Metabolism With 2-Deoxyglucose in Patients With Castrate-Resistant Prostate Cancer and Advanced Malignancies. *Prostate.* 70, 1388-94.
- [148] Chen, Z. *et al.* (2009). Role of mitochondria-associated hexokinase II in cancer cell death induced by 3-bromopyruvate. *Biochimica et Biophysica Acta.* 1787, 553-560.
- [149] Ganapathy-Kanniappan, S. *et al.* (2009). Glyceraldehyde-3-phosphate Dehydrogenase (GAPDH) Is Pyruvylated during 3-Bromopyruvate Mediated Cancer Cell Death. *Anticancer Res.* 29, 4909-18.
- [150] Le, A. *et al.* (2010). Inhibition of lactate dehydrogenase A induces oxidative stress and inhibits tumor progression. *PNAS.* 107, 2037-42.
- [151] Ganapathy-Kanniappan, S. *et al.* (2010). 3-Bromopyruvate: A New Targeted Antiglycolytic Agent and a Promise for Cancer Therapy. *Current Pharmaceutical Biotechnology.* 11, 1-8.
- [152] Sun, Y. *et al.* (2015). Mechanisms underlying 3-bromopyruvate-induced cell death in colon cancer. *J Bioenerg Biomembr.* 47, 319-329.
- [153] Valenti, D., Vacca, R. and Bari, L. (2015). 3-Bromopyruvate induces rapid human prostate cancer cell death by affecting cell energy metabolism, GSH pool and the glyoxalase system. *J Bioenerg Biomembr.* DOI 10.1007/s10863-015-9631-y
- [154] Davidescu, M. *et al.* (2015). The energy blockers bromopyruvate and lonidamine lead GL15 glioblastoma cells to death by different p53-dependent routes. *Scientific Reports.* 5, 1-12.
- [155] Guo, X. *et al.* (2016). 3-Bromopyruvate and sodium citrate induce apoptosis in human gastric cancer cell line MGC-803 by inhibiting glycolysis and promoting mitochondria-regulated apoptosis pathway. *Biochemical and Biophysical Research Communications.* 475, 37-43.
- [156] Davidescu, M. *et al.* (2012). Bromopyruvate mediates autophagy and cardiolipin degradation to monolysocardiolipin in GL15 glioblastoma cells. *J Bioenerg Biomembr.* 44, 51-60.
- [157] Verhoeven, H.A. and L.J. van Griensven (2012). Flow cytometric evaluation of the effects of 3 bromopyruvate (3BP) and dichloroacetate (DCA) on THP-1 cells: a multiparameter analysis. *J Bioenerg Biomembr.* 44, 91-99.
- [158] Bhardwaj, V. *et al.* (2010). Glycolytic enzyme inhibitors affect pancreatic cancer survival by modulating its signaling and energetics. *Anticancer Res.* 30, 743-9.

References

- [159] Ko, Y.H., Pederson, P.L. and Geschwind, J.F. (2001). Glucose catabolism in the rabbit VX2 tumor model for liver cancer: characterization and targeting hexokinase. *Cancer Letters*. 173, 83-91.
- [160] Pelicano, H. *et al.* (2006). Glycolysis inhibition for anticancer treatment. *Oncogene*. 25, 4633-46.
- [161] Pereira-Silva, A.P. *et al.* (2009). Inhibition of energy-producing pathways of HepG2 cells by 3-bromopyruvate. *Biochem. J.* 417, 717-726.
- [162] Tang, Z. *et al.* (2012). Over-expression of GAPDH in human colorectal carcinoma as a preferred target of 3-Bromopyruvate Propyl Ester. *J Bioenerg Biomembr.* 44, 117-125.
- [163] Ihrlund, L.S. *et al.* (2008). 3-Bromopyruvate as inhibitor of tumour cell energy metabolism and chemopotentiator of platinum drugs. *molecular oncology*. 2, 94-101.
- [164] Kim, S.J. *et al.* (2008). Role of reactive oxygen species-mediated mitochondrial dysregulation in 3-bromopyruvate induced cell death in hepatoma cells. *Journal of Bioenergetics and Biomembranes*. 40, 607-618.
- [165] Marrache, S. and Dhar, S. (2015). The energy blocker inside the power house: mitochondria targeted delivery of 3-bromopyruvate. *Chem. Sci.* 6, 1832-45.
- [166] Wondrak, G.T. (2009). Redox-Directed Cancer Therapeutics: Molecular Mechanisms and Opportunities. *antioxidants & redox signaling*. 11, 3013-69.
- [167] Geschwind, J.F. *et al.* (2002). Novel therapy for liver cancer: direct intraarterial injection of a potent inhibitor of ATP production. *Cancer Res.* 62, 3909-13.
- [168] Ko, Y.H. (2004) Advanced cancers: eradication in all cases using 3-bromopyruvate therapy to deplete ATP. *Biochemical and Biophysical Research Communications*. 324, 269-275.
- [169] Pederson (2007) Warburg, me and Hexokinase 2: Multiple discoveries of key molecular events underlying one of cancers' most common phenotypes, the "Warburg Effect", i.e., elevated glycolysis in the presence of oxygen. *J Bioenerg Biomembr.* 39, 211-222.
- [170] Ko, Y.H. *et al.* (2012). A translational study "case report" on the small molecule "energy blocker" 3-bromopyruvate (3BP) as a potent anticancer agent: from bench side to bedside. *J Bioenerg Biomembr.* 44, 163-170.
- [171] Ferlay, J. *et al.* (2014). Cancer incidence and mortality worldwide: sources, methods and major patterns in GLOBOCAN 2012. *International Journal of Cancer*. doi:10.1002/ijc.29210 PMID:25220842.
- [172] American Cancer Society. Global Cancer Facts & Figures 3rd Edition. Atlanta: American Cancer Society; 2015.
- [173] Mudassar, S. *et al.* (2014). Possible Role of Proto-Oncogenes in Colorectal Cancer – A Population Based Study. J. Khan (Eds), *Colorectal Cancer - Surgery, Diagnostics and Treatment*, Dr. JimKhan(Ed.), InTech, DOI:10.5772/50593, Available from: <http://www.intechopen.com/books/colorectal-cancer-surgery-diagnostics-and-treatment>.
- [174] Tarraga-López, P.J. *et al.* (2014). Primary and Secondary Prevention of Colorectal Cancer. *Clinical Medicine Insights: Gastroenterology*. 7, 33-46.
- [175] Cappellani, A. *et al.* (2013). Strong correlation between diet and development of colorectal cancer. *Frontiers in Bioscience, Landmark*. 18, 190-198.
- [176] Davis, D.M. *et al.* (2011). Is It Time to Lower the Recommended Screening Age for Colorectal Cancer?. *American College of Surgeons*. 213,352-361.
- [177] Stigliano, V. *et al.* (2014). Early-onset colorectal cancer: A sporadic or inherited disease?. *World J Gastroenterol*. 20, 12420-30.
- [178] Abdelsattar, Z.M. *et al.* (2016). Colorectal Cancer Outcomes and Treatment Patterns in Patients Too Young for Average-Risk Screening. *Cancer*. 929-934.
- [179] Schmoll, H.J. *et al.* (2012). ESMO consensus guidelines for management of patients with colon and rectal cancer: a personalized approach to clinical decision making. *Ann Oncol*. 23, 2479-2516.

- [180] Balmaña, J. *et al.* (2013). Familial risk-colorectal cancer: ESMO Clinical Practice Guidelines. *Ann Oncol.* 24, 72-79.
- [181] Numata, M. *et al.* (2012). The clinicopathological features of colorectal mucinous adenocarcinoma and a therapeutic strategy for the disease. *World Journal of Surgical Oncology.* 10, 1-8.
- [182] Tannapfel, A. *et al.* (2010). The Origins of Colorectal Carcinoma. *Dtsch Arztebl Int.* 107, 760-766.
- [183] Armaghany, T. *et al.* (2011). Genetic Alterations in Colorectal Cancer. *Gastrointest Cancer Res.* 5, 19-27.
- [184] Gonsalves, Y.I. *et al.* (2014). Patient and Tumor Characteristics and BRAF and KRAS Mutations in Colon Cancer, NCCTG/Alliance N0147. *JNCI.* 1-8.
- [185] Ahmed, D. *et al.* (2013). Epigenetic and genetic features of 24 colon cancer cell lines. *Oncogenesis.* 2, 1-8.
- [186] West, N.R. *et al.* (2015). Emerging cytokine networks in colorectal. *Cancer Nature Reviews Immunology.* 15, 615-629. doi:10.1038/nri3896.
- [187] Narayan, S. and Roy, D. (2003). Role of APC and DNA mismatch repair genes in the development of colorectal cancers. *Molecular Cancer.* 2, 1-15.
- [188] Labianca, R. *et al.* (2010). Primary colon cancer: ESMO Clinical Practice Guidelines for diagnosis, adjuvant treatment and follow-up. *Annals of Oncology.* 21, 70-77.
- [189] Labianca, R. *et al.* (2013). Early colon cancer: ESMO Clinical Practice Guidelines for diagnosis, treatment and follow-up. *Annals of Oncology.* 24, 64-72.
- [190] Sridharan, M., Hubbard, J.M. and Grothey, A. (2014). Colorectal Cancer: How Emerging Molecular Understanding Affects Treatment Decisions. *CancerNetwork.* 1-10.
- [191] Longley, D.B., (2003). 5-fluorouracil: mechanisms of action and clinical strategies. *Nature.* 3, 330-338.
- [192] Violette, S. *et al.* (2002). Resistance of colon cancer cells to long-term 5-fluorouracil exposure is correlated to the relative level of bcl-2 and bcl-xl in addition to bax and p53 status. *Int. J. Cancer.* 98, 498-504.
- [193] Zhang, N. *et al.* (2008). 5-Fluorouracil: Mechanisms of Resistance and Reversal Strategies. *Molecules.* 13, 1551-69.
- [194] Sobhani, I. *et al.* (2013). Microbial dysbiosis and colon carcinogenesis: could colon cancer be considered a bacteria-related disease?.
- [195] Kim, G.H. (2013). Gut Microbiota-Derived Short-Chain Fatty Acids, T Cells, and Inflammation. *IMMUNE NETWORK.* 14, 277-288.
- [196] Keku, T.O. *et al.* (2015). The gastrointestinal microbiota and colorectal cancer. *Ther Adv Gastroenterol.* 6, 215-229.
- [197] Donohoe, D. *et al.* (2012). The Warburg Effect Dictates the Mechanism of Butyrate Mediated Histone Acetylation and Cell Proliferation. *Mol Cell.* 48, 612-626.
- [198] Donohoe, D. *et al.* (2014). A Gnotobiotic Mouse Model Demonstrates that Dietary Fiber Protects Against Colorectal Tumorigenesis in a Microbiota- and Butyrate-Dependent Manner. *Cancer Discov.* 4, 1387-97.
- [199] Zhu, Y. *et al.* (2011). Gut Microbiota and Probiotics in Colon Tumorigenesis. *Cancer Lett.* 309, 119-127.
- [200] Myers, R. *et al.* (2015). Effects of genetic and environmental risk assessment feedback on colorectal cancer screening adherence. *J Behav Med.* 38, 777-786.
- [201] Yuan, Y., *et al.* (2003) Cobalt Inhibits the Interaction between Hypoxia-inducible Factor- α and von Hippel-Lindau Protein by Direct Binding to Hypoxia-inducible Factor- α . *The Journal of Biological Chemistry.* 278, 15911-15916.
- [20] Okail, M. (2010) Cobalt chloride, a chemical inducer of hypoxia-inducible factor-1 α in U251 human glioblastoma cell line. *Journal of Saudi Chemical Society.* 14, 197-201.
- [203] Liu, Y., *et al.* (2012) Cobalt chloride decreases fibroblast growth factor-21 expression dependent on oxidative stress but not hypoxia-inducible factor in Caco-2 cells. *Toxicol Appl Pharmacol.* 264, 212-221.
- [204] Liu, Q., *et al.* (2015) Effect of hypoxia on hypoxia inducible factor-1 α , insulin-like

References

- growth factor I and vascular endothelial growth factor expression in hepatocellular carcinoma HepG2 cells. *Oncology Letters*. 9, 1142-1148.
- [205] Hulkower, K-I. and Herber, R-I. (2011) Cell Migration and Invasion Assays as Tools for Drug Discovery. *Pharmaceutics*. 3, 107-124.
- [206] Kobayashi, M., *et al* (2005) Transport Mechanism for L-Lactic Acid in Human Myocytes Using Human Prototypic Embryonal Rhabdomyosarcoma Cell Line (RD Cells). *Biol. Pharm. Bull.* 28, 1197-1201.
- [207] Morais-Santos, F. *et al.* (2015). Targeting lactate transport suppresses in vivo breast tumour Growth. *Oncotarget*. 6, 19177-89.
- [208] Kanwar, S, Poolla, A. and Majumdar, A. (2012). Regulation of colon cancer recurrence and development of therapeutic strategies. *World J Gastrointest Pathophysiol.* 3, 1-9.
- [209] Ryuk, J.P. *et al.* (2014). Predictive factors and the prognosis of recurrence of colorectal cancer within 2 years after curative resection. *Ann Surg Treat Res.* 86,143-151.
- [210] Qin, J.Z., Xin, H. and Nickoloff, B.J. (2010). 3-Bromopyruvate induces necrotic cell death in sensitive melanoma cell lines. *Biochem Biophys Res Commun.* 396, 495-500.
- [211] Ho, N. *et al.* (2016). The effect of 3-bromopyruvate on human colorectal cancer cells is dependent on glucose concentration but not hexokinase II expression. *Biosci. Rep.* 36,1 -13.
- [212] Shoshan, M.C. (2012). 3-bromopyruvate: Targets and outcomes. *J Bioenerg Biomembr.* 1-10.
- [213] Vinette, V. *et al.* (2015). Multidrug Resistance-Associated Protein 2 Expression Is Upregulated by Adenosine 5'-Triphosphate in Colorectal Cancer Cells and Enhances Their Survival to Chemotherapeutic Drugs. *PLoS ONE.* 1-14.
- [214] Zhao, Y., Butler, E.B. and Tan, M. (2013). Targeting cellular metabolism to improve cancer therapeutics. *Cell Death and Disease.* 4, 1-10.
- [215] Nakano, A. *et al.* (2011). Glycolysis Inhibition Inactivates ABC Transporters to Restore Drug Sensitivity in Malignant Cells. *PLoS ONE.* 6, 1-10.
- [216] Lis P. *et al.* (2012). Transport and cytotoxicity of the anticancer drug 3-bromopyruvate in the yeast *Saccharomyces cerevisiae*. *J Bioenerg Biomembr.* 44, 155-161.
- [217] Bai, Y. *et al.* (2014). Importance of N-Glycosylation on CD147 for Its Biological Functions. *Int. J. Mol. Sci.* 15, 6356-77.
- [218] Christensen, J. *et al.* (2012). Defining new criteria for selection of cell-based intestinal models using publicly available databases.
- [219] Ishizy, K. *et al.* (2007). Development and Characterization of a Model of Liver Metastasis Using Human Colon Cancer HCT-116 Cells. *Biol. Pharm. Bull.* 30, 1779-83.
- [220] Flatmark, K. *et al.* (2004). Twelve colorectal cancer cell lines exhibit highly variable growth and metastatic capacities in an orthotopic model in nude mice. *European Journal of Cancer.* 40, 1593-98.
- [221] Baghdadi, H. (2017). Targeting Cancer Cells using 3-bromopyruvate for Selective Cancer Treatment. *Saudi Journal of Medicine & Medical Sciences.* 9-19.
- [222] Eales, K.L., Hollinshead, K.R and Tennant, D.A. (2016). Hypoxia and metabolic adaptation of cancer cells. *Oncogenesis.* 5, 1-8.
- [223] Xu, R-H *et al.* (2005). Inhibition of Glycolysis in Cancer Cells: A Novel Strategy to Overcome Drug Resistance Associated with Mitochondrial Respiratory Defect and Hypoxia. *Cancer Res.* 65, 613-21.
- [224] Ippolito, J.E. *et al.* (2016). Extracellular pH Modulates Neuroendocrine Prostate Cancer Cell Metabolism and Susceptibility to the Mitochondrial Inhibitor Niclosamide. *PLOS ONE.* 1-26.
- [225] Baldini, N. *et al.* (2016). Metabolism and microenvironment in cancer plasticity. *Cancer & Metabolism.* 4, 1-7.
- [226] Azevedo-Silva, J. *et al.* (2016). The anticancer agent 3-bromopyruvate: a simple but powerful molecule taken from the lab to the bedside. *J Bioenerg Biomembr.* 48, 349-362.

- [227] Pérez-Escuredo, J. *et al.* (2016). Monocarboxylate transporters in the brain and in cancer. *Biochimica et Biophysica Acta*. 1863, 2481-97.
- [228] Hadjiagapiou, C. *et al.* (2000). Mechanism(s) of butyrate transport in Caco-2 cells: role of monocarboxylate transporter 1. *Am J Physiol Gastrointest Liver Physiol*. 279, 775-780.
- [229] Oliveira, C. S. (2016). *Unraveling the Mechanisms Involved in Acetate Induced Apoptosis in Colorectal Cancer*. Dissertação de doutoramento, Universidade do Minho, Braga, Portugal.